Abstract

The tetradentate N_4-coordinate ligand *N*,*N*-bis(3,5-dimethyl-*1H*-pyrazol-1-yl)methyl-N_2-phenylethane-1,2-diamine (bdpab) has been used to synthesis a series of mononuclear complexes of the type [M(bdpab)(X)]Y, [M = Cu(II), Co(II), Zn(II). X = NCS^- / NCO^-. Y = PF_6^- / ClO_4^-], [M'' (bdpab)$(NCS)_2$] [M'' = Ni(II), Co(II)] and binuclear complexes of the type [M' (bdpab)$(NCO)]_2(Y)_2$, where M' = Ni(II), Cd(II). Y = PF_6^- / ClO_4^- by treating metal nitrate / perchlorate, NCO^-, NCS^- and PF_6^- ions using appropriate mole ratio and characterized by spectral and physico-chemical techniques. The structures of eight complexes $[Cu(bdpab)(NCS)]ClO_4$, $[Co(bdpab)(NCS)_2]$, $[Ni(bdpab)(NCS)_2]$, $[Zn(bdpab)(NCS)]PF_6$, $[Cu(bdpab)(NCO)]PF_6$, $[Co(bdpab)(NCO)]ClO_4$, $[Ni(bdpab)(\mu_{1,3}\text{-NCO})]_2(ClO_4)_2$ and $[Cd(bdpab)(\mu_{1,1}\text{-NCO})]_2(ClO_4)_2$ have been solved by single crystal X-ray diffraction studies and shows complexes $[Cu(bdpab)(NCS)]ClO_4$, $[Cu(bdpab)(NCO)]PF_6$ and $[Co(bdpab)(NCO)]ClO_4$ have distorted square pyramidal, $[Zn(bdpab)(NCS)]PF_6$ has distorted trigonal bipyramidal, [M''(bdpab)$(NCS)_2$] [M'' = Ni(II), Co(II)] has distorted octahedral and binuclear isocyanate bridged complexes [M'(bdpab)$(NCO)]_2(Y)_2$ [M' = Ni(II), Cd(II)] have distorted octahedral geometry. All complexes are ionic in nature except thiocyanate containing Co(II) and Ni(II) complexes. In the binuclear complexes, the bridging mode is end-on ($\mu_{1,1}$-NCO) for the Cd(II) complex whereas the bridging mode is end-to-end ($\mu_{1,3}$-NCO) for Ni(II) complex.

5(B). 1. Introduction

Transition metal complexes with the isocyanate and thiocyanate ligand are of special interest because both are ambidentate pseudohalides and can coordinate with metal ions as a terminal as well as bridging ligand to give mono-, di- and polymeric complexes [1-6]. They have great potential in building up of coordination networks of varied dimensionalities when it acts as bridging ligand [7-10]. When isocyanate or thiocyanate acts as monodentate ligand, it forms mononuclear complexes but as a bridging ligand it can bridge a pair of metal centers either in end-on or end-to-end coordination mode and form single or double bridged di- or multinuclear complexes [11-16]. In addition, both isocyanate and thiocyanate bridged complexes show magnetic interaction while bridging with paramagnetic metal centers [17-28].

Supramolecular metal complexes are formed by self-assembly method and weak intermolecular forces such as hydrogen bonding, π-π stacking, CH-π interaction play an important role in the assembly process [29-30]. Pseudohalides are important bridging ligand and among the pseudohalides, there are many reports on the role of intermolecular forces in the crystal packing of supramolecular complexes with azide [31-32] and thiocyanate as bridging ligand [33], but 1D and 2D crystal packing with cyanate bridging ligand is very limited [34-35].

We are interested to study the coordination behavior of thiocyanate and isocyanate ions with different transition metal ions in presence of tetradentate N_4-coordinated ligand *N,N*-bis(3,5-dimethyl-*1H*-pyrazol-1-yl)methyl-N_2-phenylethane-1,2-diamine (bdpab). In this chapter, we describe the syntheses and characterizations of mononuclear complexes of the type [M(bdpab)(X)]Y, [M = Cu(II), Co(II), Zn(II). X = NCS^-, NCO^-. Y = PF_6^- / ClO_4^-], [M''(bdpab)$(NCS)_2$] [M'' = Ni(II), Co(II)] and binuclear complexes of the type [M'(bdpab)$(NCO)]_2(Y)_2$ where M' = Ni(II), Cd(II). Y = PF_6^- / ClO_4^-. The structures of eight complexes [Cu(bdpab)(NCS)]ClO_4, [Co(bdpab)$(NCS)_2$], [Ni(bdpab)$(NCS)_2$], [Zn(bdpab)(NCS)]PF_6, [Cu(bdpab)(NCO)]PF_6, [Co(bdpab)(NCO)]ClO_4, [Ni(bdpab)($\mu_{1,3}$-NCO)$]_2(ClO_4)_2$ and [Cd(bdpab)($\mu_{1,1}$-NCO)$]_2(ClO_4)_2$ have been solved by single crystal X-ray diffraction studies. Here, two nickel(II) centers in [Ni(bdpab)$(NCO)]_2(ClO_4)_2$ are bridged by double cyanate ion with end-to-end (μ-1,3) coordination mode whereas two cadmium(II) atoms in [Cd(bdpab)$(NCO)]_2(ClO_4)_2$ are bridged by double cyanate ion

with end-on (μ-1,1) coordination mode and for Cu(II) and Co(II) complexes, the cyanate ion is acting as monodentate ligand and bonded with metal ions through nitrogen atom of the cyanate ion. Hydrogen bond and π-π stacking have been observed in the isocyanate containing complexes with perchlorate anion and they are further assembled to form 1D and 2D crystallographic network.

5(A).2. Experimental

5(A).2.1. Materials

NaNCO (Qualigens, India), KNCS, $Co(NO_3)_2.6H_2O$, $Ni(NO_3)_2.6H_2O$, $Zn(NO_3)_2.6H_2O$, $Cd(NO_3)_2.6H_2O$ (Aldrich) were reagent grade and used as received. *N*,*N*-bis(3,5-dimethyl-*1H*-pyrazol-1-yl)methyl-N_2-phenylethane-1,2-diamine (bdpab) was synthesized according to the reported method [36]. Metal perchlorate hexahydrates were prepared by reaction of metal [Ni(II), Co(II), Cd(II) and Zn(II)] carbonate with dilute $HClO_4$ acid and followed by slow evaporation of the solution.

5(A).2.2. Syntheses of complexes

Caution! Transition metal complexes with perchlorate salt, azide ion and organic ligands are potentially explosive. Only a small amount of material should be synthesized and it should be handled with care.

5(A).2.2.1. Synthesis of [Cu(bdpab)(NCS)]ClO_4 (1)

To a stirring solution of $Cu(ClO_4)_2.6H_2O$ (0.185 g, 0.5 mmol) in methanol (10 ml), ligand bdpab (0.176 g, 0.5 mmol) in methanol (10 ml) was added slowly and the colour of the solution changed to light green. After 10 min, KNCS (0.050 g, 0.5 mmol) in aqueous methanol (10 ml) was added and the light green colour solution changed to dark green and the solution was stirred for 4 h at room temperature, filtered and kept for slow evaporation. Green coloured crystalline compound was obtained after 6 days, collected by filtration and dried in vacuum.

Yield. 0.172 g (61%). Found C = 43.88, H = 4.88, N = 17.11%. Anal calc for $C_{21}H_{28}N_7O_4SClCu$: C = 43.98, H = 4.92, N = 17.09%. IR (KBr pellet) cm^{-1} : ν(-NH), 3246 m; ν(NCS^-), 2164 vs ; ν(C = C), 1603 s; ν(C = C) + ν (C = N)/pz ring, 1556 s, 1470 s; ν(ClO_4^-), 1092 br; δ(O–Cl–O), 623 s . UV-Vis spectra: λ_{max}/nm (ε_{max}/$mol^{-1}cm^{-1}$). 669 (152), 400 (943), 274 (3378), 222 (28685). Λ_M ($\Omega^{-1}cm^2\ mol^{-1}$) = 120. μ_{eff} = 1.76 BM.

5(A).2.2.2. Synthesis of [Cu(bdpab)(NCS)]PF_6 (2)

Ligand bdpab (0.176 g, 0.5 mmol) in methanol (10 ml) was added slowly to a stirring solution of $Cu(NO_3)_2.6H_2O$ (0.148 g, 0.5 mmol) in methanol (10 ml) and the colour changed to light green immediately. After 10 min, KNCS (0.050 g, 0.5 mmol) in aqueous methanol (10 ml) was added and the solution became dark green. Finally after 10 min, NH_4PF_6 (0.084 g, 0.5 mmol) in methanol (10 ml) was added. The green solution was stirred for another 4 h at room temperature, filtered and filtrate was kept for slow evaporation at room temperature. Green colour crystals were obtained after six days.

Yield. 0.230 g (73%). Found C = 40.77 , H = 4.52, N = 15.78%. Anal calc for $C_{21}H_{28}N_7SPF_6Cu$: C = 40.74, H = 4.56, N = 15.84%. IR (KBr pellet) cm^{-1}: ν(-NH), 3335 m; ν(NCS^-), 2123 vs ; ν(C = C), 1603 s; ν(C = C) + ν (C = N)/pz ring, 1555 s, 1467 s; ν(PF_6^-), 841 s. UV-Vis spectra: λ_{max}/nm (ε_{max} /$mol^{-1}cm^{-1}$). 669 (165), 400 (831), 274 (2865), 221 (34317). Λ_M ($\Omega^{-1}cm^2\,mol^{-1}$) = 120. μ_{eff} = 1.76 BM.

5(A).2.2.3. Synthesis of [Co(bdpab)$(NCS)_2$] (3)

To a stirring solution of $Co(ClO_4)_2.6H_2O$ (0.183 g, 0.5 mmol) in methanol (10 ml), ligand bdpab (0.176 g, 0.5 mmol) in methanol (10 ml) was added slowly and the colour of the solution changed to light pink. Finally after 10 min, KNCS (0.050 g, 0.5 mmol) in aqueous methanol (10 ml) was added and the pink solution was stirred for 4 h at room temperature, filtered and filtrate was kept for slow evaporation at room temperature. Pink colour diffraction quality crystals were obtained from the filtrate after 6 days.

Yield. 0.110 g (43%). Found C = 50.18, H = 5.38, N = 21.15%. Anal calc for $C_{22}H_{28}N_8S_2Co$: C = 50.08, H = 5.35, N = 21.24 %. IR (KBr pellet) cm^{-1}: ν(-NH), 3202 m; ν(NCS^-), 2087, 2057 vs; ν(C = C), 1603 s; ν(C = C) + ν (C = N)/pz ring 1554 s, 1462 s; UV-Vis spectra: λ_{max}/nm (ε_{max}/$mol^{-1}cm^{-1}$). 756 (19), 605 (319), 497 (9913), 331 (2344), 251 (10286). Λ_M ($\Omega^{-1}cm^2\,mol^{-1}$) = 10. μ_{eff} = 4.18 BM.

5(A).2.2.4. Synthesis of [Ni(bdpab)$(NCS)_2$] (4)

The complex was prepared by following the same procedure as for complex **3** except nickel perchlorate was used instead of cobalt perchlorate.

Yield. 0.120 g (46%). Found C = 50.20, H = 5.36, N = 21.30%. Anal calc for $C_{22}H_{28}N_8S_2Ni$: C = 50.11, H = 5.35, N = 21.24%. IR (KBr pellet) cm^{-1}: ν(-NH), 3294 m; ν(NCS^-), 2100, 2063 vs; ν(C = C), 1601 s; ν(C = C) + ν (C = N)/pz ring 1557 s, 1463 s ; UV-Vis spectra: λ_{max}/nm (ε_{max}/$mol^{-1}cm^{-1}$). 980 (28), 594 (17), 286 (1018), 249 (10503). Λ_M ($\Omega^{-1}cm^2\ mol^{-1}$) = 15. μ_{eff} = 2.78 BM.

5(A).2.2.5. Synthesis of [Zn(bdpab)(NCS)]ClO_4 (5)

The complex was prepared by following the same procedure as for complex **1** except zinc perchlorate was used instead of copper perchlorate**.**

Yield. 0.189 g (67%). Found C = 43.72, H = 4.86, N = 17.18%. Anal calc for $C_{21}H_{28}ClN_7O_4SZn$: C = 43.83, H = 4.90, N = 17.04%. IR (KBr Pellet) cm^{-1}: ν(-NH), 3276 m; ν(NCS^-), 2103 vs; ν(C = C), 1600 s; ν(C = C) + ν (C = N)/pz ring, 1554 s, 1469 s; ν_{asmy}(Cl–O), 1103 br; δ(O–Cl–O), 623 s. λ_{max}/nm (ε_{max}/$mol^{-1}cm^{-1}$). 298 (1212), 222 (17694). Λ_M ($\Omega^{-1}cm^2\ mol^{-1}$) = 122.

5(A).2.2.6. Synthesis of [Zn(bdpab)(NCS)]PF_6 (6)

The complex was prepared by following the same procedure as for complex **2** except zinc nitrate was used instead of copper nitrate**.**

Yield. 0.218 g (70%). Found C = 40.75, H = 4.54, N = 15.54%. Anal calc for $C_{21}H_{28}N_7F_6SPZn$: C = 40.62, H = 4.55, N = 15.79%. IR (KBr pellet) cm^{-1}: ν(-NH), 3300 m; ν(NCS^-), 2100 vs; ν(C = C), 1600 s; ν(C = C) + ν (C = N)/pz ring, 1556 s, 1470 s; ν(PF_6^-), 843 s. UV-Vis spectra: λ_{max}/nm (ε_{max}/$mol^{-1}cm^{-1}$). 298 (1024), 222 (19752). Λ_M ($\Omega^{-1}cm^2\ mol^{-1}$) = 122.

5(A).2.2.7. Synthesis of [Cu(bdpab)(NCO)]ClO_4 (7)

A methanol solution (10 ml) of copper(II) perchlorate hexahydrate (0.185 g, 0.5 mmol) was added to the methanol solution (10 ml) of ligand bdpab (0.176 g, 0.5 mmol) and the mixture was stirred at room temperature for 10 min to get a clear light green solution. A solution of KNCO (0.034 g, 0.5 mmol) in methanol (10 ml) was added to the solution and the light green colour solution changed to dark green immediately and the solution was stirred for additional 4 h. Filtered the solution and the filtrate was kept for slow evaporation at room temperature. Green crystals were collected after five days, washed with methanol and dried in vacuum.

Yield. 0.210 g (76%). Found C = 45.30, H = 5.08, N = 17.51%. Anal calc for $C_{21}H_{28}ClCuN_7O_5$: C = 45.24, H = 5.06, N = 17.59%. IR (KBr pellet) cm^{-1}: ν(-NH), 3295 m; ν(NCO^-), 2245 vs; ν(C = C), 1604 s; ν(C = C) + ν(C = N)/pz ring, 1557 s, 1476 s; ν(ClO_4^-), 1098 br; δ(O–Cl–O), 622 s. UV-Vis spectra: λ_{max}/nm (ε_{max}/$mol^{-1}cm^{-1}$). 616(297), 555(361), 276(955), 205(6985). Λ_M ($\Omega^{-1}cm^2mol^{-1}$) = 120. μ_{eff} = 1.76 BM.

5(A).2.2.8. Synthesis of [Cu(bdpab)(NCO)]PF_6 (8)

A methanol solution (10 ml) of ligand bdpab (0.176 g, 0.5 mmol) was added drop wise to a methanol solution (10 ml) of $Cu(NO_3)_2.6H_2O$ (0.148 g, 0.5 mmol). The mixture was stirred at room temperature for 10 min, then KNCO (0.034 g, 0.5 mmol) in the same solvent was added slowly. The solution changed from light green to dark green upon the addition of NH_4PF_6 (0.084 g, 0.5 mmol) in methanol. Dark green color solution was stirred for additional 4h at room temperature, filtered and the filtrate was kept for slow evaporation at room temperature. Green crystals were isolated after four days, washed with methanol and dried.

Yield. 0.270 g (75%). Found C = 41.77, H = 4.62, N = 16.40%. Anal calc for $C_{21}H_{28}CuF_6N_7OP$: C = 41.83, H = 4.68, N = 16.26%. IR (KBr pellet) cm^{-1}: ν(-NH), 3296 m; ν(NCO^-), 2239 vs ; ν(C = C), 1603 s; ν(C = C) + ν (C = N)/pz ring, 1556 s, 1475 s; ν(PF_6^-), 848 s. UV-Vis spectra: λ_{max}/nm (ε_{max}/$mol^{-1}cm^{-1}$). 615(285), 554(345), 271(1132), 206(7309). Λ_M ($\Omega^{-1}cm^2\,mol^{-1}$) = 122. μ_{eff} = 1.74 BM.

5(A).2.2.9. Synthesis of [Co(bdpab)(NCO)]ClO_4 (9)

The complexes was prepared by following the same procedure as for complex **7** except cobalt(II) perchlorate was used in the place of copper(II) perchlorate. Dark pink color block shape crystals were obtained after few days.

Yield. 0.200 g (72%). Found C = 45.88, H = 5.08, N = 17.65%. Anal calc for $C_{21}H_{28}ClCoN_7O_5$: C = 45.62, H = 5.10, N = 17.73%. IR (KBr pellet) cm^{-1}: ν(-NH), 3251 m; ν(NCO^-), 2235 vs; ν(C = C), 1601 s; ν(C = C) + ν (C = N)/pz ring, 1556 s, 1472 s; ν(ClO_4^-), 1100 br; δ(O–Cl–O), 623 s. UV-Vis spectra: λ_{max}/nm (ε_{max}/$mol^{-1}cm^{-1}$). 781(31), 606(224), 485(149), 251(2149), 219(4094). Λ_M ($\Omega^{-1}cm^2mol^{-1}$) = 118. μ_{eff} = 4.36 BM.

5(A).2.2.10. Synthesis of [Co(bdpab)(NCO)]PF_6 (10)

The complex was prepared by following the same procedure as complex **8** except cobalt(II) nitrate was used in the place of copper(II) nitrate. After few days, dark pink color block shape crystals were obtained.

Yield. 0.215 g (71%). Found C = 42.28, H = 4.68, N = 16.30%. Anal calc for $C_{21}H_{28}CoF_6N_7OP$: C = 42.15, H = 4.72, N = 16.39%. IR (KBr pellet) cm^{-1}: ν(-NH), 3297 m; ν(NCO^-), 2239 vs; ν(C = C), 1602 s; ν(C = C) + ν (C = N)/pz ring 1556 s, 1474 s; ν(PF_6^-), 840 s. UV-Vis spectra: λ_{max}/nm (ε_{max}/$mol^{-1}cm^{-1}$). 778(32), 606(237), 485(146), 250(1749), 219(3739). Λ_M ($\Omega^{-1}cm^2\,mol^{-1}$) = 116. μ_{eff} = 4.38 BM.

5(A).2.2.11. Synthesis of [Ni(bdpab)($\mu_{1,3}$ - NCO)]$_2$(ClO_4)$_2$ (11)

The complex was prepared by following the same procedure as for complex **7** except nickel(II) perchlorate was used in the place of copper(II) perchlorate**.** Light blue color plate shape crystals were obtained after few days.

Yield. 0.120 g (44%). Found C = 45.44, H = 5.06, N = 17.62%. Anal calc for $C_{42}H_{56}Cl_2N_{14}Ni_2O_{10}$: C = 45.64, H = 5.11, N = 17.74%. IR (KBr Pellet) cm^{-1}: ν(-NH), 3255 m; ν(NCO^-), 2245 vs; ν(C = C), 1602 s; ν(C = C) + ν (C = N)/pz ring, 1559 s, 1473 s; ν_{asmy}(Cl–O), 1099 br; δ(O–Cl–O), 623 s. UV-Vis spectra: λ_{max}/nm (ε_{max}/$mol^{-1}cm^{-1}$). 1062(50), 598(31), 285(514), 264(1154), 220(5249). Λ_M ($\Omega^{-1}cm^2\,mol^{-1}$) = 122. μ_{eff} = 2.74 BM.

5(A).2.2.12. Synthesis of [Ni(bdpab)($\mu_{1,3}$ - NCO)]$_2$(PF_6)$_2$ (12)

The complex was prepared by following the same procedure as that of complex **8** except nickel(II) nitrate was used in place of copper(II) nitrate**.** After one week, light blue color plate shape crystals were obtained.

Yield. 0.140 g (46%). Found C = 42.51, H = 4.68, N = 16.54%. Anal calc for $C_{42}H_{56}F_{12}N_{14}Ni_2O_2P_2$: C = 42.17, H = 4.72, N = 16.39%. IR (KBr pellet) cm^{-1}: ν(-NH), 3298 m; ν(NCO^-), 2243 vs; ν(C = C), 1603 s; ν(C = C) + ν (C = N)/pz ring, 1559 s, 1474 s; ν(PF_6^-), 877 s. UV-Vis spectra: λ_{max}/nm (ε_{max}/$mol^{-1}cm^{-1}$). 1062(53), 592(34), 286(557), 264(1204), 219(5589). Λ_M ($\Omega^{-1}cm^2\,mol^{-1}$) = 120. μ_{eff} = 2.77 BM.

5(A).2.2.13. Synthesis of [Cd(bdpab)($\mu_{1,1}$ - NCO)]$_2$(ClO$_4$)$_2$ (13)

The complex was prepared by following the same procedure as for complex **7** except cadmium(II) perchlorate was used instead of copper(II) perchlorate**.** Colorless needle shape crystals were obtained after one week.

Yield. 0.130 g (43%). Found C = 41.82, H = 4.60, N = 16.28%. Anal calc for $C_{42}H_{56}Cd_2Cl_2N_{14}O_{10}$: C = 41.60, H = 4.65, N = 16.17%. IR (KBr Pellet) cm^{-1}: ν(-NH), 3247 m; ν(NCO$^-$), 2166 vs; ν(C = C), 1603 s; ν(C = C) + ν(C = N)/pz ring, 1561 s, 1465 s; ν_{asmy}(Cl–O), 1107 br; δ(O–Cl–O), 622 s. UV-Vis spectra: λ_{max}/nm (ε_{max}/mol^{-1}cm^{-1}). 252 (2009), 224 (4345). Λ_M (Ω^{-1}cm^{2}mol^{-1}) = 115.

5(A).2.2.14. Synthesis of [Cd(bdpab)($\mu_{1,1}$-NCO)]$_2$(PF$_6$)$_2$ (14)

The complex was prepared by following the same procedure as for complex **8** except cadmium(II) nitrate was used in place of copper(II) nitrate. Colorless needle shape crystals were obtained after one week.

Yield. 0.150 g (45%). Found C = 38.35, H = 4.43, N = 15.14%. Anal calc for $C_{42}H_{56}F_{12}N_{14}Cd_2O_2P_2$: C = 38.69, H = 4.33, N = 15.04%. IR (KBr pellet) cm^{-1}: ν(-NH), 3303 m; ν(NCO$^-$), 2164 vs; ν(C = C), 1602 s; ν(C = C) + ν(C = N)/pz ring, 1558 s, 1464 s; ν(PF$_6^-$), 853 s. UV-Vis spectra: λ_{max}/nm (ε_{max}/mol^{-1}cm^{-1}). 252 (2559), 224 (4164). Λ_M (Ω^{-1}cm^2 mol^{-1}) = 118.

5(A).3. X-ray Crystallography

The crystallographic data, details of data collection and some important features of the refinement for the compounds **1**, **3, 4, 6**, **8, 9, 11** and **13** are given in Table **5(A).1**. Selected bond lengths and angles are given in Table 5(A).2 for compounds **1**, **3, 4** and **6** and Table 5(A).4 for complexes **8, 9, 11** and **13**. Crystals of suitable size were obtained by slow evaporation of methanol solution at ambient temperature. Intensity data were collected with Mo-K$_\alpha$ radiation (λ = 0.71073Å) for complexes **1**,**6**, **8**, **11** and **13** at 110 K and for complex **9** at room temperature and with Cu-K$_\alpha$ radiation (λ = 1.541841 Å) at 293 K for complexes **3** and **4**, respectively on Oxford X-CALIBUR-S diffractometer equipped with CCD area detector. The data interpretations were processed with CrysAlisPro, Agilent Technologies, Version 1.171.35.19 to give 5698, 4999, 4942, 6202, 6680, 6750, 6533, 6386 independent

reflections [37] and an absorption correction based on multi-scan method was applied [38]. The structures were solved by direct methods and refined by the full-matrix least-square based on F^2 technique using SHELXL-97 program package [39]. All calculations were carried out using WinGX system Ver-1.64 [40]. All non-hydrogen atoms were refined anisotropically. The data were collected up to 2θ angle between 6.08 and 58.28°. The positions of the hydrogen atoms were calculated from the difference Fourier map.

Table.5(A).1. Crystallographic parameters of the complexes **1**, **3**, **4** and **6.**

	[Cu(bdpab)(NCS)]ClO_4 (1)	**[Co(bdpab)$(NCS)_2$] (3)**	**[Ni(bdpab)$(NCS)_2$] (4)**	**[Zn(bdpab)(NCS)]PF_6 (6)**
Empirical formula	$C_{21}H_{28}N_7O_4SClCu$	$C_{22}H_{28}N_8S_2Co$	$C_{22}H_{28}N_8S_2Ni$	$C_{21}H_{28}N_7F_6SPZn$
Formula weight	573.55	527.57	527.33	620.91
Temperature (K)	110(30)	293(2)	293(2)	110(20)
Wavelength (Å)	0.71073	1.5418	1.5418	0.7107
Crystal system	triclinic	monoclinic	monoclinic	triclinic
Space group	*P-1*	*P21/c*	*P21/c*	*P-1*
a (Å)	8.8362(6)	9.3763(3)	9.37190(10)	8.1369(2)
b (Å)	11.7282(9)	13.3292(5)	13.2352(2)	9.6492(3)
c (Å)	13.3129(10)	19.9912(6)	19.8887(3)	17.4289(5)
α, (°)	105.230(7)	90.00	90.00	88.262(2)
β(°)	99.722(6)	92.187(3)	92.0170(10)	78.742(2)
γ (°)	103.060(6)	90.00	90.00	72.868(3)
Volume ($Å^3$)	1257.95(16)	2496.65(14)	2465.44(6)	1282.00(6)
Z	2	4	4	2
Density (g cm^{-3})	1.514	1.419	1.421	1.608

Absorption coefficient (mm^{-1})	1.100	7.165	2.933	1.171
F(000)	594.0	1104.0	1104.0	636.0
θ range for data collection (°)	6.18 to 58.06	7.98 to 146.52	8.02 to 146.3	6.26 to 58.08
Index ranges	$-12 \le h \le 11$,	$-10 \le h \le 11$,	$-11 \le h \le 11$,	$-11 \le h \le 11$,
	$-15 \le k \le 14$,	$-16 \le k \le 16$,	$-14 \le k \le 16$,	$-13 \le k \le 13$,
	$-15 \le l \le 17$	$-17 \le l \le 24$	$-22 \le l \le 24$	$-23 \le l \le 23$
Reflections collected	10790	15143	14793	27630
Independent reflections	5698	4999	4942	6202
	[R(int) = 0.0447]	[R(int) = 0.0745]	[R(int) = 0.0423]	[R(int) = 0.0293]
Data / restraints / parameters	5698/0/320	4999/0/302	4942/0/302	6202/0/338
Goodness-of-fit on F^2	1.044	1.016	1.063	1.053
Final R indices [*I*>2sigma(*I*)]	R1 = 0.0604,	R1 = 0.0615,	R1 = 0.0540,	R1 = 0.0422,
	wR2 = 0.1311	wR2 = 0.1360	wR2 = 0.1492	wR2 = 0.1143
R indices (all data)	R1 = 0.0840,	R1 = 0.1126,	R1 = 0.0612,	R1 = 0.0451,
	wR2 = 0.1419	wR2 = 0.1580	wR2 = 0.1565	wR2 = 0.1161
Largest diff. peak and hole (eA^{-3})	0.62 and -0.65	0.33 and -0.34	0.73 and -0.52	1.08 and -1.05
CCDC number	1414730	1052245	1052244	1414733

Table.5(A).1. Crystallographic parameters of the complexes **8**, **9**, **11** and **13.**

	[Cu(bdpab)(NCO)]PF_6 (8)	**[Co(bdpab)(NCO)]ClO_4 (9)**	**[Ni(bdpab)($\mu_{1,3}$-NCO)]$_2$(ClO_4)$_2$ (11)**	**[Cd(bdpab)($\mu_{1,1}$-NCO)]$_2$(ClO_4)$_2$ (13)**
Empirical formula	$C_{21}H_{28}ClCuF_6N_7OP$	$C_{21}H_{28}ClCoN_7O_5$	$C_{42}H_{56}Cl_2N_{14}Ni_2O_{10}$	$C_{42}H_{56}Cd_2Cl_2N_{14}O_{10}$
Formula weight	603.01	552.89	1105.29	1212.73
Temperature (K)	110(2)	293(2)	110(30)	110(2)
Wavelength (Å)	0.71073	0.71073	0.71073	0.71073
Crystal system	monoclinic	triclinic	triclinic	triclinic
Space group	*P 2$_1$/n*	*P-1*	*P-1*	*P-1*
a (Å)	14.5026(7)	9.1081(3)	9.2032(9)	9.2412(5)
b (Å)	9.0618(4)	11.0972(3)	10.7578(10)	11.0814(4)
c (Å)	19.5310(13)	13.4281(5)	13.4463(11)	13.3876(7)
α, (°)	90.00	103.618(3)	103.378(7)	108.019(4)
β(°)	103.427(6)	98.385(3)	99.612(7)	98.407(4)
γ (°)	90.00	103.584(3)	104.920(8)	106.622(4)
Volume (Å^3)	2496.6(2)	1252.80(8)	1214.6(2)	1207.10(10)
Z	4	2	1	1

Density (g cm^{-3})	1.604	1.4655	1.5110	1.668
Absorption coefficient (mm^{-1})	1.014	0.838	0.956	1.063
F(000)	1236.0	574.0	576.0	616.0
θ range for data collection (°)	6.22 to 58.08	6.08 to 58.28	6.32 to 58.2	6.18 to 57.9
Index ranges	$-19 \le h \le 19$, $12 \le k \le 7$, $-24 \le l \le 23$	$-12 \le h \le 12$, $-15 \le k \le 15$, $-18 \le l \le 18$	$-7 \le h \le 12$, $-14 \le k \le 14$, $-18 \le l \le 18$	$-12 \le h \le 11$, $-15 \le k \le 13$, $-18 \le l \le 18$
Reflections collected	14043	27473	9965	9877
Independent reflections	6680 [R_{int} = 0.0323]	6750 [R_{int} = 0.0393]	6533 [R_{int} = 0.0552]	6386 [R_{int} = 0.0358]
Data / restraints / parameters	6680/0/338	6750/0/323	6533/0/323	6386/0/320
Goodness-of-fit on F^2	1.062	0.828	1.015	1.087
Final R indices [*I*>2sigma(*I*)]	R_1 = 0.0523, wR_2 = 0.1286	R_1 = 0.0513, wR_2 = 0.1470	R_1 = 0.0616, wR_2 = 0.1452	R_1 = 0.0468, wR_2 = 0.1102
R indices (all data)	R_1 = 0.0762, wR_2 = 0.1430	R_1 = 0.0767, wR_2 = 0.1745	R_1 = 0.0937, wR_2 = 0.1659	R_1 = 0.0600, wR_2 = 0.1178
Largest diff. peak and hole (eA^{-3})	0.66 and -0.53	0.62 and -0.38	1.17 and -1.12	1.63 and -0.66
CCDC number	1430122	1430124	1430128	1430125

5(A).4. Results and Discussions

5(A).4.1. Syntheses

Five coordinated eight mononuclear complexes of the type [M(bdpab)(X)]Y [M = Cu(II), Co(II), Zn(II), X = NCS^-/NCO^-, Y = PF_6^-, ClO_4^-.] were obtained in good yield by treating appropriate mole ratio of metal perchlorate, ligand bdpab, KNCO/KSCN [for Y = ClO_4^-] or metal nitrate, ligand bdpab, KNCO/KSCN and PF_6^- [for Y = PF_6^-] in methanol at room temperature. Reactions of copper(II), cobalt(II) and zinc(II) salts with isocyanate/thiocyanate and ligand bdpab in different mole ratios and in different solvents always lead to the formation of complexes of the type [M(bdpab)(X)]Y. Six coordinated two mononuclear complexes of the type [M''(bdpab)$(NCS)_2$] [M'' = Co(II), Ni(II)] were synthesized by 1:1:1 molar ratio of metal perchlorate, ligand bdpab and NCS^- ion in methanol solution at room temperature. Four octahedral binuclear double NCO bridged complexes of the type [M'(bdpab)(μ-NCO)]$_2$$(Y)_2$ [M'= Ni(II) and Cd(II), Y = PF_6^-, ClO_4^-] were obtained in good yield by treating appropriate mole ratio of metal perchlorate, ligand bdpab, KNCO [for Y = ClO_4^-] or metal nitrate, ligand bdpab, KNCO and PF_6^- [for Y = PF_6^-] in methanol at room temperature [Scheme 5(A).1]. There is no change of composition of Ni(II) and Cd(II) complexes by adding excess KNCO salt. The molecular composition of the complexes confirmed by microanalysis, solution conductivity, spectral data and finally by single crystal X-ray diffraction studies. The micro analysis results are in good agreement with compositions of the complexes. The structure of the complexes **1**, **3, 4, 6**, **8, 9, 11** and **13** were determined by single crystal X-ray diffraction studies. Structural data reveal that NCS containing complexes **1**, **3, 4** and **6** are mononuclear, among them Cu(II) and Zn (II) complexes are five coordinated and Ni(II) and Co(II) complexes are six coordinated and NCO containing Cu(II) and Co(II) complexes **8** and **9** are penta-coordinated with distorted square pyramidal geometry and binuclear Ni(II) and Cd(II) complexes **11** and **13** have six coordination with distorted octahedral geometry. For binuclear Ni(II) complex, ligand NCO bridges the two nickel centers with end-to-end (μ-1,3) coordination mode whereas for Cd(II) complex, ligand NCO bridges the two cadmium centers with double end-on (μ-1,1) coordination mode. Molar conductivity data in MeCN solution (Λ_M ~ 10 $\Omega^{-1}cm^2mol^{-1}$) show all complexes

have 1:1 electrolyte whereas thiocyanate containing cobalt(II) and nickel(II) complexes are non-electrolytes [41]. All the reactions were reproducible and moisture insensitive. All the complexes are soluble in a wide range of common organic solvents such as methanol, acetonitrile, DMF, DMSO but are insoluble in water.

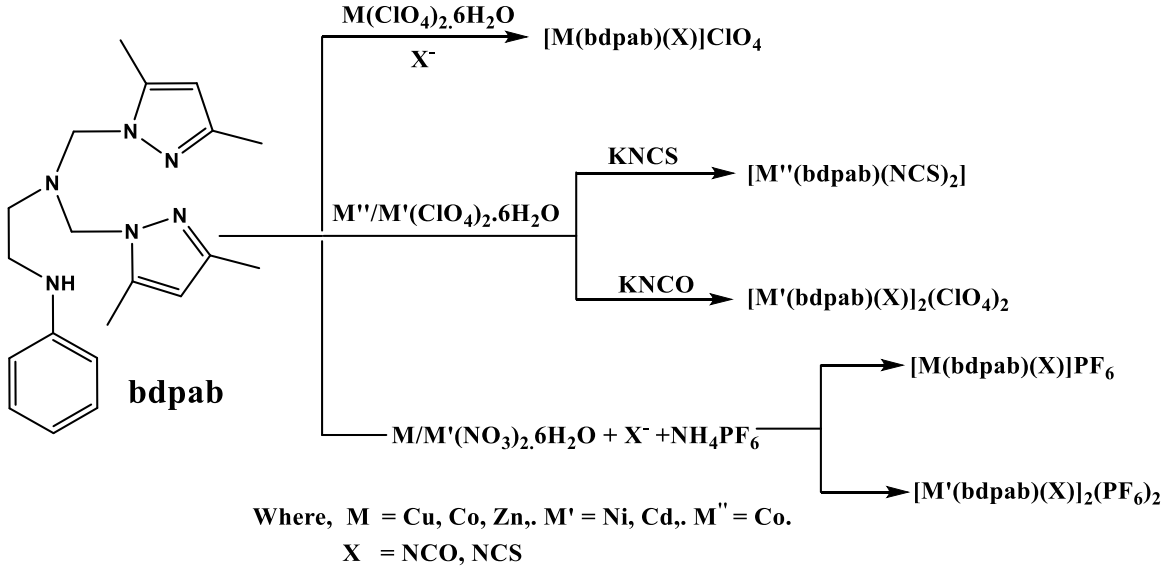

[M(bdpab)X]Y **[M''(bdpab)(NCS)$_2$]**

[Cu(bdpab)(NCS)]ClO$_4$(1) **[Cu(bdpab)(NCS)]PF$_6$(2)** **[Co(bdpab)(NCS)$_2$](3)** **[Ni(bdpab)(NCS)$_2$](4)**

[Zn(bdpab)(NCS)]ClO$_4$(5) **[Zn(bdpab)(NCS)]PF$_6$(6)** **[M'(bdpab)(X)]$_2$(Y)$_2$**

[Cu(bdpab)(NCO)]ClO$_4$(7) **[Cu(bdpab)(NCO)]PF$_6$(8)** **[Ni(bdpab)(NCO)]$_2$(ClO$_4$)$_2$(11)** **[Ni(bdpab)(NCO)]$_2$(PF$_6$)$_2$(12)**

[Co(bdpab)(NCO)]ClO$_4$(9) **[Co(bdpab)(NCO)]PF$_6$(10)** **[Cd(bdpab)(NCO)]$_2$(ClO$_4$)$_2$(13)** **[Cd(bdpab)(NCO)]$_2$(PF$_6$)$_2$(14)**

Scheme 5(A).1. Syntheses of complexes.

5(A).4.2. IR data

IR spectra data of the ligand exhibits a medium intensity band at 3200 cm^{-1} due to *ν*(-NH) and two strong bands at 1553 and 1467 cm^{-1} which are assigned as *ν*(C=C) and *ν*(C=N) due to pyrazole ring. The infrared spectra of all the complexes show two intense bands at ~1561 and ~1465 cm^{-1} due to ν(C=C) + ν(C=N) of pyrazole groups and a medium intensity band at the ~3295 cm^{-1} assigned as ν(-NH) group. All these bands are also present in the ligand molecule but with change of frequencies, indicating the coordination of ligand with the metal ions. The binding mode of NCS^- anion to the metal

centers are confirmed by the strong IR band which occurs above 2000 cm^{-1}. The CN stretching vibration for N-bonded SCN^- ion usually appears below 2100 cm^{-1} and that of S-bonded thiocyanate appear above 2100 cm^{-1} [42-43]. The complexes **1**, **2**, **5** and **6** show one intense band at ~ 2100 cm^{-1} and complexes **3** and **4** show two intense bands at less than 2100 cm^{-1} indicating the presence of N-bonded thiocyanate group present in the complexes. The coordination mode of the cyanate anion in the transition metal complexes is detected by the strong infrared band due to *ν*(NCO) which occurs above 2100 cm^{-1}. The asymmetric stretch of (μ-1,1) bridging *ν*(NCO) shows at lower frequencies than the (μ-1,3) bridging *ν*(NCO) or terminal NCO [44-45]. Complexes **7** and **8** show broad band at 2245 and 2239 cm^{-1} respectively, whereas complexes **9** and **10** exhibits broad band at 2235 and 2239 cm^{-1} respectively, confirming the coordination of terminal N bonded NCO in the complexes. For complexes **11** and **12** with end-to-end (μ-1,3) bridging mode, the ν(NCO) bands appeared at 2245 cm^{-1} and 2243 cm^{-1} whereas the *ν*(NCO) band with end-on (μ-1,1) bridging mode exhibited at ~ 2165 cm^{-1} for the complexes **13** and **14**. These data support the versatile coordination modes of NCO group in the complexes. Nature of the coordination mode of cyanate ligand in the complexes is also confirmed by the crystal structure determination of the complexes. The IR spectra of complexes **1, 5, 7, 9, 11** and **13** exhibited two bands: one broad band at ~ 1100 cm^{-1} due to ν_{asmy}(Cl-O) and a band at ~ 623 cm^{-1} due to δ(O-Cl-O), confirming the presence of perchlorate ion outside the coordination sphere in the complexes. Similarly, one strong band at ~ 844 cm^{-1} due to ν(PF_6^-) indicating the presence of counter anion for complexes **2, 6, 8, 10, 12** and **14**. For complexes **3** and **4** no bands were observed at 1100 or at 844 cm^{-1} indicating the absence of ClO_4^- or PF_6^- ion as counter anion in the complexes and the molecules are nonionic [46].

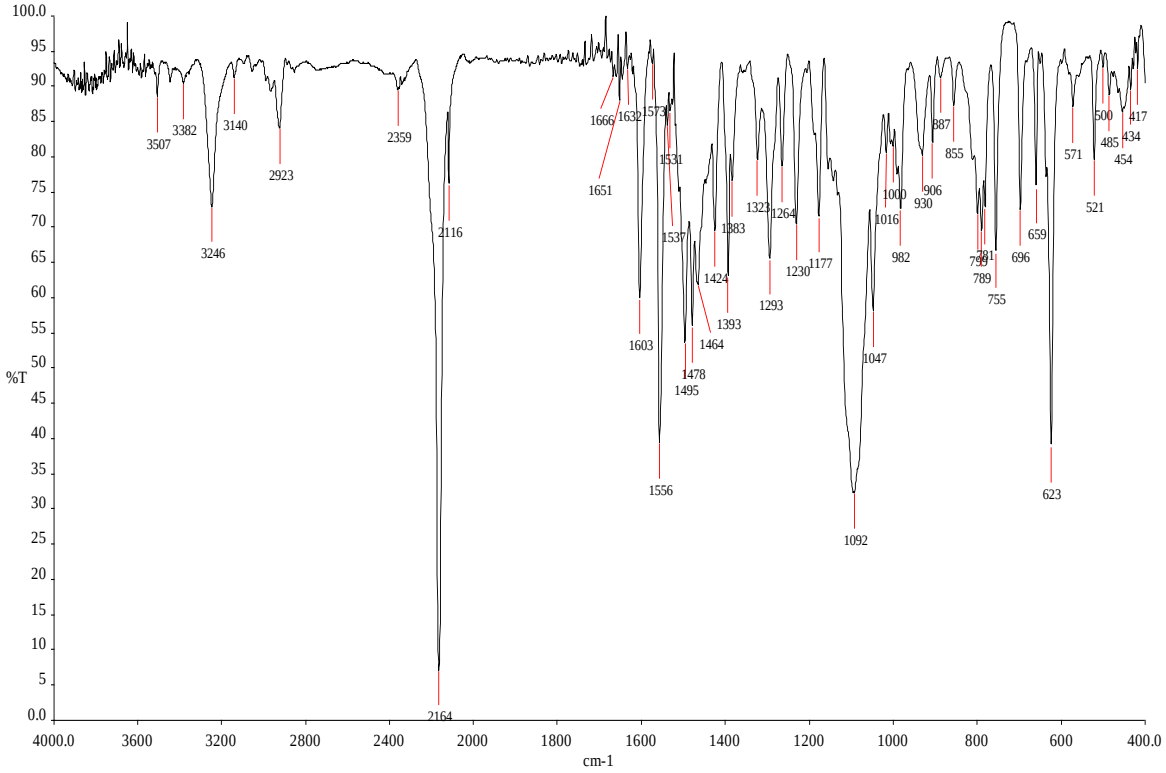

Fig.5(A).1. IR spectrum of [Cu(bdpab)(NCS)]ClO_4 (**1**).

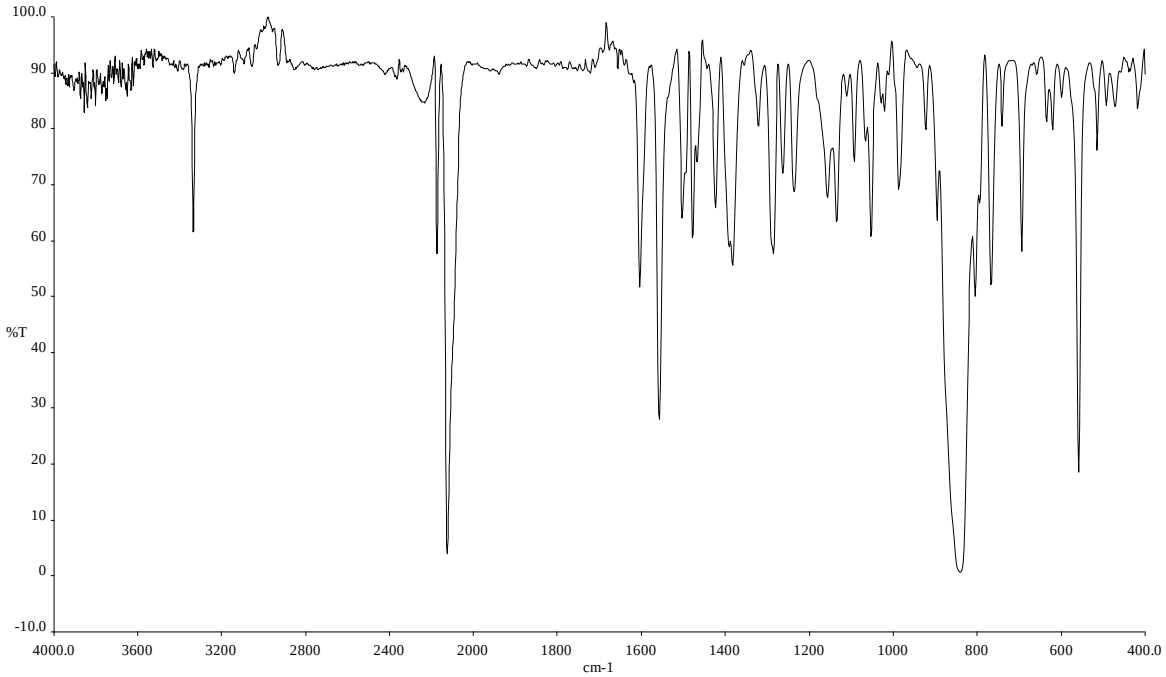

Fig.5(A).2. IR spectrum of [Cu(bdpab)(NCS)]PF_6 (**2**).

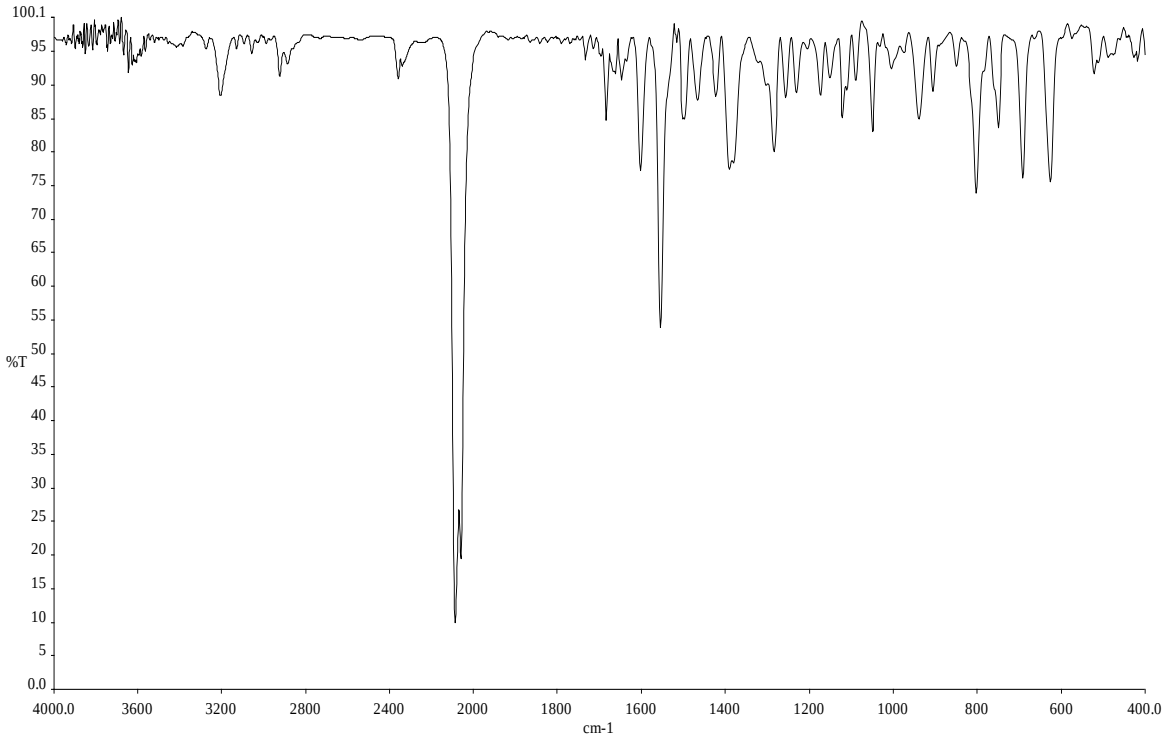

Fig.5(A).3. IR spectrum of [Co(bdpab)$(NCS)_2$] (**3**).

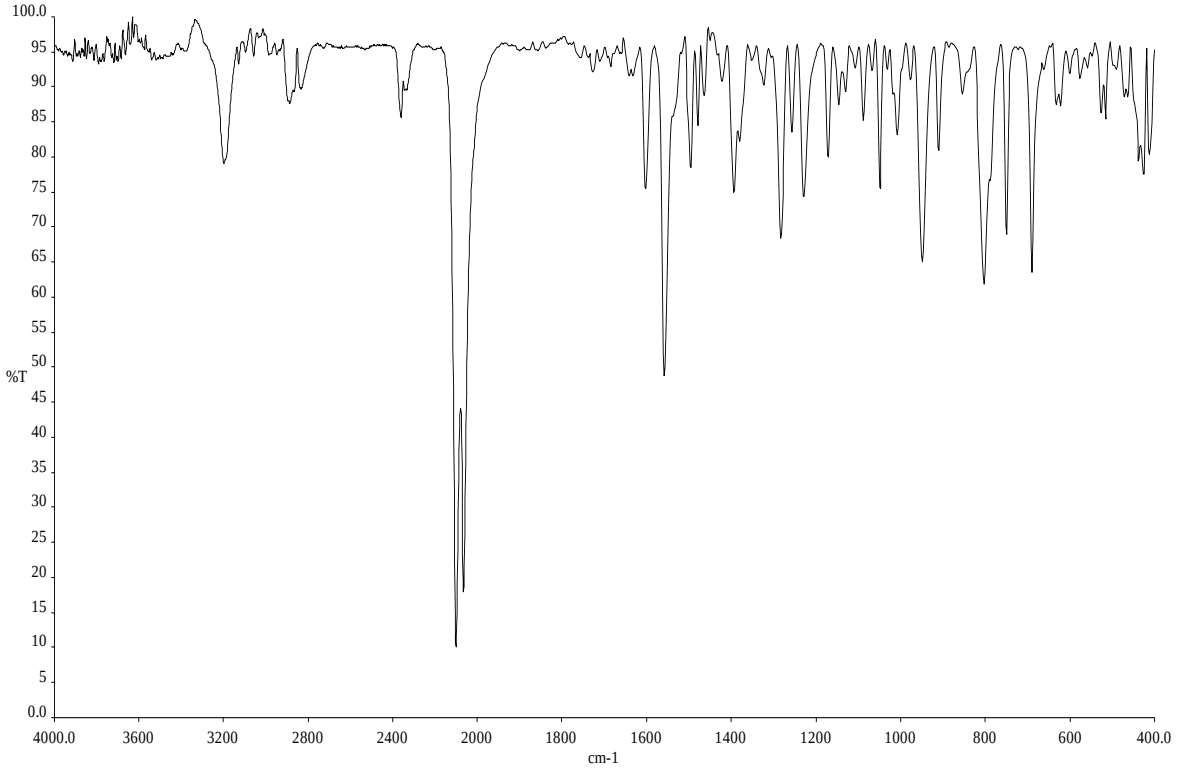

Fig.5(A).4. IR spectrum of [Ni(bdpab)$(NCS)_2$] (**4**).

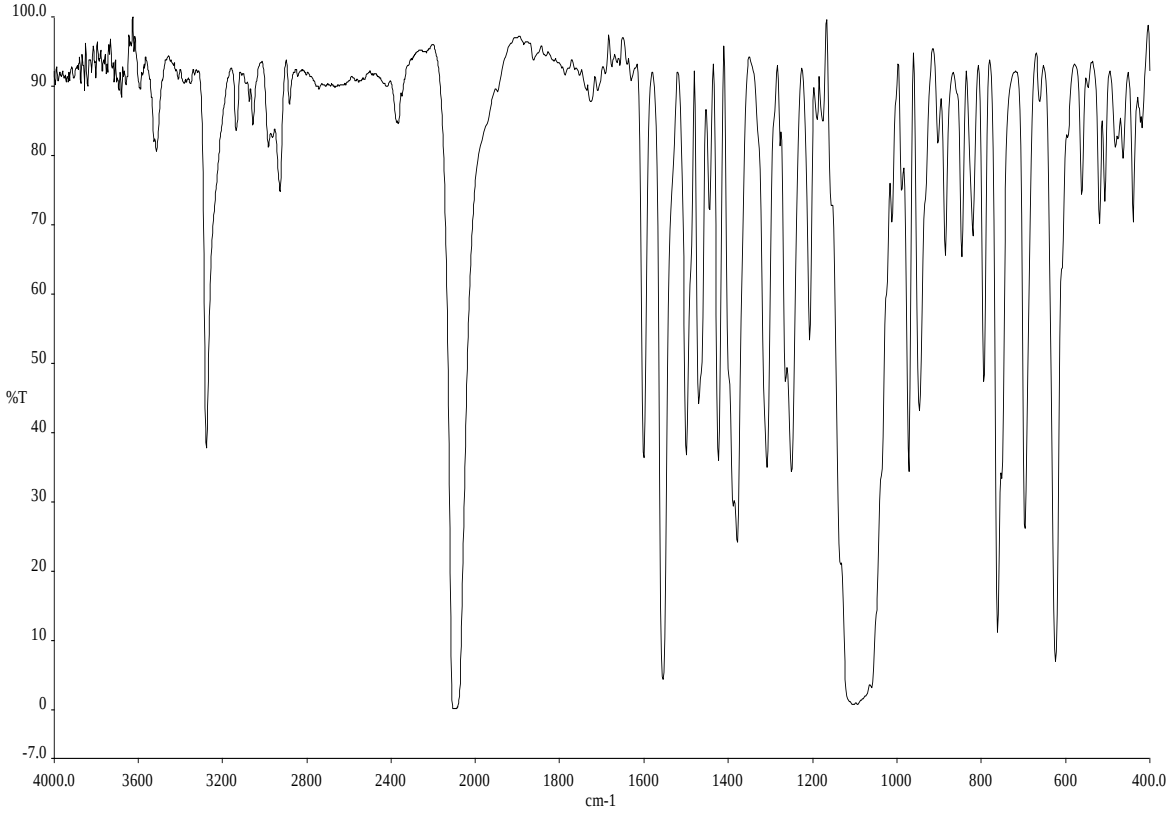

Fig.5(A).5. IR spectrum of $[Zn(bdpab)(NCS)]ClO_4$ (**5**).

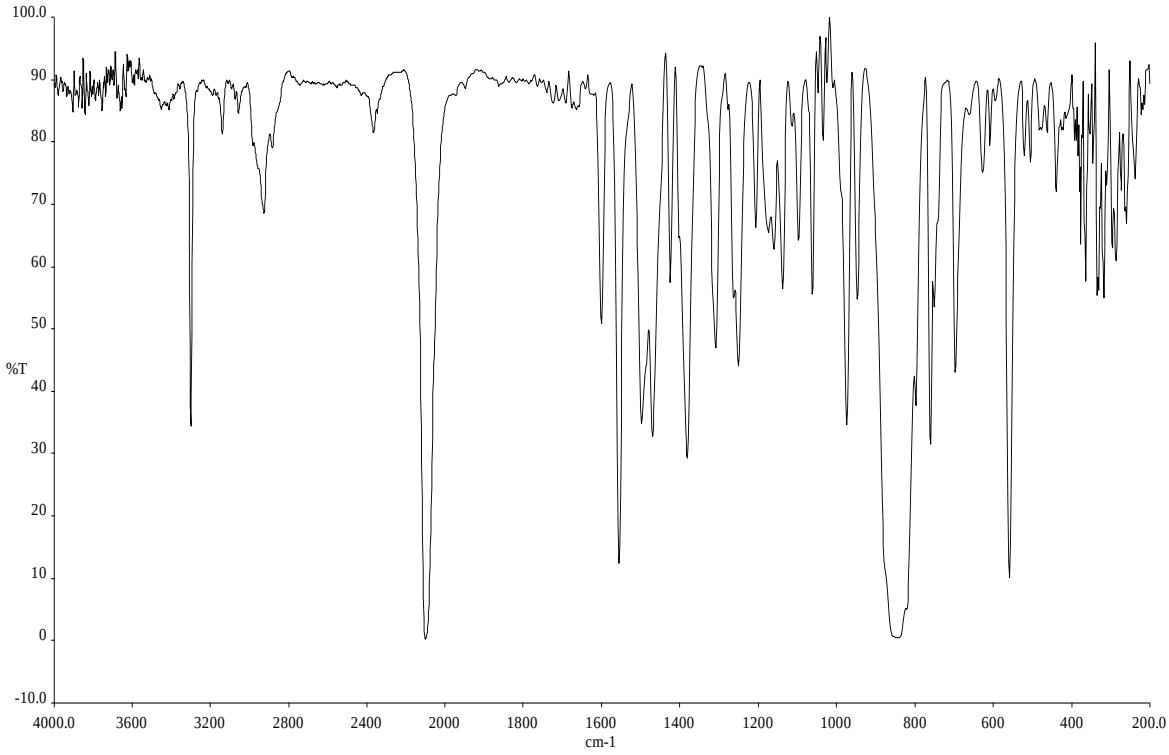

Fig.5(A).6. IR spectrum of $[Zn(bdpab)(NCS)]PF_6$ (**6**).

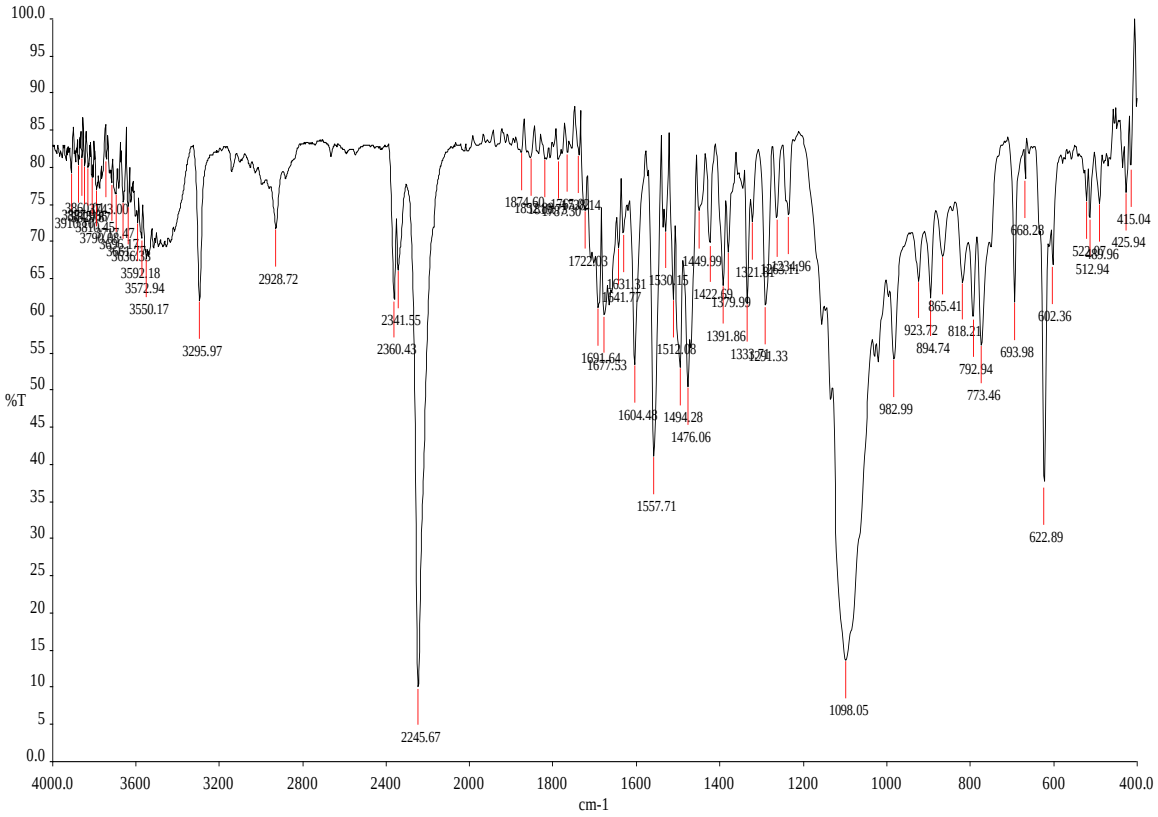

Fig.5(A).7. IR spectrum of [Cu(bdpab)(NCO)]ClO_4 (**7**).

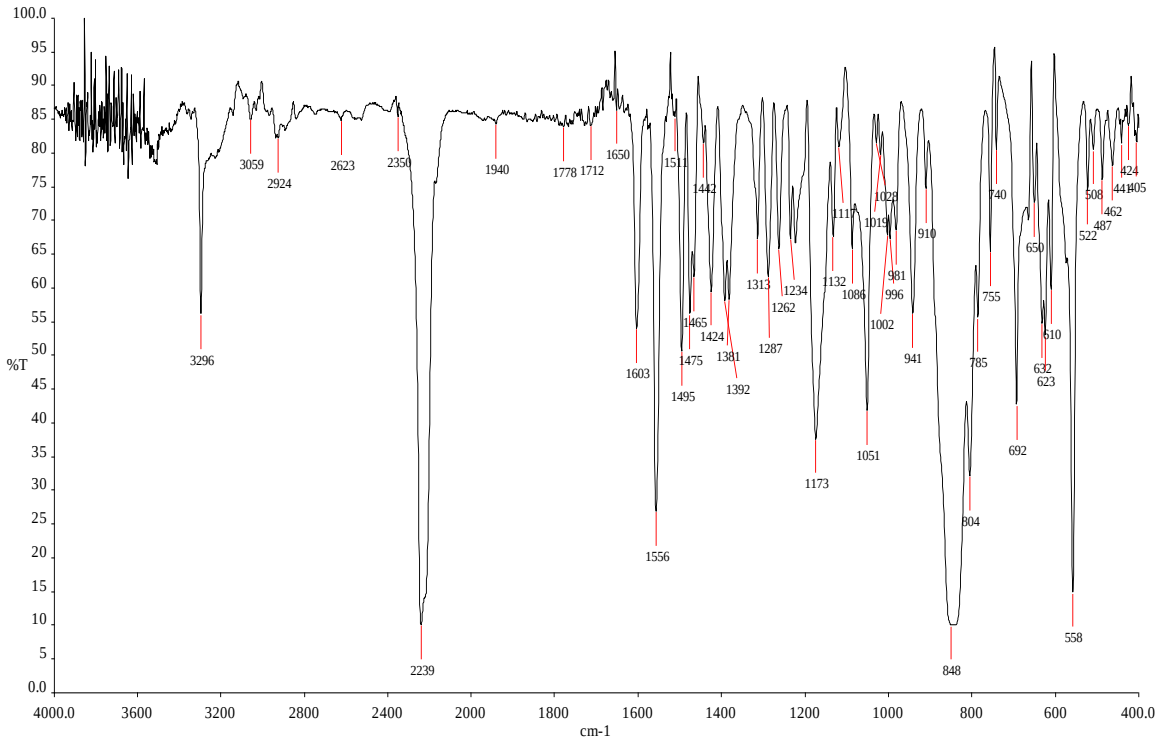

Fig.5(A).8. IR spectrum of [Cu(bdpab)(NCO)]PF_6 (**8**).

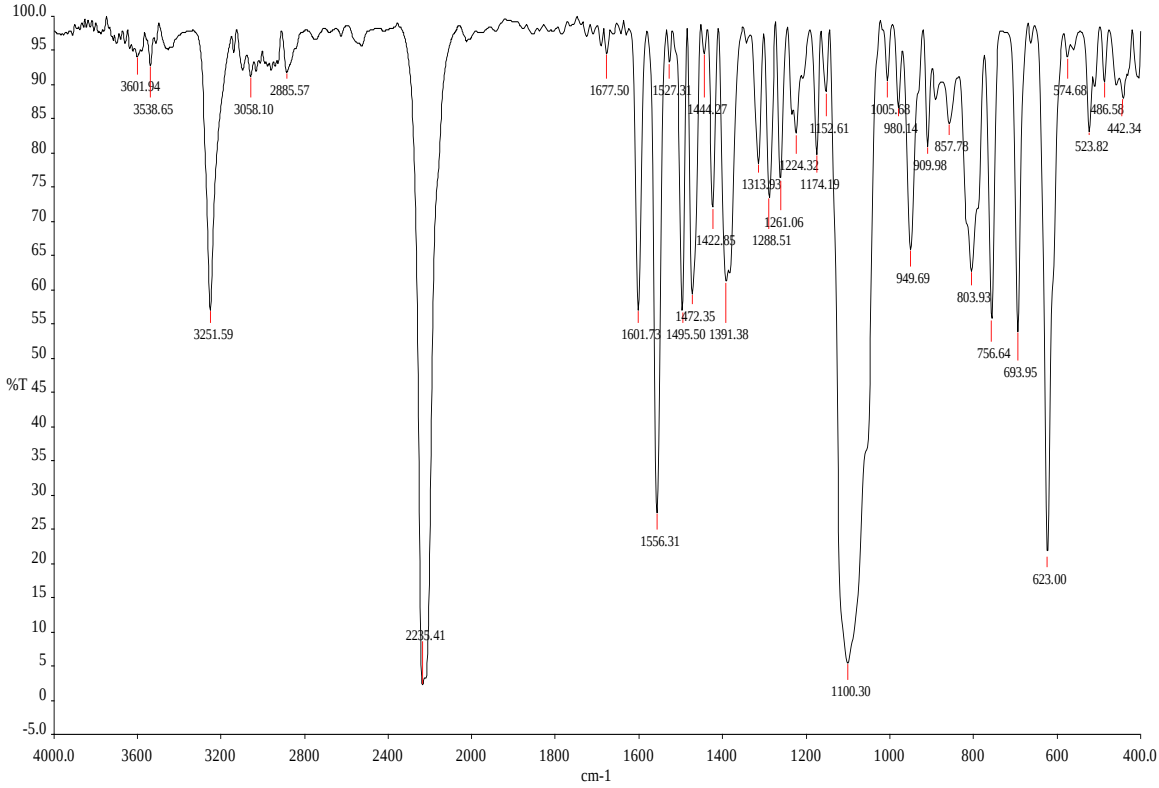

Fig.5(A).9. IR spectrum of [Co(bdpab)(NCO)]ClO_4 (**9**).

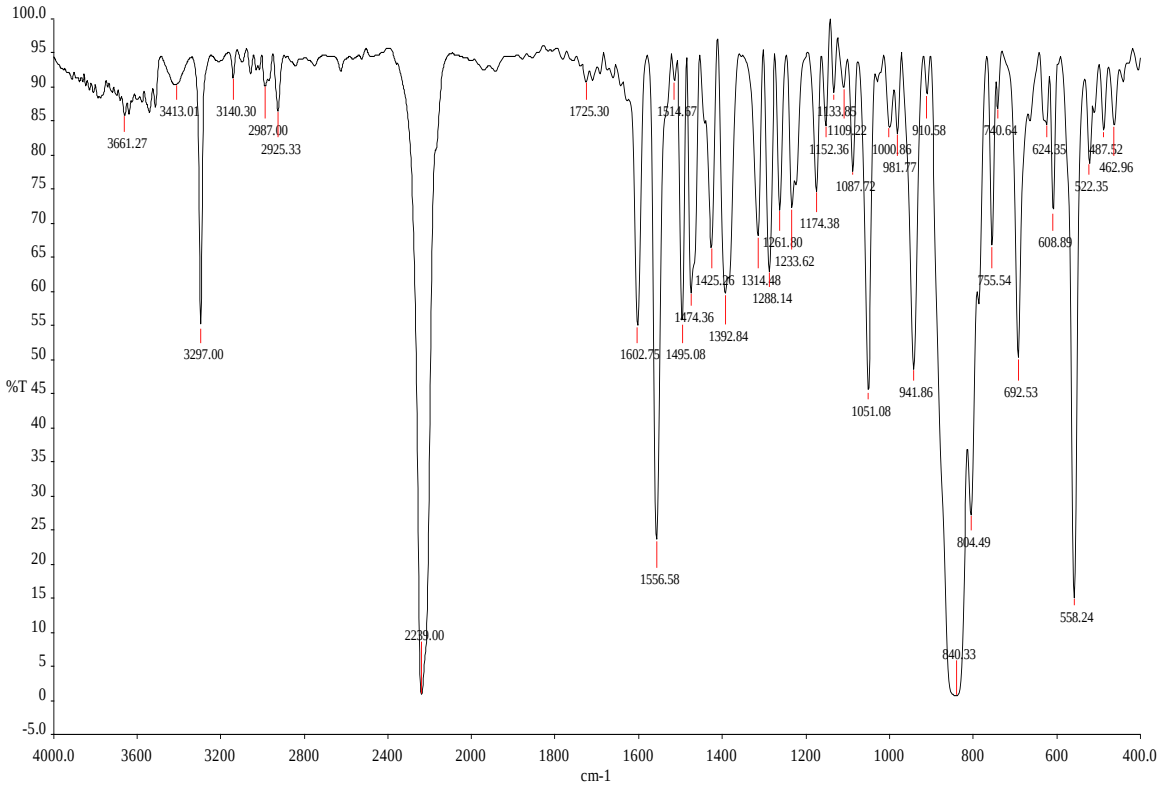

Fig.5(A).10. IR spectrum of [Co(bdpab)(NCO)]PF_6 (**10**).

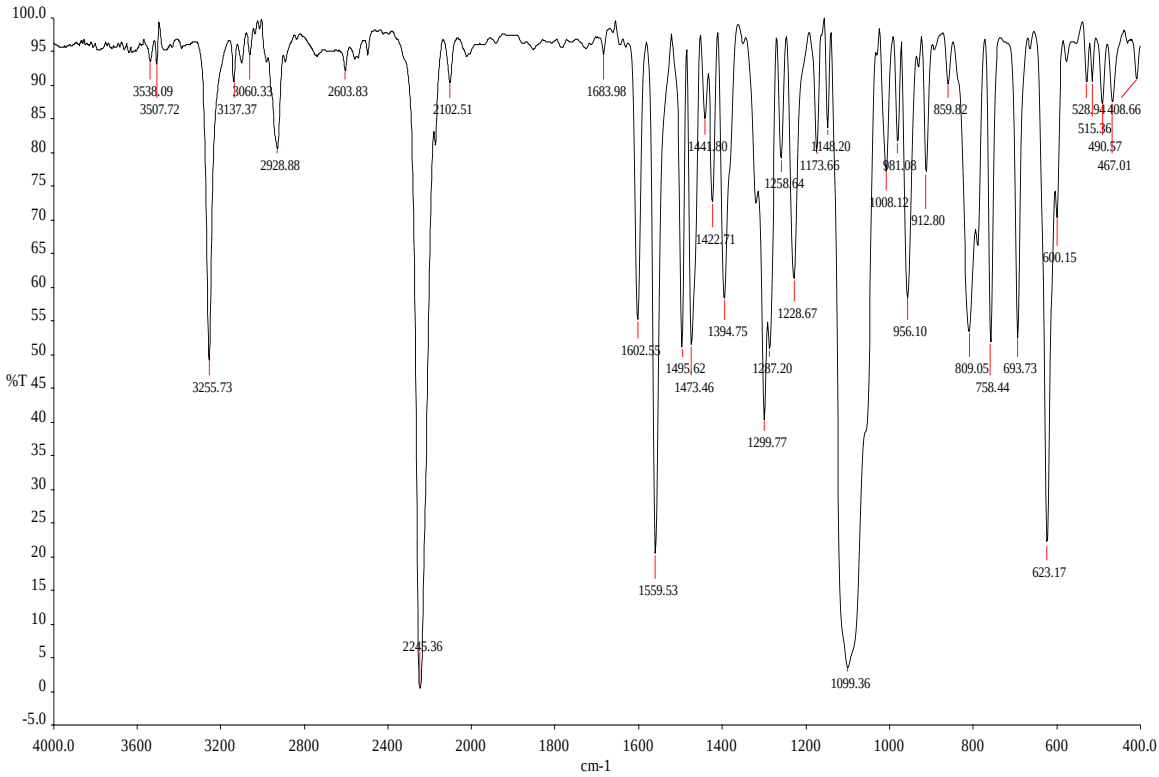

Fig.5(A).11. IR spectrum of $[Ni(bdpab)(\mu_{1,3}\text{-}NCO)]_2(ClO_4)_2$ (**11**).

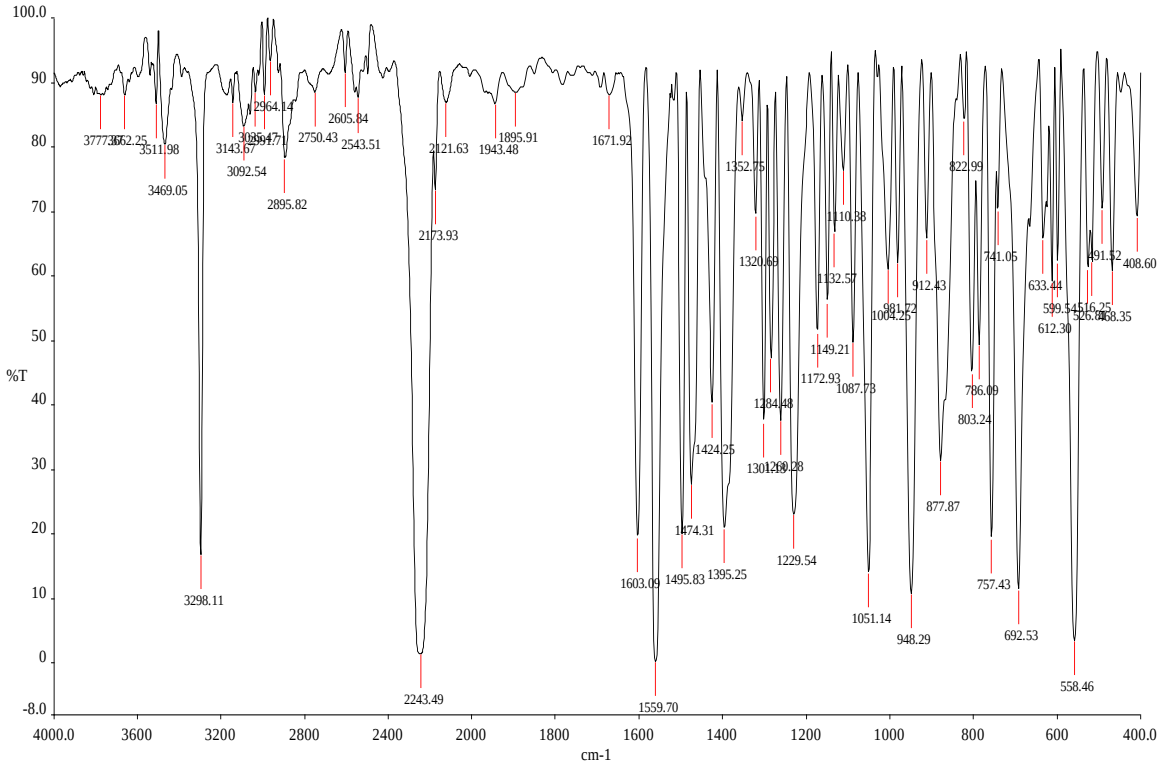

Fig.5(A).12. IR spectrum of $[Ni(bdpab)(\mu_{1,3}\text{-}NCO)]_2(PF_6)_2$ (**12**).

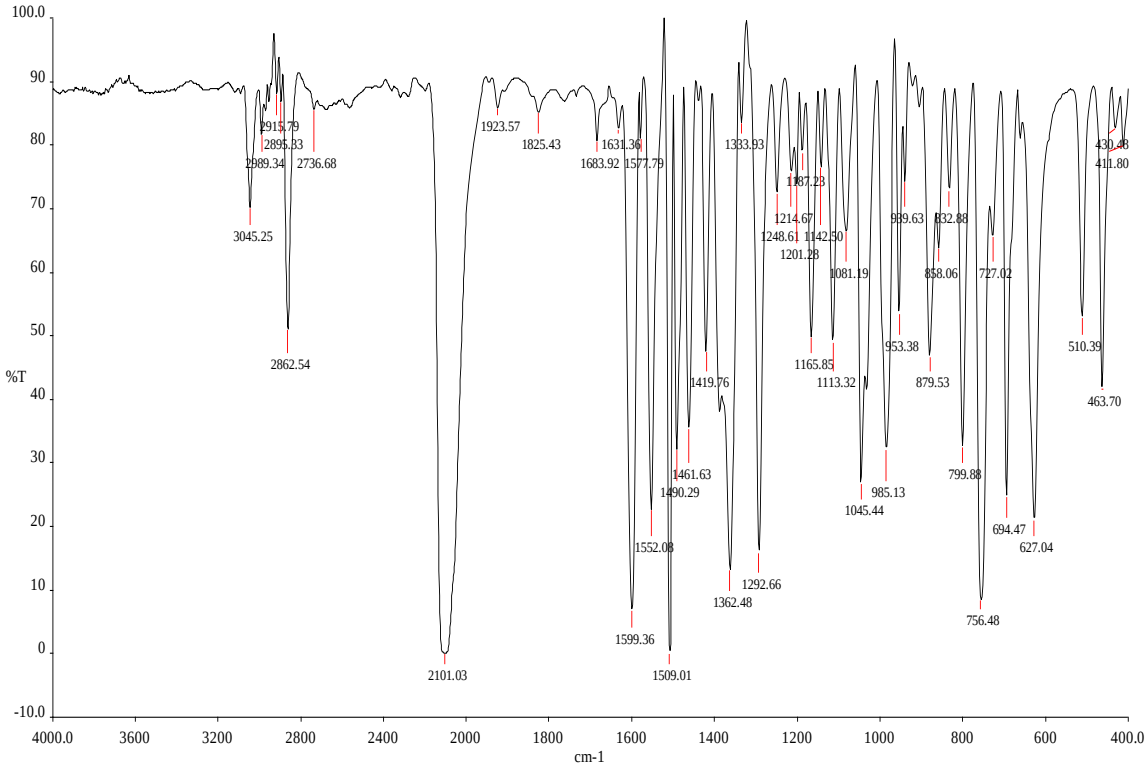

Fig.5(A).13. IR spectrum of [Cd(bdpab)($\mu_{1,1}$-NCO)]$_2$(ClO$_4$)$_2$ (**13**).

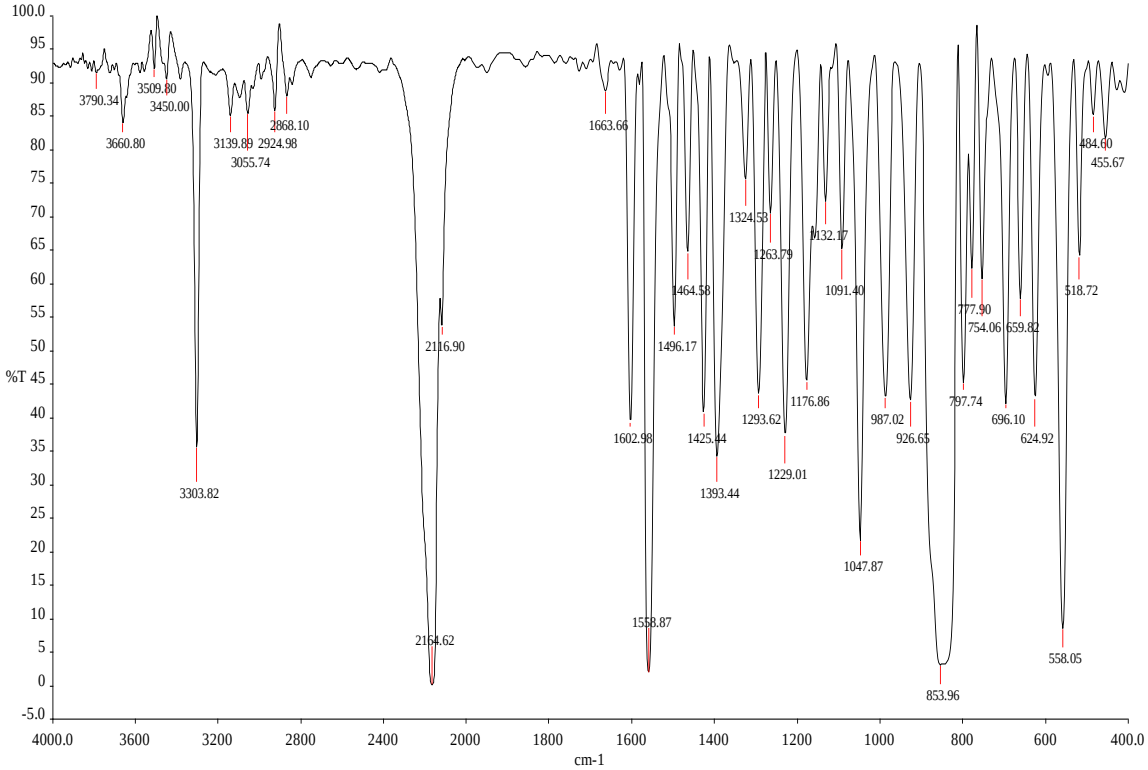

Fig.5(A).14. IR spectrum of [Cd(bdpab)($\mu_{1,1}$-NCO)]$_2$(PF$_6$)$_2$ (**14**).

5(A).4.3. UV-Visible spectra and magnetic data

The UV-Visible spectra of all the complexes were recorded in acetonitrile solution (10^{-3} M). For all complexes the high intensity bands appeared at < 400 nm are due to n-π^* / π-π^* intra ligand charge transfer transition. For copper(II) complexes **1**, **2**, **7** and **8** a broad absorption band observed at ~ 669 nm with molar extinction coefficient ~ 155 $mol^{-1}cm^{-1}$ due to d_{xz}, $d_{yz} \rightarrow d_{x^2-y^2}$ transition. Generally, square pyramidal or distorted square pyramidal Cu(II) complexes show spectral band in the region of 550-670 nm whereas copper(II) complexes with trigonal bipyrmidal geometry shows two bands: one band at $\lambda > 800$ nm (d_{xy}, $d_{x^2-y^2} \rightarrow d_{z^2}$) and a weak transition at higher energy region at $\lambda <$ 750 nm (d_{xy}, $d_{yz} \rightarrow d_{z^2}$). Absence of two spectral bands in the copper(II) complexes also indicate the geometry around copper(II) center is distorted square pyramidal [47-49]. Cobalt(II) complexes **3**, **9**, and **10** shows three absorption bands appeared at ~ 781, ~ 606 and ~ 485 nm and these are either due to d-d or ligand field transitions [50]. Similarly for nickel(II) complexes **4**, **11** and **12,** there are two absorption bands at ~ 1062 and ~ 592 nm with low molar absorption coefficient and these are due to d-d transitions. There is no change of λ_{max} in solution even after 2h indicating no dissociation or change of geometry after dissolution.

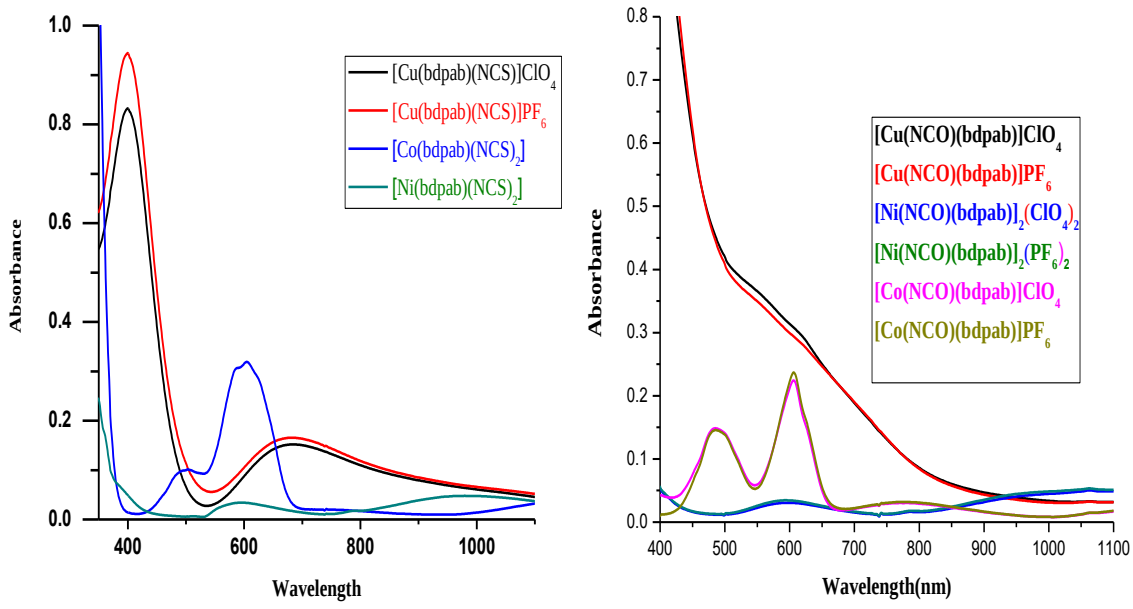

Fig.5(A).15(a). Electronic spectra of complexes in CH_3CN (10^{-3} M).

Room temperature magnetic susceptibility measurements of powder samples of the complexes show all copper(II) complexes have μ_{eff} ~ 1.75 BM indicating one electron paramagnetism, all cobalt(II) complexes have μ_{eff} ~ 4.37 BM indicating three electron paramagnetism and nickel(II) complexes have μ_{eff} ~ 2.75 BM indicating octahedral geometry with two electron paramagnetism of all nickel(II) complexes. Magnetic susceptibility of cobalt(II) complex with tetradentate N_4-coordinate ligand fall in this region [51-52].

5(A).4.4. Description of Crystal Structures

5(A).4.4.1. Crystal structures of [Cu(bdpab)(NCS)]ClO_4 (1) and [Zn(bdpab)(NCS)]PF_6 (6)

The ORTEP diagrams with atom numbering schemes of the complexes **1** and **6** are shown in Fig.5 (A).16(a) and 17, respectively. Both compounds are isostructural and crystallize in the triclinic system with space group *P-1* with MN_5 coordination environment. In both the complexes ligand bdpab acts as tetradentate N_4-coordinated and bonded through one nitrogen atom from secondary amine, one nitrogen atom from tertiary amine and two pyrazole ring's nitrogen atom. In their crystal structures, the metal cations are coordinated by one nitrogen atom from NCS and four nitrogen atoms of the ligand bdpab with a slightly distorted square pyramidal [for Cu(II)] or distorted trigonal bipyramidal [for Zn(II)] geometry.

In complex **1**, the copper(II) ion has adopted distorted square pyramidal geometry as revealed from trigonality index $\tau = 0.31$ [53]. In the equatorial plane, there are three nitrogen atoms N(4), N(6), N(2) from ligand bdpab and one nitrogen atom N(7) of NCS^- ion. Secondary amine nitrogen atom N(1) of the ligand is occupied the axial position. The equatorial bond distances Cu-N(2) [1.993(3) Å], Cu-N(4) [2.102(3) Å], Cu-N(6) [1.995(3) Å] and Cu-N(7) [1.924(4) Å] are shorter than the axial bond length Cu(1)-N(1) [2.380(2)Å]. The bond angels of the coordination sphere are in the range of 81.06(13) to 178.63(13)°. The NCS^- ion is linear with bond angel [N(7)-C(21)-S(1)] 178.92° but its bonding with copper center [Cu-N(7)-C(21)] is not linear [169.46°]. The

bond lengths are similar to reported five coordinated mononuclear copper(II) complex with tetradentate tripodal N_4-coordinated ligand [54].

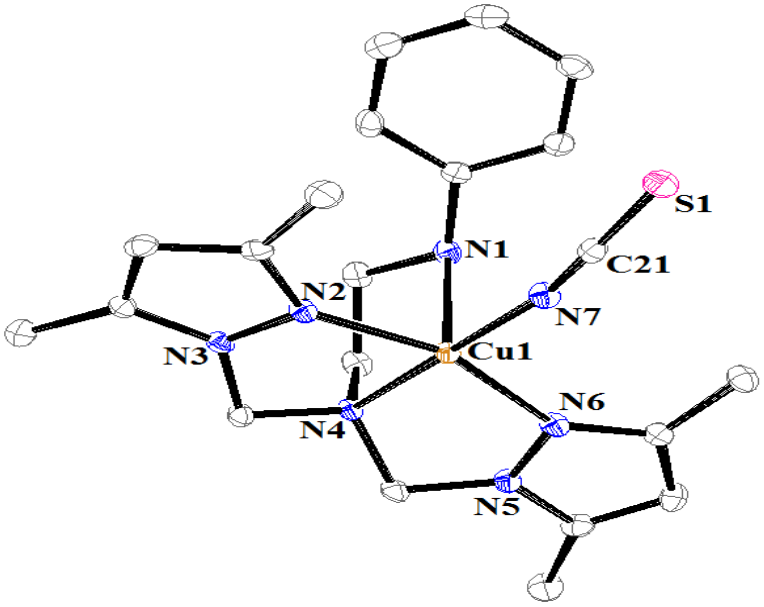

(a)

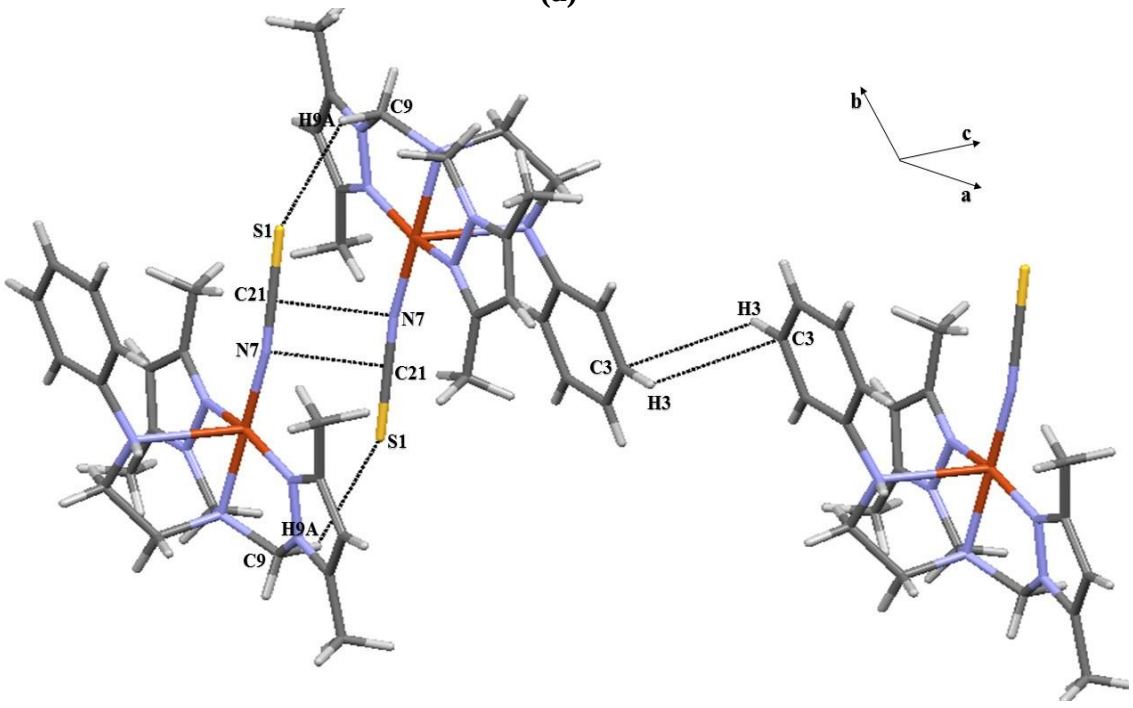

(b)

Fig.5(A)16(a). ORTEP diagram depicting the cationic part of the [Cu(bdpab)(NCS)]ClO_4 (**1**) with atom numbering scheme (40% probability factor for the thermal ellipsoids). **(b).** Intermolecular interaction of complex **1.**

Table.5(A).2. Important bond lengths (Å) of complexes **1**, **3**, **4** and **6.**

Bond lengths (Å)							
[Cu(bdpab)(NCS)]ClO_4 (1)		**[Co(bdpab)$(NCS)_2$] (3)**		**[Ni(bdpab)$(NCS)_2$] (4)**		**[Zn(bdpab)(NCS)]PF_6 (6)**	
Cu(1)-N(7)	1.924(4)	Co(1)-N(7)	2.023(4)	Ni(1)-N(7)	2.010(2)	Zn(1)-N(7)	1.966(2)
Cu(1)-N(2)	1.993(3)	Co(1)-N(5)	2.103(3)	Ni(1)-N(5)	2.071(2)	Zn(1)-N(2)	2.020(2)
Cu(1)-N(6)	1.995(3)	Co(1)-N(6)	2.104(4)	Ni(1)-N(6)	2.089(2)	Zn(1)-N(5)	2.044(2)
Cu(1)-N(4)	2.102(3)	Co(1)-N(1)	2.123(4)	Ni(1)-N(1)	2.092(2)	Zn(1)-N(1)	2.152(2)
Cu(1)-N(1)	2.389(3)	Co(1)-N(3)	2.233(4)	Ni(1)-N(3)	2.157(2)	Zn(1)-N(4)	2.3555(19)
		Co(1)-N(8)	2.302(4)	Ni(1)-N(8)	2.218(2)		

Bond angles (º) of complexes **1**, **3**, **4** and **6.**

Bond angles (º)							
[Cu(bdpab)(NCS)]ClO_4 (1)		**[Co(bdpab)$(NCS)_2$] (3)**		**[Ni(bdpab)$(NCS)_2$] (4)**		**[Zn(bdpab)(NCS)]PF_6 (6)**	
N(7)-Cu(1)-N(2)	98.79(14)	N(7)-Co (1)-N(5)	101.72(15)	N(7)-Ni (1)-N(5)	99.99(9)	N(7)-Zn(1)-N(2)	105.45(9)
N(7)-Cu(1)-N(6)	98.07(14)	N(7)-Co(1)-N(6)	96.17(17)	N(7)-Ni(1)-N(6)	93.45(10)	N(7)-Zn(1)-N(5)	102.98(9)
N(2)-Cu(1)-N(6)	160.31(14)	N(5)-Co(1)-N(6)	92.15(15)	N(5)-Ni(1)-N(6)	90.72(9)	N(2)-Zn(1)-N(5)	116.69(8)
N(7)-Cu(1)-N(4)	178.63(13)	N(7)-Co(1)-N(1)	104.11(16)	N(7)-Ni(1)-N(1)	101.78(9)	N(7)-Zn(1)-N(1)	99.90(9)
N(2)-Cu(1)-N(4)	82.24(13)	N(5)-Co(1)-N(1)	154.00(16)	N(5)-Ni(1)-N(1)	158.22(9)	N(2)-Zn(1)-N(1)	105.98(8)
N(6)-Cu(1)-N(4)	81.08(13)	N(6)-Co(1)-N(1)	88.01(15)	N(6)-Ni(1)-N(1)	87.56(9)	N(5)-Zn(1)-N(1)	123.00(8)
N(7)-Cu(1)-N(1)	98.00(14)	N(7)-Co(1)-N(3)	174.43(15)	N(7)-NI(1)-N(3)	176.40(9)	N(7)-Zn(1)-N(4)	178.15(8)
N(2)-Cu(1)-N(1)	91.39(13)	N(5)-Co(1)-N(3)	78.21(14)	N(5)-Ni(1)-N(3)	80.33(8)	N(2)-Zn(1)-N(4)	76.35(7)
N(6)-Cu(1)-N(1)	96.27(13)	N(6)-Co(1)-N(3)	89.40(15)	N(6)-Ni(1)-N(3)	90.13(9)	N(5)-Zn(1)-N(4)	75.73(7)
N(4)-Cu(1)-N(1)	81.06(13)	N(1)-Co(1)-N(3)	75.79(14)	N(1)-Ni(1)-N(3)	77.97(8)	N(1)-Zn(1)-N(4)	79.85(7)
		N(7)-Co(1)-N(8)	95.36(15)	N(7)-Ni(1)-N(8)	95.09(9)		
		N(5)-Co(1)-N(8)	87.43(14)	N(5)-NI(1)-N(8)	89.64(8)		
		N(6)-Co(1)-N(8)	168.31(16)	N(6)-Ni(1)-N(8)	171.26(9)		
		N(1)-Co(1)-N(8)	87.28(14)	N(1)-Ni(1)-N(8)	88.87(9)		
		N(3)-Co(1)-N(8)	79.07(14)	N(3)-Ni(1)-N(8)	81.32(8)		

The NCS^- ion of each molecule of the complex has face-to-face π---π interaction with another NCS^- ion of the nearest molecule [Fig. 5(A).16(b)]. The intermolecular distance between the two parallel planes of two NCS^- ion equal to 3.228 Å. The network is stabilized by two weak intermolecular interactions S1—H9A-C9 between S(1) atom of NCS^- and H9A atom of CH_2- of nearest molecule and two weak intermolecular interactions between C3 and H3 of two benzene rings of two nearest molecules [Table.5(A).3].

Table.5(A).3. Intermolecular interactions of the complexes **1**, **3** and **4**.

Compounds/ parameters	D-H(Å)	H---A(Å)	D----A(Å)	<(DHA)
[Cu(bdpab)(NCS)]ClO_4 (1)				
C9-H9A----S1	0.970	2.822	3.792	130.45
C3-H3---H3A	0.931	2.865	3.796	122.62
[Co(bdpab)$(NCS)_2$] (3)				
C13-H13----S2	0.930	2.992	3.922	142.16
C5-H5---H20	0.929	2.275	3.204	134.00
N8-H22---S1	0.839	2.715	3.554	155.79
[Ni(bdpab)$(NCS)_2$] (4)				
C11-H11----H5	0.960	2.260	3.191	162.93
C18-H18---S1	0.930	2.970	3.900	143.21
N8-H21---S2	0.816	2.717	3.533	156.7

In the complex **6**, zinc(II) centre adopts a trigonal bipyramidal geometry (τ = 0.91) with ZnN_5 coordination environment. The trigonal plane consists of three nitrogen atoms from the ligand (bdpab) - two nitrogen atoms N(2) and N(5) of the two pyrazole

rings and the N(1) of secondary amine. The axial positions are occupied by two nitrogen atoms- N(4) of the tertiary amine of the ligand and N(7) of NCS^- ion. The bond distances in the triangular plane Zn-N(1), Zn-N(2) and Zn-N(5) are in the range of 2.020(2) to 2.152(2) (Å) but the axial bond distance Zn-N(4) [2.356(19)Å] is longer than Zn-N(7) [1.966(2)Å] of terminal NCS unit. The linear N-donor NCS^- ion (179.34°) is ligated to zinc(II) center in a bending fashion as is reflected from bond angle Zn-N(7)-C(21) is 168.88º. The axial bond angle N(4)-Zn-N(7) is nearly linear (178.15°). The Zn-NCS bond length is comparable to other reported Zn-NCS bond length reported with mononuclear penta coordinate complex with tripodal ligand [55-56].

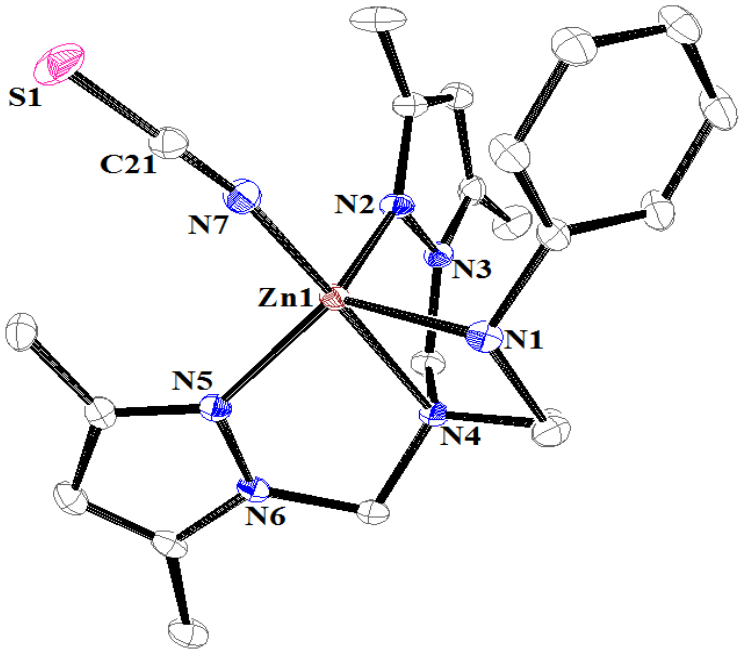

Fig.5(A).17. ORTEP diagram depicting the cationic part of the complex $[Zn(bdpab)(NCS)]PF_6$ (**6**) present in the asymmetric unit with atom numbering scheme (30% probability factor for the thermal ellipsoids).

5(A).4.4.2. Crystal structures of $[Co(bdpab)(NCS)_2]$ (3) and $[Ni(bdpab)(NCS)_2]$ (4)

The ORTEP diagrams of the complexes **3** and **4** are shown in Fig.5(A).18(a) and 19(a), respectively. The X-ray crystal structure determination confirmed that both the complexes are nonionic, iso-structural, crystallized in monoclinic $P2_1/c$ space groups. In

both the complexes, the metal atoms have MN_6 chromophores with distorted octahedral geometry. Each metal center is coordinated by four donor nitrogen atoms [N(1), N(3), N(5) and N(8)] of ligand (bdpab) and the remaining two sites are occupied by two nitrogen atoms N(6) and N(7) of two NCS^- ions. The two NCS^- ions are coordinated in the cis position with respect to metal center in both the complexes.

The CoN_6 octahedra is slightly distorted with distances ranging from 2.023(4) to 2.302(4) Å and angles between 75.79(14)° and 174.43(15)° [Table.5(A).2]. Four equatorial bond distances Co-N(1) [2.123(4) Å], Co-N(5) [2.103(3) Å], Co-N(3) [2.233(4) Å] and Co-N(7) [2.023(4) Å] are not equal. The axial bond Co-N(8) [2.302(4) Å] is longer than Co-N(6) [2.104(4) Å]. The NCS ions (178.37°) are nearly linear but are bonded with metal centres with different bond angles 167.58° [Co-N(7)-C(21)] and 148.87° [Co-N(6)-C(22)].

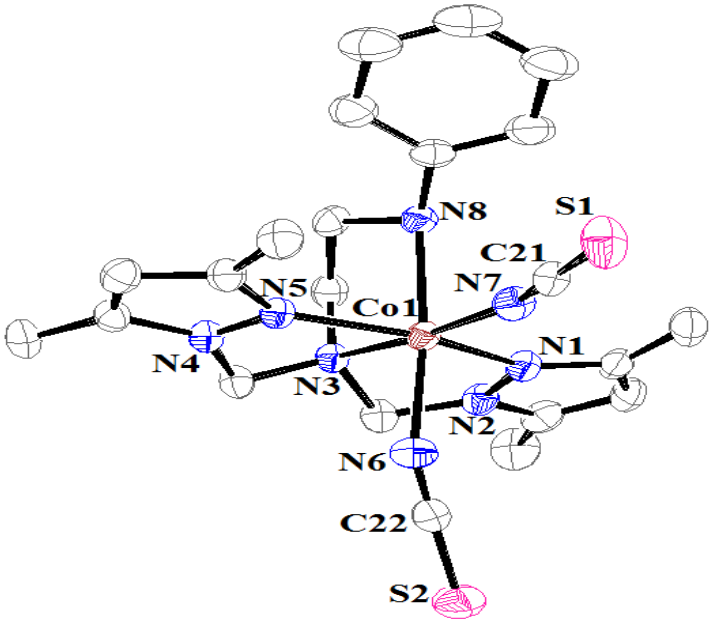

Fig.5(A).18(a). ORTEP diagram depicting the cationic part of the complex $[Co(bdpab)(NCS)_2]$ (**3**) with atom numbering scheme (40% probability factor for the thermal ellipsoids).

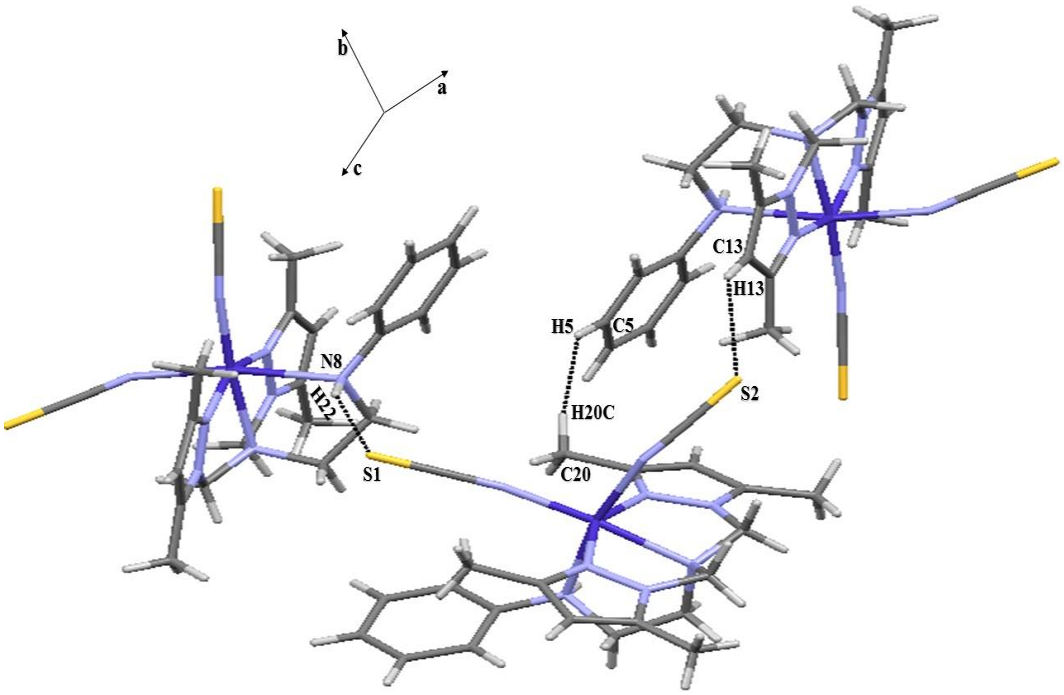

Fig.5(A).18(b). Intermolecular interactions of complex **3.**

Two sulphur atoms of the two NCS^- ion of each molecule has weak intermolecular interactions with hydrogen atoms of two nearest molecules [Fig.5(A).18(b)]. S(2) has weak intermolecular interaction with H13 of H13C13 of the pyrazole and S(1) has intermolecular interaction with H22 of H22N8 of the secondary amine attached with benzene ring of the nearest molecules. The H20 of methyl group [H20C20] attached with pyrazole ring has weak intermolecular interaction with H5 of H5C5 of the benzene ring of the nearest molecule [Table 5(A).3].

In complex **4**, the NiN_6 octahedral are slightly distorted as four equatorial bond distances Ni-N(1) [2.092(2)) Å], Ni-N(5) [2.071(2) Å], Ni-N(3) [2.157(2) Å], Ni-N(7) [2.010(2) Å] are nearly equal and the axial bond Ni-N(6) distance [2.089(2) Å] is shorter than Ni-N(8) [2.218(2) Å]. The bond angles varies from 77.97(8)° to 176.40(9)° [Table.5(A).2]. The bond M-N (secondary amine) of the tripodal ligand is most elongated and is always greater than other three M-N (i.e. N atom from tertiary amine and pyrazoles) bond distances in all the complexes. The axial bond angle N(8)-Ni-N(6) [171.27°] is not linear. The quasi linear NCS ions (178.37°) are bonded with metal centres with bond angle 167.98° [Ni-N(7)-C(21)] and 148.81° [Ni-N(6)-C(22)],

respectively. The two M-NCS distances are nearly equal to both the complexes and comparable to other mononuclear octahedral complexes with two NCS^- ion reported earlier [57-58].

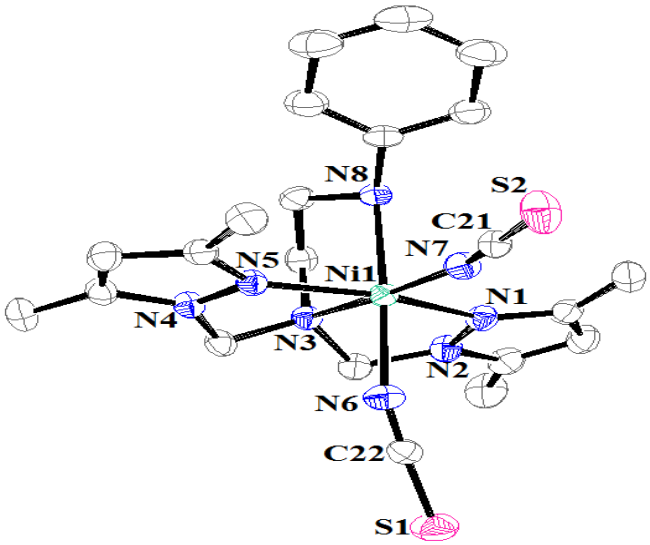

Fig.5(A).19(a). ORTEP diagram depicting the cationic part of the complex $[Ni(bdpab)(NCS)_2]$ (**4**) with atom numbering scheme (30% probability factor for the thermal ellipsoids).

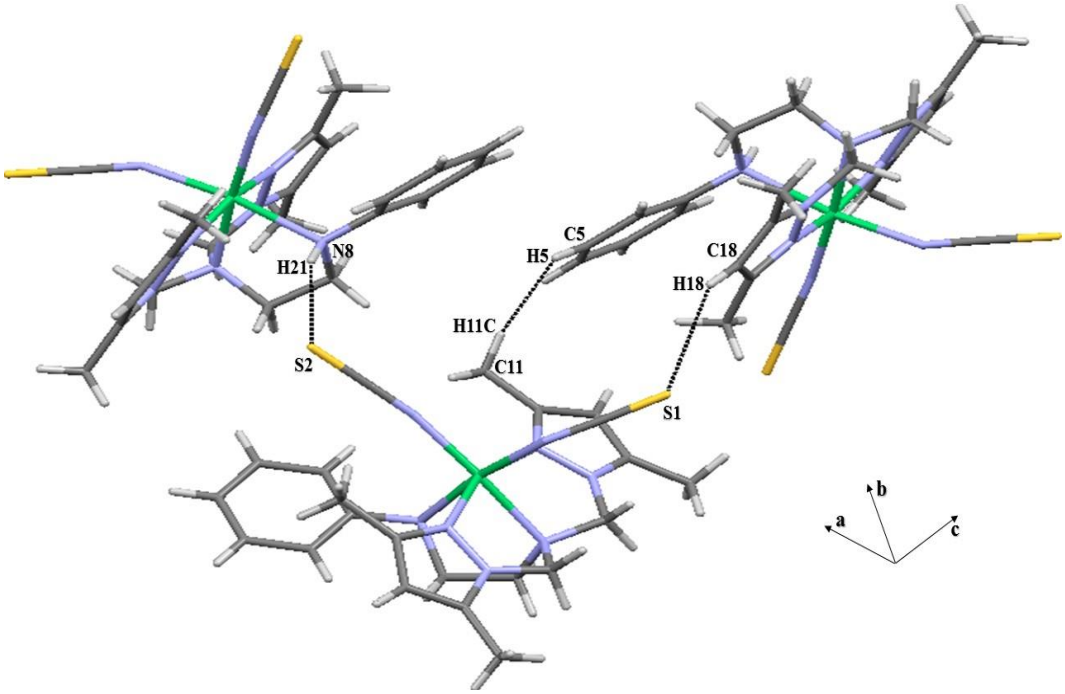

Fig.5(A).19(b). Intermolecular interactions of the complex **4**.

Two sulphur atoms of the two NCS^- ion of each molecule has weak intermolecular interactions with hydrogen atoms of two nearest molecules [Fig.5(A).19(b)]. S1 has weak intermolecular interaction with one nearest molecule through H18 of H18C18 of the pyrazole molecule. S2 has intermolecular interaction with H21 of H21N8 of the secondary amine attached with benzene ring. The H11 of (H11C11) of the methyl group attached with pyrazole ring has weak intermolecular interaction with H5 of H5C5 of benzene ring of the nearest molecule [Table.5(A).3].

5(A).4.4.3. Crystal structures of $[Cu(bdpab)(NCO)]PF_6$ (8) and $[Co(bdpab)(NCO)]ClO_4$ (9)

The ORTEP diagram with the atom labeling schemes for complexes **8** and **9** are depicted in Fig.5(A).20(a) and 21(a) and confirmed that compounds are mononuclear. Complexes **8** and **9** crystallize in monoclinic and triclinic crystal system with $P2_1/n$ and *P-1* space group, respectively. Both the complexes are iso-structural, penta coordinated with MN_5 coordination environment. For both the complexes metal centres are coordinated by five nitrogen donor atoms–four nitrogen atoms from the ligand bdpab and one nitrogen from cyanate ion. The geometry of both the metal centres may be regarded as distorted square pyramidal geometry as described by the τ parameter, the degree of trigonality index [$\tau = 0.23$ for complexes **8** and 0.42 for complexes **9**] [53].

For both the complexes, the equatorial positions are occupied by tertiary nitrogen N(2), two pyrazole nitrogen atoms N(4) and N(6) of ligand bdpab and nitrogen N(7) of the NCO group and the axial position is occupied by secondary nitrogen atom N(1) of ligand bdpab. The four Cu-N bonds distances in the basal plane are in the range 1.919(3)-2.097 Å for complex **8** which are much shorter than the axial Cu-N(1) bonds distance [2.405(3) Å] but for complex **9**, the four equatorial Cu-N bond distances are in the range of 1.993 (3)-2.244(2) Å and the axial Cu–N(1) bond distance is 2.178(3) Å. In both the complexes NCO ion is nearly linear [~179.18º for N(7)-C(21)-O] whereas the M-N(7)-C(21) linkage is somewhat bent [171.18(3)º for Cu(II) and 156.32(3)º for Co(II)]. For both the complexes [M-N(NCO)] distance is ~1.992 Å which is comparable with reported metal complexes with N_4-tripodal ligand [59-60]. The M-NH distances are not equal and Cu-NH distance (2.405Å) is much longer than Co-NH distance (2.178Å). The

bond angles of the complex **8** varies from 80.27(11) to 174.23(12) whereas for complex **9** the angle varies from 77.12(9) to 177.13(10)º. The unequal bond lengths and bond angles produces maximum distortion in the molecules. For both the complexes, the bond distance between C and N (~1.15Å) has triple bond character and this is smaller than the bond distance between the C and O (~1.203Å) in N bonded NCO^- ion.

Table.5(A).4. Important Bond lengths (Å) of complexes **8**, **9, 11** and **13.**

Bond lengths (Å)							
[Cu(bdpab)(NCO)]PF_6 (8)		**[Cd(bdpab)($\mu_{1,1}$-NCO)]$_2$(ClO_4)$_2$ (13)**		**[Ni(bdpab)($\mu_{1,3}$-NCO)]$_2$(ClO_4)$_2$ (11)**		**[Co(bdpab)(NCO)]ClO_4 (9)**	
Cu(1)-N(7)	1.919(3)	Cd(1)-N(7)	2.281(3)	Ni(1)-O(1)	2.221(3)	Co(1)-N(6)	2.091 (3)
Cu(1)-N(6)	2.000(3)	Cd(1)-N(4)	2.296(3)	Ni(1)-N(1)	2.138(3)	Co(1)-N(2)	2.244 (2)
Cu(1)-N(4)	2.016(3)	Cd(1)-N(6)	2.299(3)	Ni(1)-N(2)	2.149(3)	Co(1)-N(1)	2.178 (3)
Cu(1)-N(2)	2.097(3)	Cd(1)-N(1)	2.408(4)	Ni(1)-N(6)	2.062(4)	Co(1)-N(4)	2.078 (3)
Cu(1)-N(1)	2.405(3)	Cd(1)-N(7i)	2.482(3)	Ni(1)-N(7)	2.001(3)	Co(1)-N(7)	1.993 (3)
		Cd(1)-N(2)	2.534(3)	Ni(1)-N(4)	2.055(4)		
		Cd(1)-Cd(1i)	3.593	Ni(1)-Ni(1i)	5.165		

Important Bond angles (Å) of complexes **8**, **9, 11** and **13.**

Bond angles (°)							
[Cu(bdpab)(NCO)]PF_6 (8)		**[Co(bdpab)(NCO)]ClO_4 (9)**		**[Cd(bdpab)($\mu_{1,1}$-NCO)]$_2$(ClO_4)$_2$ (13)**		**[Ni(bdpab)($\mu_{1,3}$-NCO)]$_2$(ClO_4)$_2$ (11)**	
N(7)-Cu(1)-N(6)	99.41(13)	N(2)-Co(1)-N(6)	77.12(9)	N(7)-Cd(1)-N(4)	107.16(11)	N(1)-Ni(1)-O(1)	170.05(10)
N(7)-Cu(1)-N(4)	98.25(13)	N(1)-Co(1)-N(6)	95.40(10)	N(7)- Cd(1)-N(6)	111.74(11)	N(2)-Ni(1)-O(1)	87.30(10)
N(6)-Cu(1)-N(4)	160.52(11)	N(1)-Co(1)-N(2)	80.67(9)	N(4)-Cd(1)-N(6)	140.58(12)	N(2)-Ni(1)-N(1)	82.87(11)
N(7)-Cu(1)-N(2)	174.23(12)	N(4)-Co(1)-N(6)	151.82(11)	N(7)-Cd(1)-N(1)	105.68(12)	N(6)-Ni(1)-O(1)	86.59(12)
N(6)-Cu(1)-N(2)	81.34(11)	N(4)-Co(1)-N(2)	78.02(10)	N(4)-Cd(1)-N(1)	88.99(12)	N(6)-Ni(1)-N(1)	93.25(13)
N(4)-Cu(1)-N(2)	80.27(11)	N(4)-Co(1)-N(1)	93.47(10)	N(6)-Cd(1)-N(1)	86.66(12)	N(6)-Ni(1)-N(2)	80.06(11)
N(7)-Cu(1)-N(1)	104.02(12)	N(7)-Co(1)-N(6)	100.55(11)	N(7)-Cd(1)-N(7i)	82.12(13)	N(7)-Ni(1)-O(1)	92.40(11)
N(6)-Cu(1)-N(1)	90.17(11)	N(7)-Co(1)-N(2)	177.13(10)	N(4)-Cd(1)-N(7i)	89.38(11)	N(7)-Ni(1)-N(1)	97.48(12)
N(4)-Cu(1)-N(1)	93.47(12)	N(7)-Co(1)-N(1)	101.32(10)	N(6)-Cd(1)-N(7i)	89.74(11)	N(7)-Ni(1)-N(2)	177.85(15)
N(2)-Cu(1)-N(1)	81.67(11)	N(7)-Co(1)-N(4)	103.84(12)	N(1)-Cd(1)-N(7i)	172.16(12)	N(7)-Ni(1)-N(6)	97.79(15)
				N(7)-Cd(1)-N(2)	177.03(11)	N(4)-Ni(1)-O(1)	84.24(12)
				N(4)-Cd(1)-N(2)	70.08(11)	N(4)-Ni(1)-N(1)	92.66(13)
				N(6)-Cd(1)-N(2)	71.13(11)	N(4)-Ni(1)-N(2)	81.20(11)
				N(1)-Cd(1)-N(2)	73.45(12)	N(4)-Ni(1)-N(6)	159.48(12)
				N(7i)-Cd(1)-N(2)	98.79(11)	N(4)-Ni(1)-N(7)	100.89(15)

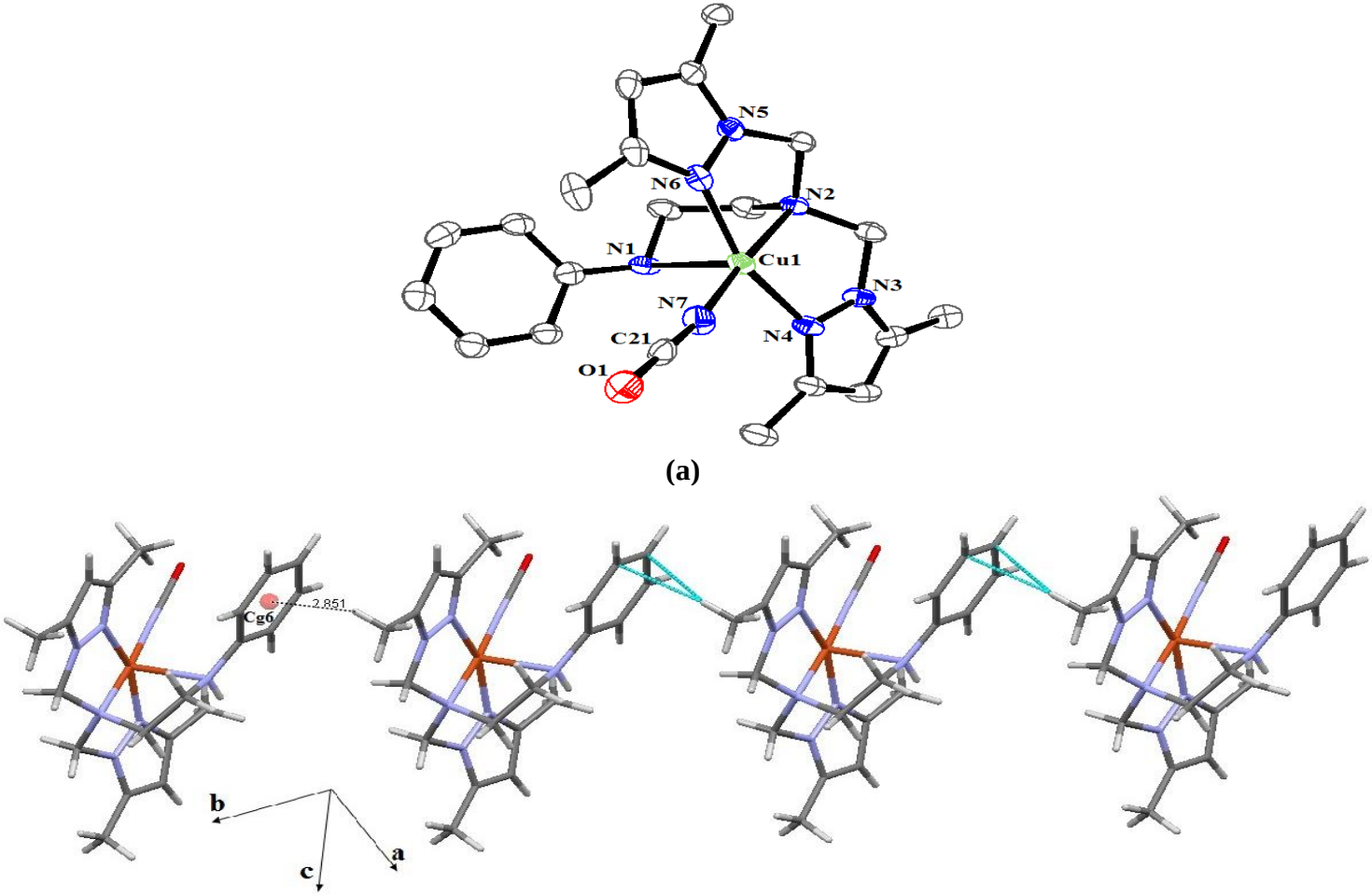

Fig.5(A).20(a). ORTEP diagram depicting the cationic part of the complex [Cu(bdpab)(NCO)]PF_6 (**8**) with atom numbering scheme (30% probability factor for the thermal ellipsoids).**(b).** The 1D network formed through C-H--- π interaction along *b*-axis in complex **8**.

Table.5(A).5. The intermolecular hydrogen bonds of the complexes **9**, **11** and **13.**

	N-H----O bond					C-H----O bond			
Compounds/ parameters	D-H(Å)	H---A(Å)	D----A(Å)	<(DHA)	Compounds/ parameters	D-H(Å)	H---A(Å)	D----A(Å)	<(DHA)
[Co(bdpab)(NCO)]ClO_4					**[Co(bdpab)(NCO)]ClO_4**				
N1-H1---O4	0.803	2.247	3.05	166.21	C11-H11c---O3	0.961	2.541	3.502	163.19
					C18-H18---O4	0.930	2.649	3.579	154.73
[Ni(bdpab)($\mu_{1,3}$-NCO)]$_2(ClO_4)_2$					**[Ni(bdpab)($\mu_{1,3}$-NCO)]$_2(ClO_4)_2$**				
N1-H1---O4	0.736	2.292	3.028	166.13	C15-H15c---O3	0.960	2.568	3.528	148.21
					C18-H18---O4	0.930	2.677	3.607	155.98
[Cd(bdpab)($\mu_{1,1}$-NCO)]$_2(ClO_4)_2$					**[Cd(bdpab)($\mu_{1,1}$-NCO)]$_2(ClO_4)_2$**				
N1-H21---O4	0.777	2.253	3.03	160.69	C6-H6---O5	0.930	2.544	3.474	138.99
					C11-H11b---O1	0.961	2.667	3.628	154.26

In complex **8**, two $[Cu(bdpab)(NCO)]^+$ cations are joined by H atom i.e. H16b of -CH_3 group of pyrazole ring of ligand bdpab of one molecule and π-electron density of the benzene [Cg6: C(1)-(C2)-(C3)-(C4)-(C5)-(C6)] ring of the nearest molecule and the distance between H16b and centroid is 2.851Å and thus form 1D chain along b - axis [Fig.5(A).20(b)].

In complex **9**, two nearest molecules are connected by non-coordinated oxygen atoms of the perchlorate ion and three different H atoms namely H1 atom of HN, H18 atom of pyrazole and H11c atom from -CH_3 of the ligand bdpab [Fig.5(A).21(b)]. A list of H-bonds and short intermolecular interactions of the complexes are given in Table.5**(**A).5. Mononuclear cobalt units [Fig.5(A).21(c)] are arranged by means of face-to-face π---π stacking interaction between phenyl and pyrazole ring and form 1D linear polymer. The centroid-centroid separation is 4.223Å with dihedral angle between phenyl and pyrazole ring is 19.37º indicating a significant intermolecular face-to-face π---π stacking interaction [61]. This adjacent 1D chain are further linked to form 2D network through the intermolecular C-H---O and N-H---O hydrogen bond interaction [Fig.5(A).21(b) and (c)].

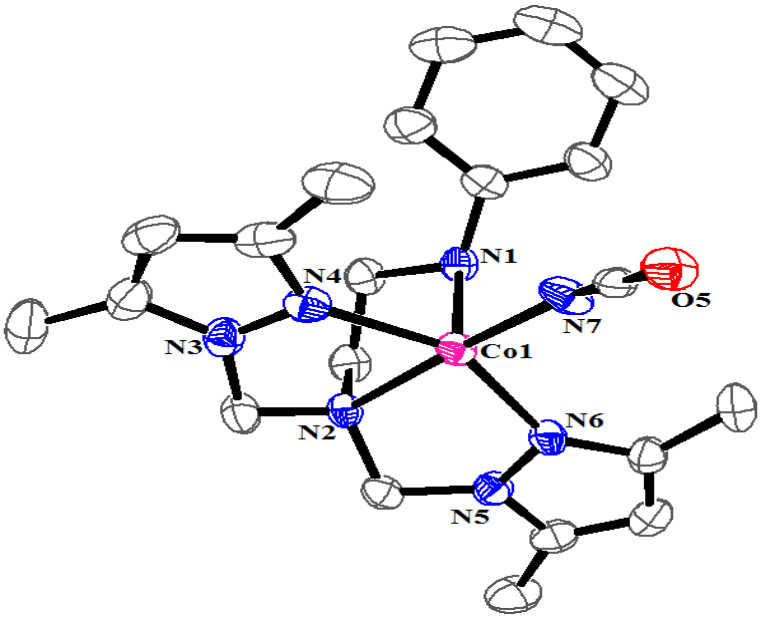

Fig.5(A).21(a). ORTEP diagram depicting the cationic part of the complex $[Co(bdpab)(NCO)]ClO_4$ (**9**) with atom numbering scheme (30% probability factor for the thermal ellipsoids).

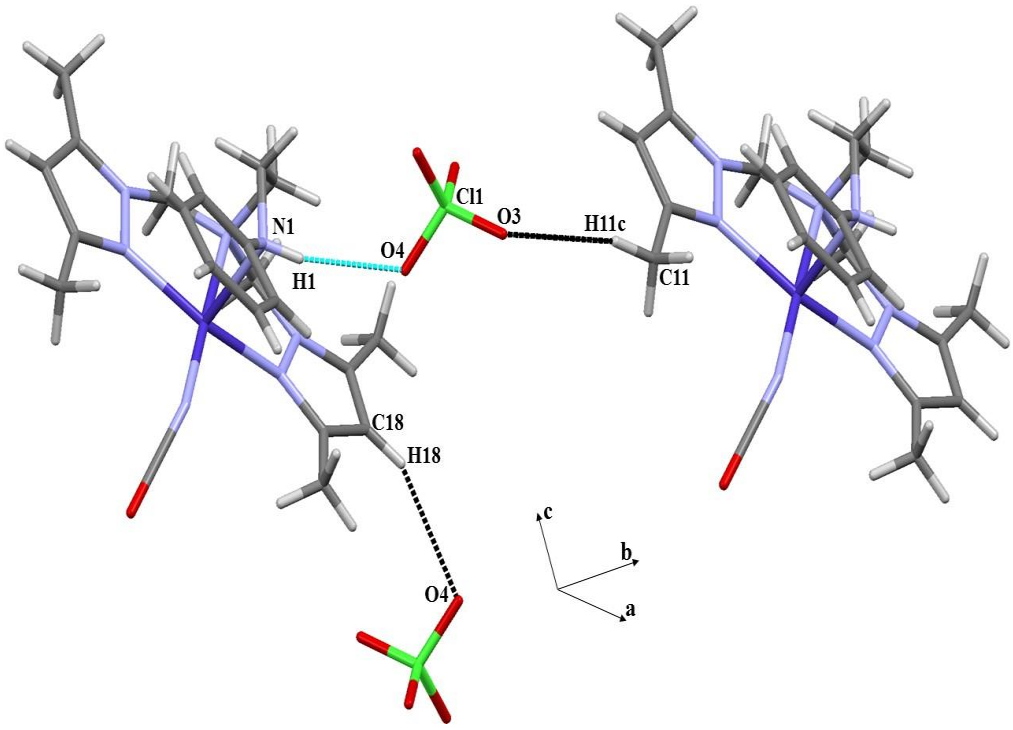

Fig.5(A).21(b). Arrangement of the intermolecular H-bonding interactions in complex **9**.

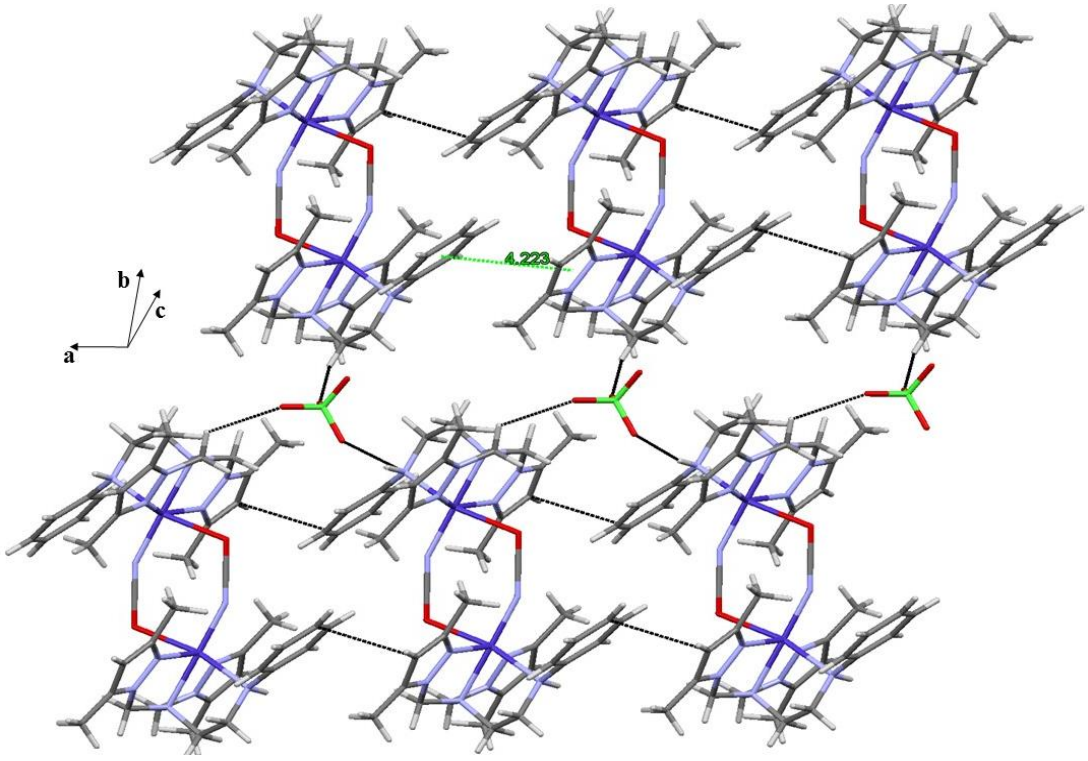

Fig.5(A).21(c). The 2D network formed through face-to-face π---π stacking and interchain H-bonding interactions in complex **9**.

5(A).4.4.4. Crystal structures of [Ni(bdpab)($\mu_{1,3}$-NCO)]$_2$(ClO$_4$)$_2$ (11) and [Cd(bdpab)($\mu_{1,1}$-NCO)]$_2$(ClO$_4$)$_2$ (13)

The ORTEP diagram representations of binuclear complexes **11** and **13** with the atom labeling schemes are depicted in Fig.5(A).22(a) and 23(a). Both complexes were crystallized in triclinic crystal system with *P-1* space group and each atom has distorted octahedral geometry and surrounded by ligand bdpab and two bridging NCO ions.

In Complex **11,** two nickel centres are joined by double end-to-end (μ-1,3) NCO coordination mode and Ni….Ni separation is 5.165 Å. The coordination environment of each nickel atom is N_5O and surrounded by four nitrogen atoms [N(1), N(2), N(4) and N(6)] from ligand bdpab and N(7) and O(1) atoms from two bridging cyanate ligand. The equatorial positions are occupied by two nitrogen atoms- N(1), N(2) from ligand bdpab and one nitrogen atom N(7) from cyanate and one oxygen atom O(1) and two nitrogen atoms N(4) and N(6) from ligand are in the axial position. The equatorial bond distances are Ni-N(1) [2.138(3) Å], Ni-N(2) [2.149(3) Å], Ni-N(7) [2.001(3) Å] and O(1) [2.221(3) Å] are close but not equal. The axial bond distances Ni-N(4) [2.055(4)] and Ni-N(6) [2.062(4) Å] are equal. The axial bond angle N(4)-Co(1)-N(6) [151.82(11)] is deviated from ideal value 180º. The two trans equatorial bond angles N(7)-Co(1)-N(2) [177.13(10)º] and N(1)-Ni(1)-O(1) [170.05(10)] are nearly same. Two bridged NCO ions are parallel to each other and the angle of NCO ions [N(7)-C(21)-O(1)] is 179.66º. Unequal bond lengths and deviation of axial bond length produce distortion in the molecule. Nickel-cyanate bridging bond lengths i.e. Ni-N (NCO) [2.001Å] and Ni-O(NCO) [2.221Å] are comparable to similar end-to-end NCO nickel(II) complex with tetradentate pyrazole based ligand [62]. The bond length between the C and N is 1.143 Å and between C and O is 1.206 Å respectively in the bridging NCO^- ion in the complex and these values are similar to terminal N bonded NCO ion containing complexes **8** and **9**.

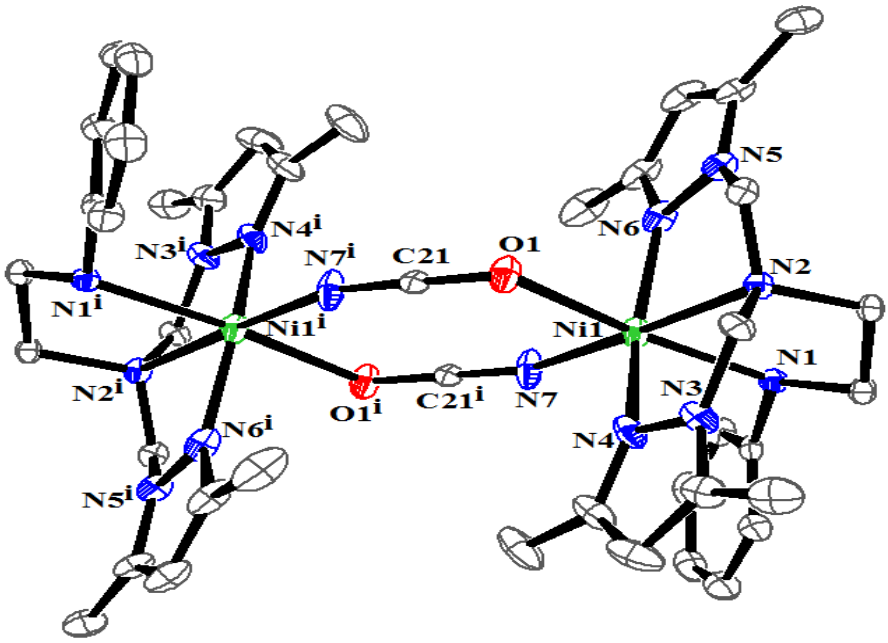

Fig.5(A).22(a). ORTEP diagram depicting the cationic part of the complex $[Ni(bdpab)(\mu_{1,3}\text{-}NCO)]_2(ClO_4)_2$ (**11**) with atom numbering scheme (30% probability factor for the thermal ellipsoids).

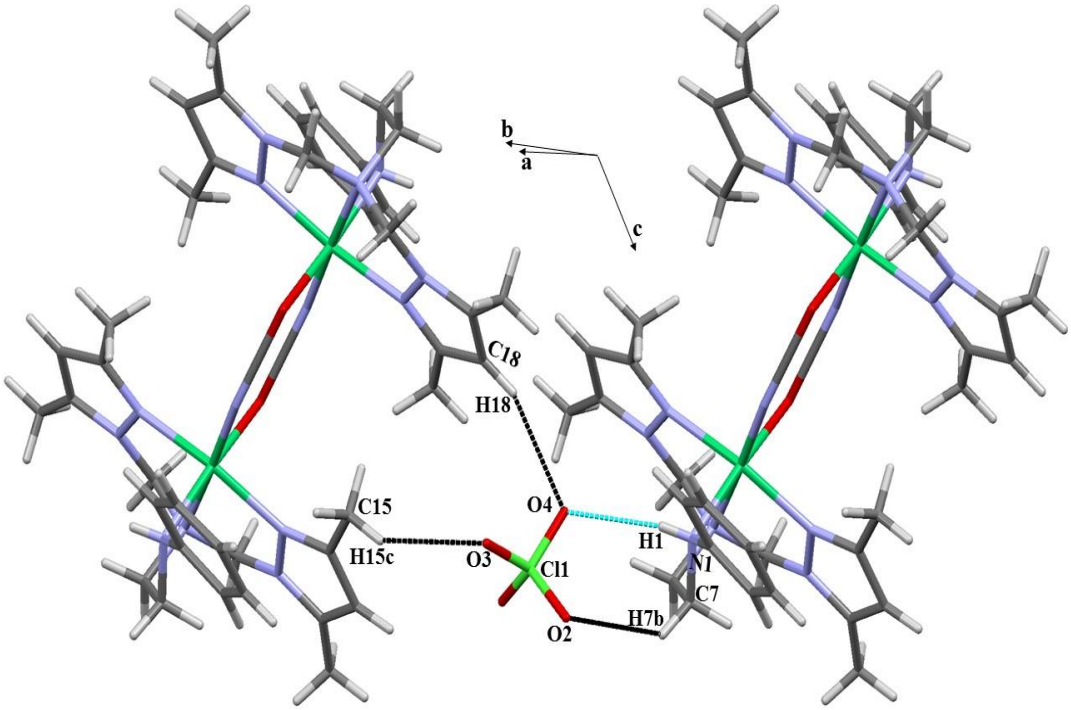

Fig.5(A).22(b). Arrangement of the intermolecular H-bonding interactions in complex **11**.

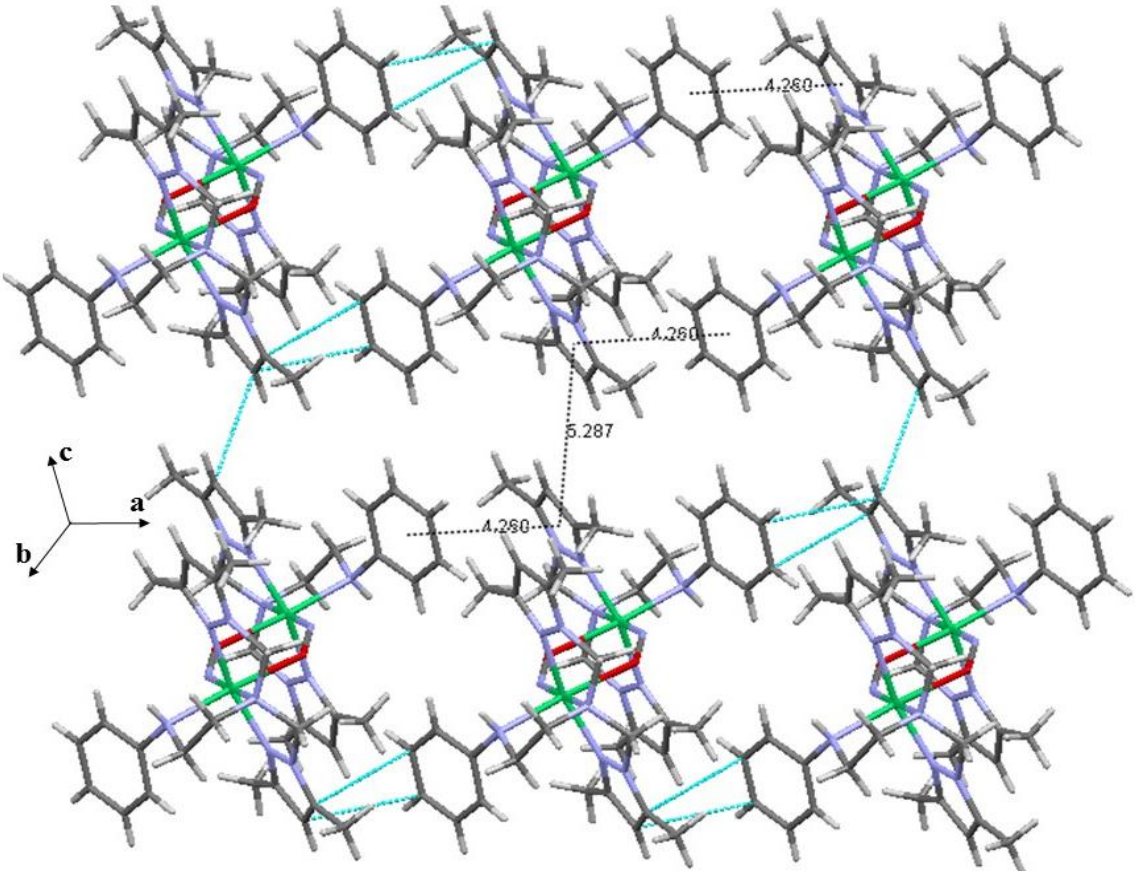

Fig.5(A).22(c). The 2D network formed through face-to-face π---π stacking in complex **11**.

In complex **11,** two nearest molecules are connected by non-coordinated oxygen atoms of the perchlorate ion and four different H atoms namely H1 atom of HN (secondary amine), H18 atom of pyrazole HC, H7b atom of methylene HC and H15c atom from $–CH_3$ of the ligand bdpab [Fig.5(A).22(b)]. A list of H-bonds and short intermolecular interactions of the complexes are given in Table.5**(**A).5. The binuclear molecules are assembled by means of intermolecular π-π interaction between phenyl ring and pyrazole ring of two nearest molecules with the centroid-centroid distance is 4.260 Å and the dihedral angle between them is 19.52º. This π-π interaction gives a 1D linear polymer along a- axis [61]. The resulting 1D chain is further propagated towards c - axis through π-π interaction between two pyrazole rings of nearest molecules. The cumulative effect of these interactions resulted into the formation of 2D molecular framework [Fig.5(A).22(c)].

In Complex **13,** two cadmium centres are joined by double bridged NCO anions with end-on coordination mode and the Cd….Cd separation is 3.593 Å. The structure shows each cadmium atom has CdN_6 coordination environment and surrounded by four nitrogen atoms [N(1). N(2), N(4) and N(6)] from ligand bdpab and two nitrogen atoms N(7) and N(7i) from two bridging cyanate ligand.

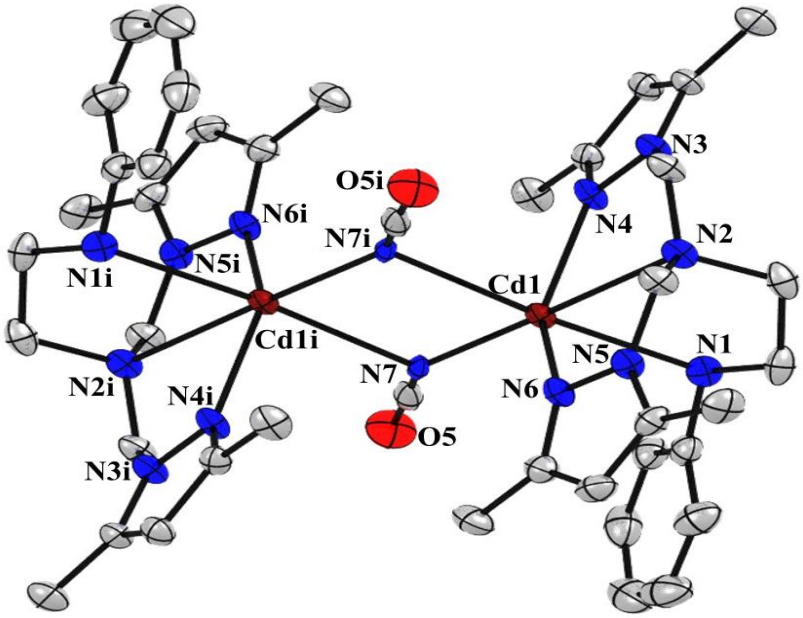

Fig.5(A).23(a). ORTEP diagram depicting the cationic part of the complex $[Cd(bdpab)(\mu_{1,1}\text{-}NCO)]_2(ClO_4)_2$ (**13**) with atom numbering scheme (30% probability factor for the thermal ellipsoids).

Two axial sites of the cadmium(II) centres are occupied by two pyrazole nitrogen atoms N(4) and N(6) of ligand bdpab and the two axial bonds distances Cd-N(4) [2.296(3) Å] and Cd-N(6) [2.299(3) Å] are same. The equatorial sites of the cadmium centre are occupied by four nitrogen atoms-secondary amine nitrogen N(1) and tertiary amine nitrogen N(2) of ligand bdpab, and two cyanate nitrogen atoms N(7) and N(7i) and all the bonds distances in the basal plane Cd-N(1) [2.408(4) Å], Cd-N(2) [2.534(3) Å], Cd-N(7) [2.281(3) Å] and Cd-N(7i) [2.482(3) Å] are long but not equal. Bond angle of cadmium centre involving NCO ion Cd(1)-N(7)-C(21), Cd(1)-N(7i)-C(21i) and N(7)-Cd(1)-N(7i) are 143.31º, 116.37º and 82.12º, respectively. The axial bond angle N(4)-Cd-N(6) [140.58(12)] has maximum deviation. The two bond length of the equatorial planes

N(7)-Cd(1)-N(2) [177.03(11)] and N(1)-Cd(1)-N(7i) [172.16(12)] are nearly same. The unequal bond lengths and bond angles produce maximum distortion in the molecule. Different coordination modes of NCO^- ion in cadmium(II) and nickel(II) complexes are also reflected in the bond distances between C and N [1.064Å for Cd(II) complex and 1.143 Å for Ni(II) complex] and also in C and O [1.237Å for Cd(II) complex and 1.206 Å for Ni(II) complex] in the NCO ligand.

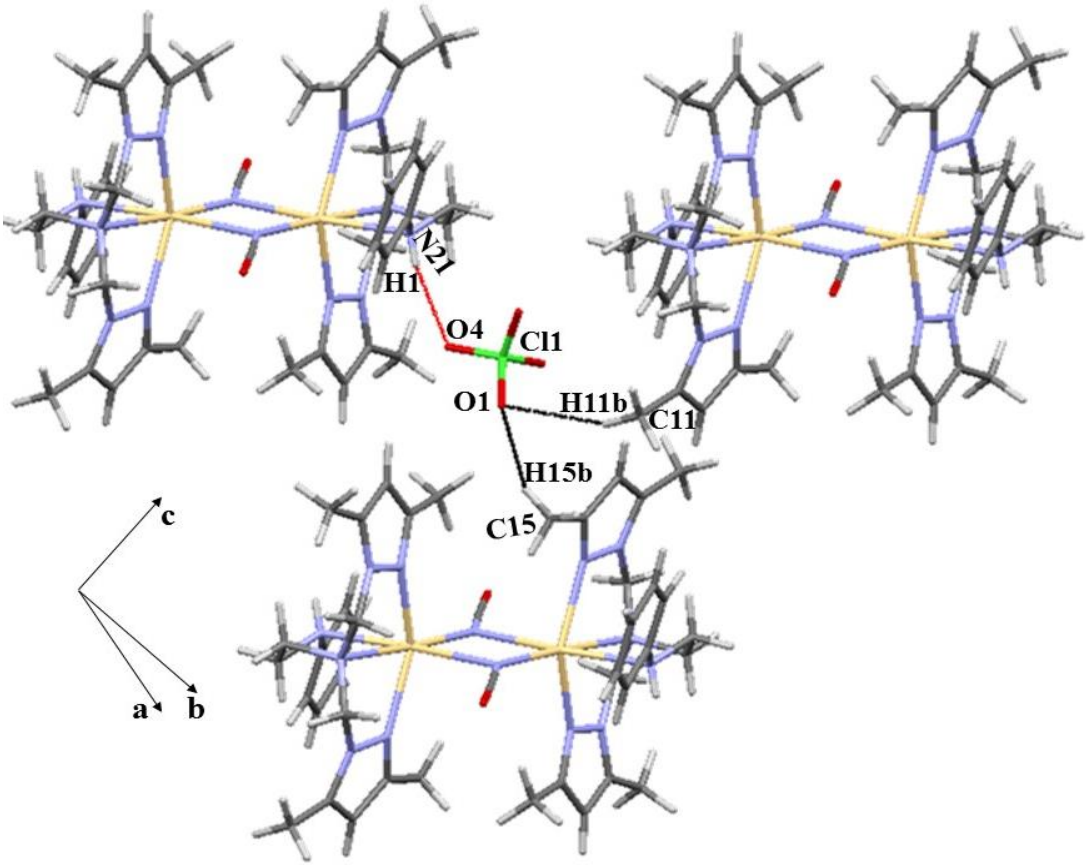

Fig.5(A).23(b). Arrangement of the intermolecular H-bonding interactions in complex **13**.

In complex **13**, two nearest molecules in the unit cell are connected by non-coordinated oxygen atoms of the perchlorate ion and three different H atoms namely H1 atom of HN (secondary amine), H11b atom of methylene pyrazole HC, H15b atom of methylene pyrazole HC [Fig.5(A).23(b)]. A list of H-bonds and short intermolecular interactions of the complexes are given in Table.5**(**A).5. The binuclear cadmium units [Fig.5(A).23(a)] are arranged by means of face-to-face π---π stacking interaction between

the phenyl and pyrazole ring, forming a 1D linear polymer along a- axis. The separation between the centroids of phenyl and pyrazole ring is 4.295 Å with dihedral angle 18.97º indicating a significant intermolecular face-to-face π---π stacking interaction [61]. This resulting 1D chain is further propagated towards c – axis through C-H---π supramolecular interactions between the two phenyl rings. The cumulative effect of these interactions resulted into the formation of 2D molecular framework [Fig.5(A).23(c)].

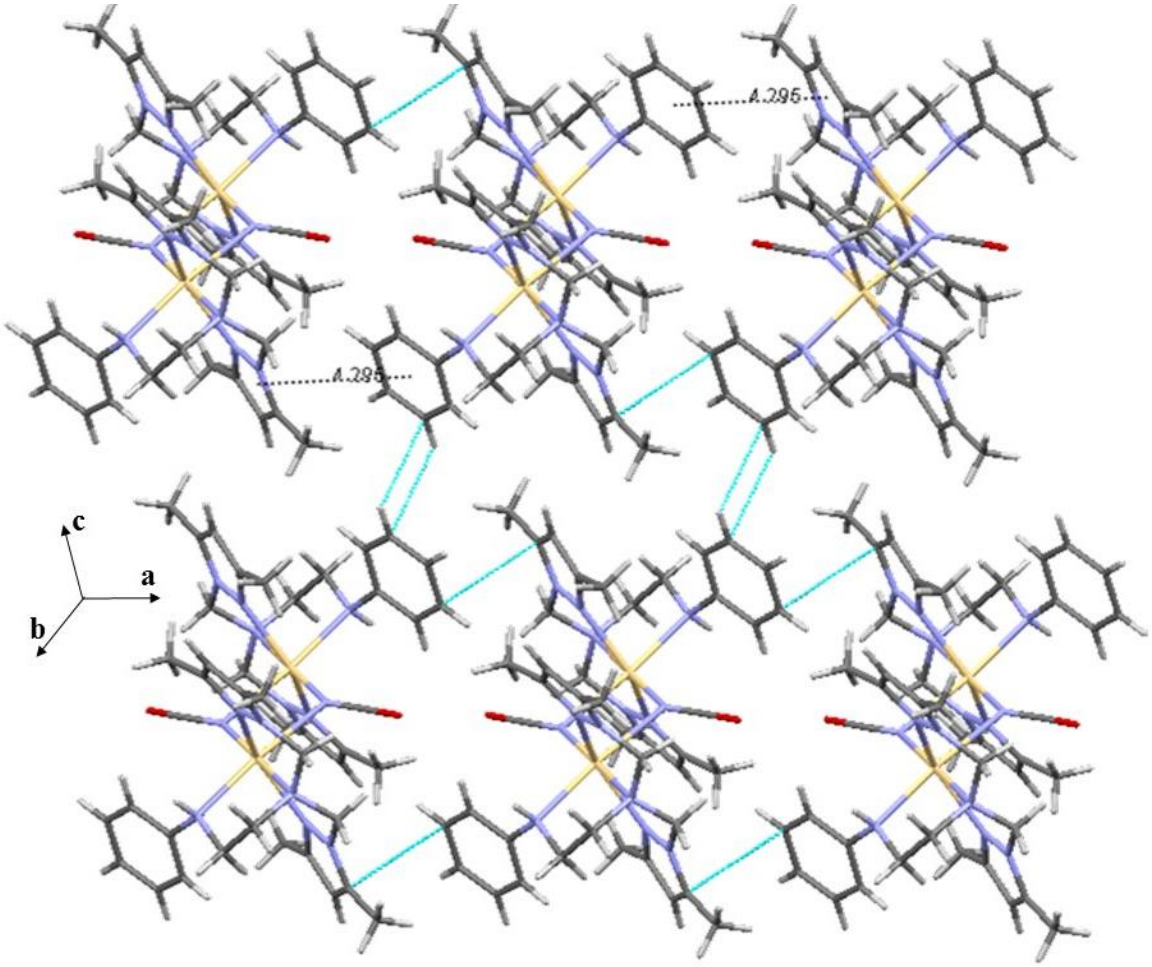

Fig.5(A).23(c). The 2D network formed through face-to-face π---π stacking and C-H--- π interaction in complex **13**.

5(A).5. Conclusions

A series of mononuclear complexes of the type [M(bdpab)(X)]Y, [M = Cu(II), Co(II), Zn(II). X = NCS^-, NCO^-. Y = PF_6^- / ClO_4^-] , [M''(bdpab)$(NCS)_2$], [M'' = Ni(II), Co(II)] and binuclear complexes of the type [M'(bdpab)$(NCO)]_2(Y)_2$ where M' = Ni(II), Cd(II). Y = PF_6^- / ClO_4^- have been synthesized with ligand bdpab = *N*,*N*-bis(3,5-dimethyl-*1H*-pyrazol-1-yl)methyl-N_2-phenylethane-1,2-diamine and characterized. X-ray single crystal structural data shows five coordinated copper(II), Zinc(II) and cobalt(II) complexes are mononuclear with distorted square pyramidal geometry [for Cu(II) and Co(II)] or distorted trigonal bipyramidal geometry [for zinc(II)]. Mononuclear [M''(bdpab)$(NCS)_2$] [M'' = Co(II), Ni(II)] complexes have octahedral geometry and the geometry around each metal center in binuclear isocyanate bridged [M'(bdpab)$(NCO)]_2(Y)_2$ complexes are distorted octahedral. All complexes are ionic in nature except thiocyanate containing Co(II) and Ni(II) complexes. In binuclear isocyanate bridged complexes, the bridging mode is end-on ($\mu_{1,1}$-NCO) in the Cd(II) complex whereas the bridging mode is end-to-end ($\mu_{1,3}$-NCO) for Ni(II) complex. Complexes **9**, **11** and **13** have π-π stacking between the phenyl ring and pyrazole ring of the two nearest molecules and intermolecular hydrogen bonding between the oxygen atom of perchlorate ion and different H-atoms present in the ligand and finally 1D and 2D crystallographic network were obtained.

5(A).6. References:

1. A. Solanki, M.H. Sadhu, S.B. Kumar, P. Mitra, J. Mol. Struct. 1076 (2014) 475.
2. J.C. Liu, G.C. Guo, J. S. Huang, X.Z. You, Inorg. Chem. 42 (2003) 235.
3. B. Machura, A. Switlicka, I. Nawrot, J. Mrozinski, R. Kruszynski, Polyhedron 30 (2011) 832.
4. F.A. Mautner, M. Scherzer, C. Berger, R.C. Fischer, R. Vicente, S.S. Massoud, Polyhedron 85 (2015) 20.
5 S. Jana, R. Chandra Santra, S. Das, S. Chattopadhyay, J. Mol. Struct. 1074 (2014) 703.
6. P. Bhowmik, S. Chattopadhyay, M.G.B. Drew, A. Ghosh, Inorg. Chim. Acta 395 (2013) 24.
7. A. Beheshti, A. Lalegani, A. Noshadian, G. Bruno, H.A. Rudbari, Polyhedron 85 (2015) 690.
8. M. Gotzone Barandika, M.L. Hernandez-Pino, M.K. Urtiaga, R. Cortes, L. Lezama, M.I. Arriortua, T. Rojo, J. Chem. Soc., Dalton Trans. (2000) 1469.
9. H. Grove, M. Julve, F. Lloret, P.E. Kruger, K.W. Tornroos, J. Sletten, Inorg. Chim. Acta 325 (2001) 115.
10. M.S. El Fallah, A. Escuer, R. Vicente, F. Badyine, X. Solans, M. Font-Bardia, Inorg. Chem. 43 (2004) 7218.
11. T. Mallah, O. Kahn, J. Gouteron, S. Jeannin, Y. Jeannin, J. O'Connor, Inorg. Chem. 26 (1987) 1375
12. N. Kitanovski, A. Golobic., B. Ceh, Inorg. Chem. Commun. 8 (2005) 397.
13. P.K. Bhaumik, K. Harms, S. Chattopadhyay, Polyhedron 67 (2014) 181.
14. Y.-P. Quan, P. Yin, N.-N. Han, Ai.-H. Yang, H.-L. Gao, J.-Z. Cui, W. Shi, P. Cheng., Inorg. Chem. Commun. 12 (2009) 469.
15. N.K. Karan, S. Mitra, T. Matsushita, V. Gramlich, G. Rosair, Inorg. Chim. Acta 332 (2002) 87.
16. T. Silha, I. Nemec, R. Herchel, Z. Travnicek, Cryst. Eng. Comm. 15 (2013) 5351.
17. S. Sen, S. Mitra, D.L. Hughes, G. Rosair, C. Desplanches, Polyhedron 26 (2007)

1740.

18. P. Bhowmik, S. Chattopadhyay, M.G.B. Drew, C. Diaz, A. Ghosh, Polyhedron 29 (2010) 2637.
19. R. W. Saalfrank, I. Bernt, M.M. Chowdhry, F. Hampel, G.B.M. Vaughan, Chem. Eur. J. 7 (2001) 2765.
20. X.Y. Wang, B.L. Li, X. Zhu, S. Gao, Eur. J. Inorg. Chem. (2005) 3277.
21. X. Zhu, X.-Y. Wang, B.-L. Li, J. Wang, S. Gao, Polyhedron 31 (2012) 77.
22. T. Mallah, M.-L. Boillot, O. Kahn, J. Gouteron, S. Jeannin, Y. Jeannin, Inorg. Chem. 25 (1986) 3058.
23. O. Kahn, T. Mallah, J. Gouteron, S. Jeannin, Y. Jeannin, J. Chem. Soc., Dalton Trans. (1989) 1117.
24. O.J. Parker, M.P. Wolther, G.L. Breneman, Acta. Crystallogr, Sect. C 52 (1996) 1089.
25. T. Rojo, R. Cortes, L. Lezama, J.L. Mesa, J. Via, M.I. Arriortua, Inorg. Chim. Acta 165 (1989) 91.
26. J.A. Real, M. Mollar, R. Ruiz, J. Faus, F. Lloret, M. Julve, M.P. Levisalles, J. Chem. Soc. Dalton Trans. (1993) 1483.
27. G. Vuckovic, Z.M. Miodragovic, S. Tanaskovic, J. Serb. Chem. Soc. 69 (2001) 17.
28. F. Lloret, M. Julve, J. Faus, R. Ruiz, I. Castro, M. Mollar, M. Philoche-Levisalles, Inorg. Chem. 31 (1992) 784.
29. P. Gomez, G.A. Van Albada, I. Mutikainen, U. Turpeinen, J. Reedijk, Inorg. Chim. Acta 358 (2005) 1975.
30. J.-M. Lehn, 'Supramolecular Chemistry: Concepts and Perspectives', VCH, Weinheim, (1995).
31. B. Chand, U. Ray, G. Mostafa, T. Lu, C. Sinha, Polyhedron 23 (2004) 1669.
32. H. Chowdhury, R. Ghosh, S.H. Rahaman, B.K. Ghosh, Polyhedron 26 (2007) 5023.
33. D. Bose, J. Banerjee, S.H. Rahaman, G. Mostafa, H.-K. Fun, R.D. Bailey Walsh, M.J. Zaworotko, B.K. Ghosh, Polyhedron 23 (2004) 2045.
34. P. Kar, R. Biswas, M.G.B. Drew, A. Frontera, A. Ghosh, Inorg. Chem. 51 (2012)

1837.

35. L.K. Das, C. Diaz, A. Ghosh, Cryst. Growth Des. 15 (2015) 3939.
36. M.H. Sadhu, A.Solanki, S.B. Kumar, Polyhedron 100 (2015) 206.
37. Agilent, CrysAlis PRO. Agilent Technologies UK Ltd, Yarnton, England, (2011)
38. G.M. Sheldrick, SAINT, 5.1 ed. Siemens Industrial Automation Inc., Madison, WI, (1995)
39. G.M. Sheldrick. SHELXL-97: Program for Crystal Structure Refinement, University of Gottingen, Gottingen, (1997).
40. L.J. Farrugia, J. Appl. Cryst. 32 (1999) 837.
41. W.J. Geary, Coord. Chem. Rev.7 (1971) 81.
42. A. Turco, C. Pecile, Nature 191 (1961) 66.
43. P.J. Arnold, S.C. Davies, M.C. Durrant, D.V. Griffiths, D.L. Hughes, P.C. Sharpe, Inorg. Chim. Acta 348 (2003) 143.
44. S.R. Ananias, A.E. Mauro, V.A. de LucaaNeto, Trans. Met. Chem. 26 (2001) 570.
45. S.R. Ananias, A.E. Mauro, K. Zutin, Trans. Met. Chem. 29 (2004) 284.
46 K. Nakamoto, Infrared and Raman Spectra of Inorganic and Coordination Compounds, 3rd edn. Wiley Interscience, New York, (1978).
47. B.J. Hathaway, in: G. Wilkinson, R.D. Gillard, J.A. McCleverty (Eds.), Comprehensive Coordination Chemistry, vol. 5, Pergamon Press, Oxford, England, (1987) 533
48 F.A. Moutner, C.N. Landry, A.A. Gallo, S.S. Massoud, J. Mol. Struct. 837 (2007) 72.
49. U. Mukhopadhayay, I. Bernal, S.S. Massoud, F.A. Moutner, Inorg. Chim. Acta 357 (2004) 3673.
50. A. Garoufis, S. Kasselouri, C.P. Raptopoulou, Inorg. Chem. Commun. 3 (2000) 251.
51. J. Matsumoto, T. Suzuki, Y. Kajita, H. Masuda, Dalton Trans. 41 (2012) 4107.
52. S. Sabiah, B. Varghese, N.N. Murthy. Dalton Trans. (2009) 9770.
53. A.W. Addison, T.N. Rao, J.Reedijk, J.V. Rijn, G.C. Verschoor, J. Chem. Soc. Dalton Trans. (1984) 1349.

54. F.A. Mautner, F.R. Louka, T. LeGuet, S.S. Massoud, J. Mol. Struct. 919 (2009) 196.
55. F.A. Mautner, M. Scherzer, C. Berger, R.C. Fischer, S.S. Massoud, Inorg. Chim Acta 425 (2015) 46.
56. B.A. Yamgar, V.A. Sawant, S.K. Sawant, S.S. Chavan, J. Coord. Chem. 62 (2009) 2367.
57. J. Vallejo, Isabel Castro, R. Ruiz-García, J. Cano, M. Julve, F. Lloret, G. De. Munno, W. Wernsdorfer, E. Pardo, J. Am. Chem. Soc. 134 (2012) 15704.
58. F.A. Mautner, M. Scherzer, C. Berger, R.C. Fischer, R. Vicente, S.S. Massoud, Polyhedron 85 (2015) 20.
59. A. Solanki, Y. Patil, S.B. Kumar, J. Coord. Chem. 68 (2015) 4017.
60. A. Solanki, S.B. Kumar, A.A. Doshi , C.R. Prabha, Polyhedron 63 (2013) 147.
61. K. Avasthi, L. Shukla, R. Kant, K. Ravikumarc, Acta Cryst. C70 (2014) 555.
62. M. Zala, A. Solanki, S.B. Kumar, A. Escuer, E.Suresh, Inorg. Chim. Acta 375 (2011) 333.

Abstract

Four mononuclear selenocyanate containing complexes namely $[Ni(bdpab)(NCSe)_2]$, $[Co(bdpab)(NCSe)_2]$, $[Zn(bdpab)(NCSe)]Y$ ($Y = ClO_4^-$, PF_6^-) and two one-dimensional polymeric selenocyanato and thiocyanato bridged cadmium(II) complexes $[Cd(dpip)(\mu_{1,3}\text{-}SeCN)_2]_n$ and $[Cd(dpip)(\mu_{1,3}\text{-}SCN)_2]_n$, where bdpab = *N*,*N*-bis(3,5-dimethyl-*1H*-pyrazol-1-yl)methyl-N_2-phenylethane-1,2-diamine and dpip = 3,5-dimethyl-1-((3-phenylimidazolidin-1-yl)-methyl)-*1H*-pyrazole have been synthesized and characterized by microanalyses, spectroscopic methods and single crystal X-ray diffraction studies. The bidentate N_2-coordinated ligand dpip is formed from N_4-coordinated tetradentate ligand bdpab due to unusual transformation during in situ complexation reaction. Structural data confirmed that mononuclear zinc(II) complex is five coordinated with distorted trigonal bipyramidal geometry whereas mononuclear Ni(II) and Co(II) complexes and polynuclear Cd(II) complexes are six coordinated with distorted octahedral geometry. In both the polymeric Cd(II) complexes, two Cd centres are bridged by end-to-end (μ-1,3) (EE) NCS/NCSe ligands and form 1D zig-zag chain. The DFT calculations performed with cadmium(II) complexes $[Cd(dpip)(\mu_{1,3}\text{-}SCN)_2]_n$ and $[Cd(dpip)(\mu_{1,3}\text{-}SeCN)_2]_n$ corroborated the observed crystal structures and the structural parameter were found to be in good agreement in both calculated and X-ray geometries. The distortions in the above two cadmium molecules are due to two unequal Cd-N (organic ligand dpip) bond lengths and small bite angle of the unsymmetrical organic ligand.

5(B). 1. Introduction

Thiocyanate (SCN^-) and selenocyanate ($SeCN^-$) are ambidentate ligands and they generally coordinate with metal ions through the nitrogen atom while acting as monodentate ligand and form mononuclear complexes [1-7]. They can also act as bridging ligands and bridges the metal centres with different coordination modes such as μ-1,3(NCS/Se) or μ-1,1(NCS/Se) and form different types of bridging networks [8-11] and also form supramolecular complexes [12-18]. The tetradentate N_4-coordinate ligand (bdpab) shows an interesting coordination behaviour towards Cu(II), Co(II), Zn(II), Ni(II) and Cd(II) ion in presence of co-ligand like $SeCN^-$ and NCS^- in methanol. The ligand bdpab used its four potential donor sites and formed mononuclear complexes with distorted trigonal bipyramidal geometry with metal ions like Cu(II), Co(II), Zn(II) and Ni(II) in presence of co-ligands such as $SeCN^-$ and NCS^- ions [19-20]. In the case of Cd(II), however, the ligand molecule undergo two changes during in situ complexation reaction (i). The ligand molecule losses one pryazolyl arm by the activation of C-N single bond and the ligand bdpab is transformed into bidentate N_2-coordination ligand from tetradentate ligand. (ii). A new five member saturated imidazole type ring formed by cyclization. There are few examples where in situ tetradentate ligand is transformed into tridentate ligand after losing one pyrzolyl arm but there is probably no report where tetradentate ligand transformed into bidentate ligand and formation of saturated imidazole type ring [21-25].

In this chapter, we discuss the synthesis, characterization, crystal structures of six coordinate $[Ni(bdpab)(NCSe)_2]$, $[Co(bdpab)(NCSe)_2]$ complexes and five coordinate zinc(II) complexes $[Zn(bdpab)(NCSe)]Y$ [Y = ClO_4^- or PF_6^-] with N_4-coordinated tetradentate ligand *N,N*-bis(3,5-dimethyl-*1H*-pyrazol-1-yl)methyl-N_2-phenylethane-1,2-diamine (bdpab) and two polymeric octahedral cadmium(II) complexes $[Cd(dpip)(SCN)_2]_n$ and $[Cd(dpip)(SeCN)_2]_n$ where dpip is 3,5-dimethyl-1-((3-phenylimidzolidin-1-yl)-*1H*-pyrazole, a bidentate N_2-coordinate ligand (dpip) formed from tetradentate N_4-coordinate ligand *N,N*-bis(3,5-dimethyl-*1H*-pyrazol-1-yl)methyl-N_2-phenylethane-1,2-diamine (bdpab). DFT calculations have been performed to examine the structural parameters of two cadmium(II) complexes $[Cd(dpip)(\mu_{1,3}\text{-}SCN)_2]_n$ and $[Cd(dpip)(\mu_{1,3}\text{-}SeCN)_2]_n$.

5(B).2. Experimental

5(B).2.1. Materials

Materials used for the syntheses of ligands and complexes are discussed in Chapter 5(A) [section 5(A).2.1.]. KSeCN (Aldrich) was reagent grade and used as received.

5(B).2.2. Syntheses of complexes

Caution! Transition metal complexes with perchlorate ion and organic ligands are potentially explosive. Only a small amount of material should be synthesized and should be handled with care.

5(B).2.2.1. Synthesis of [Ni(bdpab)(NCSe)$_2$] (1)

To a methanol solution (10 ml) of $Ni(ClO_4)_2.6H_2O$ (0.183 g, 0.5 mmol), a solution of the ligand (bdpab) (0.176 g, 0.5 mmol) in the same solvent (10 ml) was slowly added with stirring at room temperature. After 10 min, methanol solution (10 ml) of KSeCN (0.072 g, 0.5 mmol) was added drop by drop. The stirring was continued for an additional 3h in the dark and filtered. The filtrate was left for slow evaporation at room temp. Light green colour crystals suitable for X-ray diffraction were obtained after several days. The crystal were isolated by filtration and dried in vacuum.

Yield. 0.072 g (46%). Found %. C = 42.70, H = 4.56, N = 18.13% Anal calc for $C_{22}H_{28}NiN_8Se_2$: C = 42.54 , H = 4.54, N = 18.04%. IR (KBr pellet) cm^{-1}: ν(-NH), 3172 vs; ν($NCSe^-$), 2103, 2063 vs; ν(C = C)/ph ring, 1601 s; ν(C = C) + ν (C = N)/pz ring 1557 s, 1479 s. UV-Vis spectra: λ_{max}/nm (ε_{max}/$mol^{-1}cm^{-1}$). 943 (22), 578 (21), 295 (415), 219 (29606). Λ_M ($\Omega^{-1}cm^2\,mol^{-1}$) = 16. μ_{eff} = 2.76 BM.

5(B).2.2.2. Synthesis of [Co(bdpab)(NCSe)$_2$] (2)

A methanol solution of ligand bdpab (0.176 g, 0.5 mmol) was slowly added to a stirring methanol solution (10 ml) of $Co(ClO_4)_2.6H_2O$ (0.183 g, 0.5 mmol) at room temperature. After 10 min, a methanol solution (10 ml) of KSeCN (0.072 g, 0.5 mmol) was added into it drop by drop. The stirring was continued for an additional 3h in the dark and then the reaction mixture was filtered. The filtrate was left for slow evaporation at room temp. Light pink colour crystals suitable for X-ray diffraction

were obtained after several days. The crystal were isolated by filtration and dried in vacuum.

Yield. 0.083 g (53%). Found C = 42.48, H = 4.51, N = 18.10%. Anal calc for $C_{22}H_{28}CoN_8Se_2$: C = 42.53, H = 4.54, N = 18.03%. IR (KBr pellet) cm^{-1}: ν(-NH), 3176 vs; ν($NCSe^-$), 2090,2056 vs; ν(C = C)/ph ring, 1601 s; ν(C = C) + ν (C = N)/pz ringЬ 1553 s, 1499 s. UV-Vis spectra: λ_{max}/nm (ε_{max}/$mol^{-1}cm^{-1}$). 578 (159), 492 (132), 295 (1415), 247 (7525). Λ_M ($\Omega^{-1}cm^2\ mol^{-1}$) = 12. μ_{eff} = 3.76 BM.

5(B).2.2.3. Synthesis of [Zn(bdpab)(NCSe)]ClO_4 (3)

The compound was synthesized by following the procedure for complex **1** except $Zn(ClO_4)_2.6H_2O$ (0.186 g, 0.5 mmol) was used instead of nickel perchlorate. Colour less crystals suitable for X-ray diffraction were obtained after several days.

Yield. 0.112 g (72%). Found C = 40.61, H = 4.52, N = 15.53%, Anal calc for $C_{21}H_{28}ClN_7SeO_4Zn$: C = 40.53, H = 4.54, N = 15.76%. IR (KBr pellet) cm^{-1}: ν(-NH), 3276 vs; ν($NCSe^-$), 2090 vs; ν(C = C)/ph ring, 1600 s; ν(C = C) + ν (C = N)/pz ring, 1554 s, 1467 s; ν(ClO_4^-), 1108 br. UV-Vis spectra: λ_{max}/nm (ε_{max}/$mol^{-1}cm^{-1}$). 297 (2725), 247 (15032). Λ_M ($\Omega^{-1}cm^2\ mol^{-1}$) = 120.

5(B).2.2.4. Synthesis of [Zn(bdpab)(NCSe)]PF_6 (4)

To a methanol solution (10 ml) of $Zn(NO_3)_2.6H_2O$ (0.148 g, 0.5 mmol) a solution of the ligand (bdpab)(0.176 g, 0.5 mmol) in the same solvent (10 ml) was slowly added with stirring at room temperature. After 10 min, methanol solution (10 ml) of KSeCN (0.072 g, 0.5 mmol) was added slowly. Finally after 10 min, NH_4PF_6 (0.084 g, 0.5 mmol) in methanol (10 ml) was added and the stirring was continued for an additional 3h in dark chamber. Filtered the solution and the colour less filtrate was left for slow evaporation at room temperature. Colourless crystals suitable for X-ray diffraction were obtained from the filtrate after several days. The crystal were isolated by filtration and air-dried.

Yield. 0.128 g (78%). Found C = 40.87, H = 4.52 , N = 15.78%. Anal calc for $C_{21}H_{28}N_7SePF_6Zn$: C = 40.77, H = 4.23, N = 14.68%. IR (KBr pellet) cm^{-1}: ν(-NH), 3299 vs; ν($NCSe^-$), 2099 vs ; ν(C = C)/ph ring, 1600 s; ν(C = C) + ν (C = N)/pz ring, 1555 s, 1469 s; ν(PF_6^-), 840 br. UV-Vis spectra: λ_{max}/nm (ε_{max}/$mol^{-1}cm^{-1}$). 278 (1794), 240 (10385). Λ_M ($\Omega^{-1}cm^2\ mol^{-1}$) = 122.

5(B).2.2.5. Synthesis of $[Cd(dpip)(SCN)_2]_n$ (5)

The complex $[Cd(dpip)(SCN)_2]_n$ was synthesized by the addition of ligand bdpab (0.176 g, 0.5 mmol) in methanol (10 ml) to a stirring solution of cadmium perchlorate (0.210 g, 0.5 mmol) in methanol (10 ml) at room temperature. After 10 min, a solution (10 ml) of KNCS (0.050 g, 0.5 mmol) in aqueous methanol (1:20) was added slowly. The final resulting colourless solution was stirred for 3 h at room temperature, filtered and the filtrate was kept for slow evaporation. Colourless square shape crystals were isolated after one week.

Yield. 0.078 g (62%). Found C = 42.25, H = 4.20, N = 17.41%. Anal calc for $C_{17}H_{20}CdN_6S_2$: C = 42.11, H = 4.16, N = 17.33%. IR (KBr pellet) cm^{-1}: $\nu(NCS^-)$, 2101vs; ν(C=C), 1599s; ν(C=C)+ν(C=N)/pz ring, 1552s,1461s. ^{1}H NMR (400 MHz, DMSO-d_6, 20°C), δ/ppm: 2.13 (s, 3H, -CH_3 of pz), 2.26 (s, 3H, -CH_3 of pz), 3.06-3.09 (t, J = 6.8 Hz, 2H, -N-CH_2-CH_2), 3.27-3.30 (t, J = 6.4 Hz,2H, -N-CH_2-CH_2), 4.1 (s, 2H, N-CH_2-N-pz ring), 4.9 (s, 2H, N-CH_2-N), 5.9 (s, 1H, pz ring), 6.46-6.48 (d, 2H, J = 7.6 Hz, phenyl ring), 6.6-6.65 (t, 1H, J = 7.2, 7.6 Hz, phenyl ring), 7.15-7.19 (m, 2H, phenyl ring).

5(B).2.2.6. Synthesis of $[Cd(dpip)(SeCN)_2]_n$ (6)

The complex $[Cd(dpip)(SeCN)_2]_n$ was synthesized by the addition of ligand bdpab (0.176 g, 0.5 mmol) in methanol (10 ml) to a stirring solution of cadmium perchlorate (0.210 g, 0.5 mmol) in methanol (10 ml) at room temperature. After 10 min, an aqueous methanol (1:20) (10ml) solution of KSeCN (0.072 g, 0.5 mmol) was slowly added and the resulting solution was stirred at room temperature in dark for additional 3 h, filtered and the filtrate was kept it for slow evaporation. Colourless square shape crystals were isolated after one week.

Yield. 0.108 g (64%). Found C = 43.43, H = 3.51, N = 14.61%. Anal calc for $C_{17}H_{20}CdN_6Se_2$: C = 43.28, H = 3.48, N = 14.52%. IR (KBr pellet) cm^{-1}: $\nu(NCSe^-)$, 2109, 2098 vs ; ν(C = C), 1599 s; ν(C = C) + ν(C = N)/pz ring, 1559 s, 1460 s. ^{1}H NMR (400 MHz, DMSO-d_6, 20°C), δ/ppm: 2.09 (s, 3H, -CH_3 of pz), 2.27 (s, 3H, -CH_3 of pz), 3.05-3.08 (t, J = 6.4 Hz, 2H, -N-CH_2-CH_2), 3.24-3.27 (t, J = 6.4 Hz, 2H, -N-CH_2-CH_2), 4.2 (s, 2H, N-CH_2-N-pz ring), 4.92 (s, 2H, N-CH_2-N), 5.86 (s, 1H, pz ring), 6.45-6.69 (d, 2H, J = 7.6 Hz, phenyl ring), 6.62 (t, 1H, J = 7.2, 7.6 Hz, phenyl ring), 7.14-7.18 (m, 2H, phenyl ring).

5(B).3. X-ray structure determination

The summary of data collection and structure refinement parameters for the compounds **1**-**3**, **5** and **6** are given in Table 5(B).1 and selected bond lengths (Å) and angels (º) are given in Table 5(B).2. Crystals of suitable size of complexes [crystal size: **1**, 0.25 x 0.17 x 0.12 mm; **2**, 0.25 x 0.17 x 0.12 mm; **3**, 0.34 x 0.27 x 0.25 mm; **5**, 0.22 x 0.19 x 0.16 mm; **6**, 0.25 x 0.17 x 0.12 mm] were obtained by slow evaporation of methanol solution. Data were collected with Mo-K_α radiation (λ = 0.71073Å) at 273 and 110 K for **1** and **2**, respectively and with Cu-K_α radiation (λ = 1.54184 Å) at 150 K for **3** and at 110 K for both polynuclear cadmium(II) complexes on an Oxford X-CALIBUR-S diffractometer with CCD area detector. The data interpretations were processed with CrysAlisPro, Agilent Technologies, Version 1.171.35.19 [26] and an absorption correction based on multi-scan method was applied [27]. All structures were solved by using direct methods and refined by the full-matrix least-square based on F^2 technique using SHELXL-97 program package [28]. At convergence, the final residual were R1 = 0.0899 (for complex **1**), 0.0981 (for complex **2**), 0.0710 (for complex **3**), 0.0985 (for complex **5**) and 0.0689 (for complex **6**); R2 = 0.2679 (for complex **1**), 0.2790 (for complex **2**), 0.1872 (for complex **3**), 0.2492 (for complex **5**) and 0.1887 (for complex **6**) with I >2σ (I), goodness fit = 1.049 (for complex **1**), 1.082 (for complex **2**), 1.054 (for complex **3**), 1.087 (for complex **5**) and 1.045 (**6**). The final differences Fourier map showed the maximum and minimum peak heights of 2.07 and -1.85 eA^{-3} for **1**, 1.64 and -1.76 eA^{-3} for **2**, 0.63 and -1.72 eA^{-3} for **3**, 2.70 and -2.26 eA^{-3} for **5**, and 1.53 and -1.71 eA^{-3} for **6**. All calculations were carried out using WinGX system Ver-1.64 [29]. All non-hydrogen atoms were refined anisotropically. The positions of the hydrogen atoms were located at their calculated position and treated as riding on the respective atoms to which they are attached.

Table 5(B).1. Crystal parameters of complexes **1**, **2**, **3, 5** and **6.**

Empirical formula	$C_{22}H_{28}NiN_8Se_2$ **(1)**	$C_{22}H_{28}CoN_8Se_2$ **(2)**	$C_{21}H_{28}ClN_7O_4SeZn$ **(3)**	$C_{17}H_{20}CdN_6S_2$ **(5)**	$C_{17}H_{20}CdN_6Se_2$ **(6)**
Formula weight	621.12	621.36	622.29	484.92	578.72
Temperature (K)	293(2)	293(2)	110(2)	110(2)	110(2)
Wavelength (Å)	0.71073	1.54184	0.71073	1.54184	1.54184
Crystal system	monoclinic	monoclinic	triclinic	monoclinic	monoclinic
Space group	*P21/c*	*P21/c*	*P -1*	$P2_1/c$	$P2_1/c$
a (Å)	9.4523(11)	9.3920(5)	7.8654(5)	19.2236(9)	19.0676(7)
b (Å)	13.4524(15)	13.5214(6)	9.7267(6)	10.8909(4)	10.9606(4)
c (Å)	20.1926(19)	20.2511(8)	17.8747(13)	9.9493(4)	10.1716(4)
α, (°)	90.00	90.0	87.706(5)	90.00	90.0
β(°)	91.328(9)	91.526(4)	79.697(6)	101.106(4)	100.464(3)
γ (°)	90.00	90.00	72.279(6)	90.00	90.00
Volume ($Å^3$)	2566.9(5)	2570.8(2)	1281.46(16)	2044.00(15)	2090.43(14)
Z	4	4	2	4	4
Density (g cm^{-3})	1.516	1.685	1.6127	1.576	1.794
Absorption coefficient (mm^{-1})	2.900	1.094	2.525	10.571	12.435
F(000)	1248	1288	633	976.0	1120.0

θ range for data collection (°)	6.38 to 58.02	7.86 to 146.54	6.34 to 57.86	9.38 to 146.5	9.34 to 146.16
Index ranges	$-10 \le h \le 12$,	$11 \le h \le 11$,	$-10 \le h \le 8$,	$-23 \le h \le 23$,	$-23 \le h \le 23$,
	$-18 \le k \le 16$,	$-15 \le k \le 16$,	$-12 \le k \le 12$,	$-13 \le k \le 13$,	$-13 \le k \le 13$,
	$-19 \le l \le 26$	$-24 \le l \le 25$	$-24 \le l \le 21$	$-8 \le l \le 12$	$-9 \le l \le 12$
Reflections collected	11977	16158	10120	11356	12663
Independent reflections	5858	5151	5758	4114	4196
	[R(int) = 0.0362]	[R(int) = 0.0614]	[R(int) = 0.0270]	[R(int) = 0.1007]	[R(int) = 0.0932]
Data / restraints / parameters	5858/0/302	5151/0/302	5758/0/313	4114/0/237	4196/0/235
Goodness-of-fit on F^2	1.049	1.082	1.054	1.087	1.045
Final R indices [I>2sigma(I)]	*R1* = 0.0899,	*R1* = 0.0981,	*R1* = 0.0710,	*R1* = 0.0985,	*R1* = 0.0689,
	wR2 = 0.2679	*wR2* = 0.2790	*wR2* = 0.1872	*wR2* = 0.2492	*wR2* = 0.1887
R indices (all data)	*R1* = 0.1320,	*R1* = 0.1371,	*R1* = 0.0855,	*R1* = 0.1073,	*R1* = 0.0737,
	wR2 = 0.3084	*wR2* = 0.3110	*wR2* = 0.2017	*wR2* = 0.2718	*wR2* = 0.1995
Largest diff. peak and hole (eA^{-3})	2.07 and -1.85	1.64 and -1.76	0.63 and -1.72	2.70 and -2.26	1.54 and -1.71
CCDC number	1401708	1401707	1401709	1501914	1501915

5(B).4. Results and Discussion

5(B).4.1. Syntheses

Mononuclear octahedral cobalt(II) and nickel(II) complexes of the type $[M(bdpab)(NCSe)_2]$ [M = Ni(II) or Co(II)], five coordinate Zn(II) complexes [Zn(bdpab)(NCSe)]Y [Y^- = ClO_4 **(3)** or, PF_6 **(4)**] and double end-to-end zig-zag SeCN/NCS bridged polymeric cadmium complexes of the type $[Cd(dpip)(X)_2]_n$ [X^- = NCS (**5)** or SeCN(**6)**] were obtained with good yield (~ 65 %) upon one-pot synthesis of 1:1:1 molar ratio of metal perchlorate, tetradenatate ligand bdpab and potassium thiocyanate / potassium selenocyanate in a methanol solvent at room temperature (Scheme 5(B).1). The molecular compositions of the complexes were confirmed by microanalyses and spectroscopic studies. The structures of complexes **1-3, 5** and **6** were determined by single crystal X-ray diffraction studies [Figs.5(B).10(a), 11(a), 12(a), 13(b) and 14(b).]. The structural data revealed that the mononuclear Co(II) and Ni(II) complexes are six coordinated and the zinc(II) complex is five coordinated whereas cadmium complexes are six coordinated with μ-1,3 NCS/SeCN bridged and form 1D polymeric chain. The important aspect of the synthesis is that the tetradentate N_4-coordinate ligand bdpab is transformed into bidentate N_2-coordinte ligand 3,5-dimethyl-1-((3-phenylimidzolidin-1-yl)methyl)-1-H-pyrazole (dpip) with the formation of saturated imidazole ring due to cyclization of $-CH_2$ group of one pyrazolyl arm between two N atoms of the ethylene spacer. When the same reaction was carried out using other than alcohol, it is obtained as soluble mass but without any crystal. Molar conductivity data of complexes **1-4** in CH_3CN (10^{-3} M) show that the Co(II) and Ni(II) complexes are non- electrolytes (Λ_M = 10 $\Omega^{-1}cm^2\,mol^{-1}$) whereas zinc the complexes are 1:1 electrolytes (Λ_M ~120 $\Omega^{-1}cm^2\,mol^{-1}$) [30]. Complexes **1-4** are soluble in common organic solvents such as methylene chloride, acetonitrile, methanol, ethanol etc and complexes **5** and **6** are soluble in DMF/DMSO and insoluble in common organic solvent.

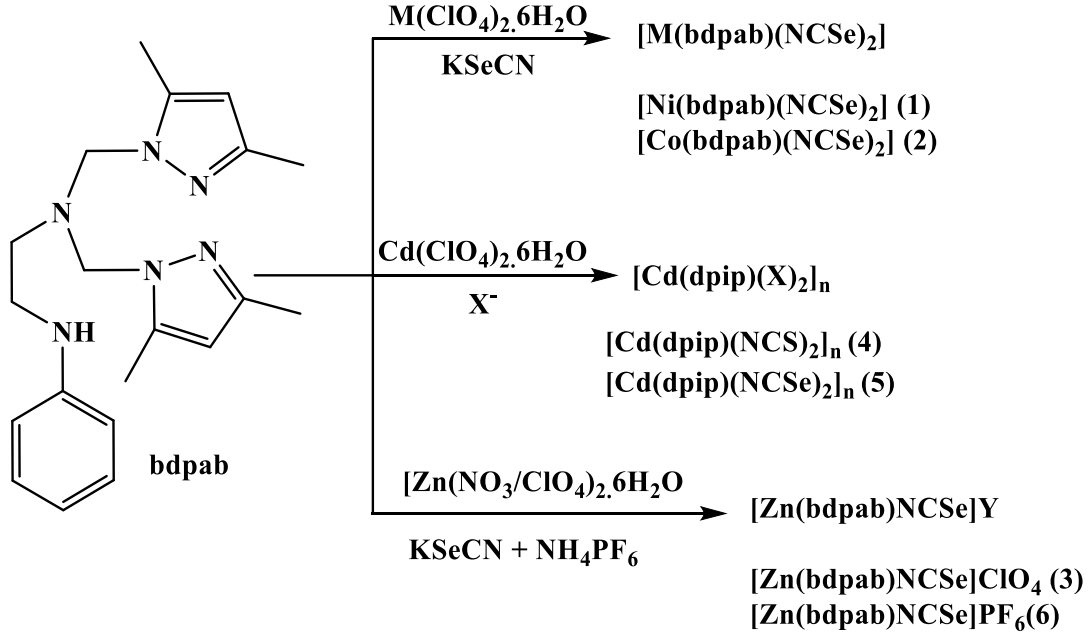

Scheme 5(B).1. Synthesis of complexes.

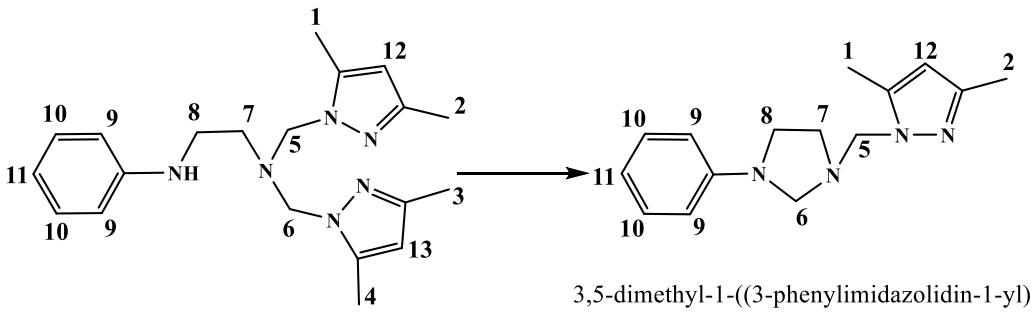

N^1,N^1-bis((3,5-dimethyl-1*H*-pyrazol-1-yl)methyl)-N^2-phenylethane-1,2-diamine
(bdpab)

3,5-dimethyl-1-((3-phenylimidazolidin-1-yl) methyl)-1*H*-pyrazole
(dpip)

Since ligand and co-ligands (NCS^-/$SeCN^-$) were same for copper(II), nickel(II), cobalt(II) and zinc(II) complexes [19-20] but ligand transformation had taken place in cadmium(II) complexes, it can be assumed that moderate acidic cadmium(II) and bridging nature of the ambidentate NCS/SeCN ions are responsible for the removal of pyrazole molecule and the formation of imidazole type ring in the serendipitous synthesis.

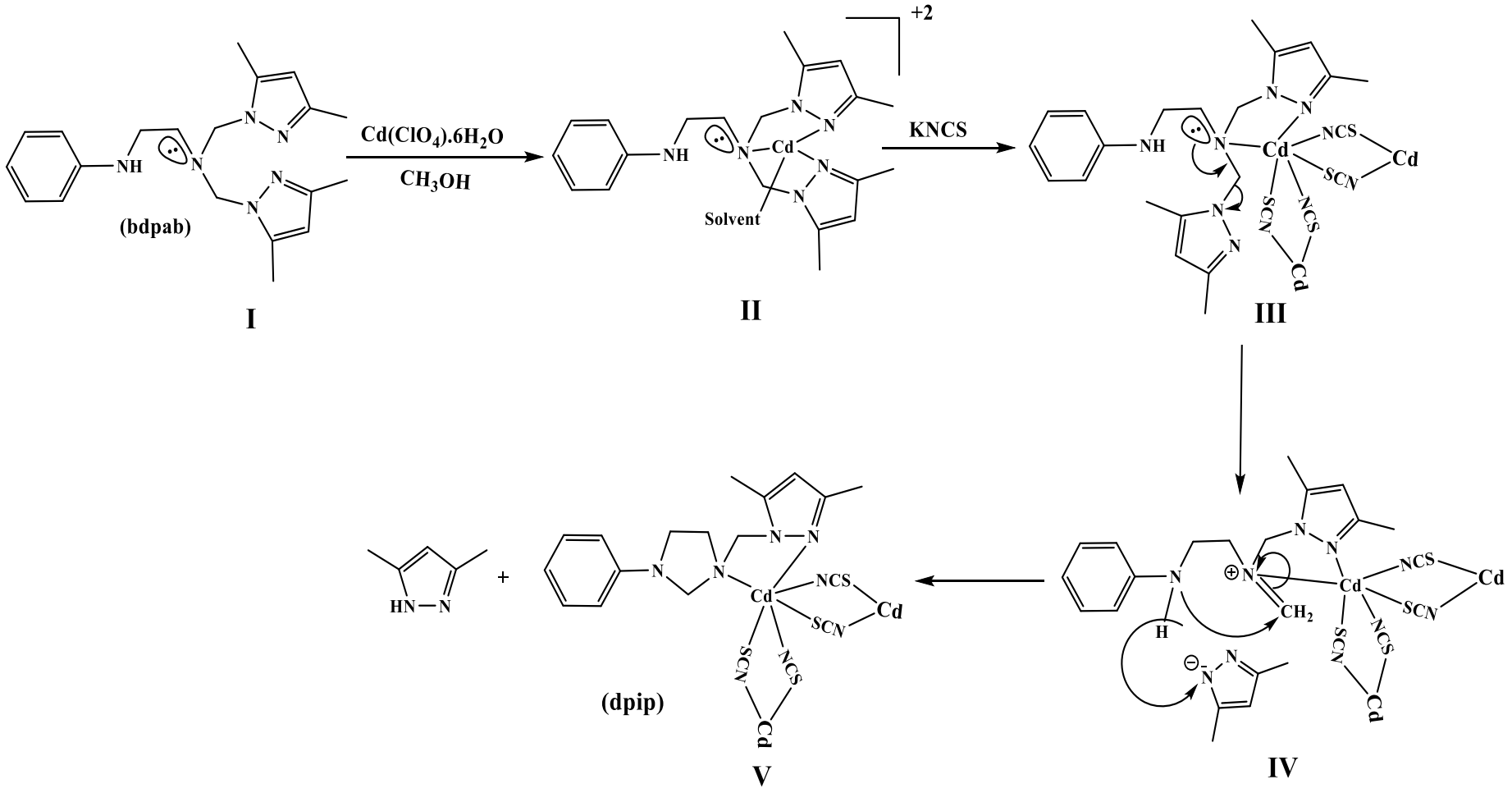

Scheme 5(B).2. Mechanism of in situ ligand transformation reaction of complexes **5** and **6**.

When ligand bdpab is added to Cd(II) solution, $[Cd(bdpab)(solvent)]^{+2}$ complex was formed and three coordination sites of the ligand and one solvent molecule were coordinate with cadmium centre [31]. Since moderate acidic Cd(II) has affinity towards both nitrogen and sulphur / selenium atom of the ambidentate NCS/SeCN ligand, four coordination sites of the Cd(II) centre were occupied by co-ligand NCS or SeCN ions for the formation polynuclear bridged complex when SCN/SeCN ions are added into the solution and forced bdpab ligand acts as bidentate for the formation of octahedral complex, leaving one weakly coordinated pyrazolyl group remain uncoordinated [23]. The pendant arm of tetradentate ligand was removed by cleaving one C-N bond between N(pyrazole)-CH_2 of N(pyrazole)-CH_2-N(amine) arm and thereby formation of N^+(amine)=CH_2 and pz^- ion [21]. This N^+(amine)=CH_2 is then react with –NH group attached with phenyl ring in a C-N bond formation reaction and form a saturated imidazole type ring with removal of pyrazole molecule [Scheme 5(B).2].

5(B).4.2. IR and ^{1}H NMR data

The infrared spectra of complexes **1-6** showed two strong bands at ~1553 and ~1464 cm^{-1} which are assigned as ν(C = C) + ν (C = N) of pyrazole ring. These bands are also present in the spectrum of the free ligand (bdpab) which indicating the coordination of pyrazole ring to the metal centres in the complexes. Ligand bdpab and complexes **1-4** have one medium intensity band at ~3205 cm^{-1} assigned as *ν*(-NH) stretching frequency and this *ν*(-NH) band is missing in the IR spectra of Cd(II) complexes **5** and **6** indicating the formation of new bond. The binding mode of the SeCN ligand is confirmed by the strong IR band below 2100 cm^{-1}. The ν(CN) asymmetric stretching vibration for N-bonded SeCN- usually appears below 2100 cm^{-1}, whereas Se-bonded $SeCN^-$ appears above 2100 cm^{-1} [32-33]. For NCS ligand bridging $\mu_{1,1}$–NCS ion band appears at ~2050 cm^{-1} and $\mu_{1,3}$–NCS ion band appears at ~2100 cm^{-1}. The spectra show a strong band at ~2089 and 2099 cm^{-1} for zinc(II) complexes **3** and **4** respectively, which are assigned as N-bonded ν($NCSe^-$). Similarly, two bands each at ~2100 and ~2090 cm^{-1} for both the Ni(II) and Co(II) complexes can be assigned as two N-bonded ν($NCSe^-$) modes. Complex **5** shows sharp intense band at 2101 cm^{-1}, indicating two cadmium metal centres are bridged by $\mu_{1,3}$ – NCS ion [34-35]. IR spectra of complex **6** shows two bands at 2098 and 2109 cm^{-1} indicating the presence of the bridging μ-1,3 selenocyanate groups. The

coordination modes of SCN and SeCN ions and formation of C-N bond of Cd(II) complexes are also confirmed by the single crystal structures of the complexes. For complex **3**, a strong band at 1108 cm^{-1} is assigned to $\nu(ClO_4^-)$, and a weak band at 624 cm^{-1} due to δ(Cl-O-Cl), while for complex **4**, a strong band at 840 nm is due to $\nu(PF_6^-)$, confirming the presence of perchlorate and hexaflurophosphate ions outside the coordination sphere [36]. All other major bands of the ligand are also present in the spectra of the complexes.

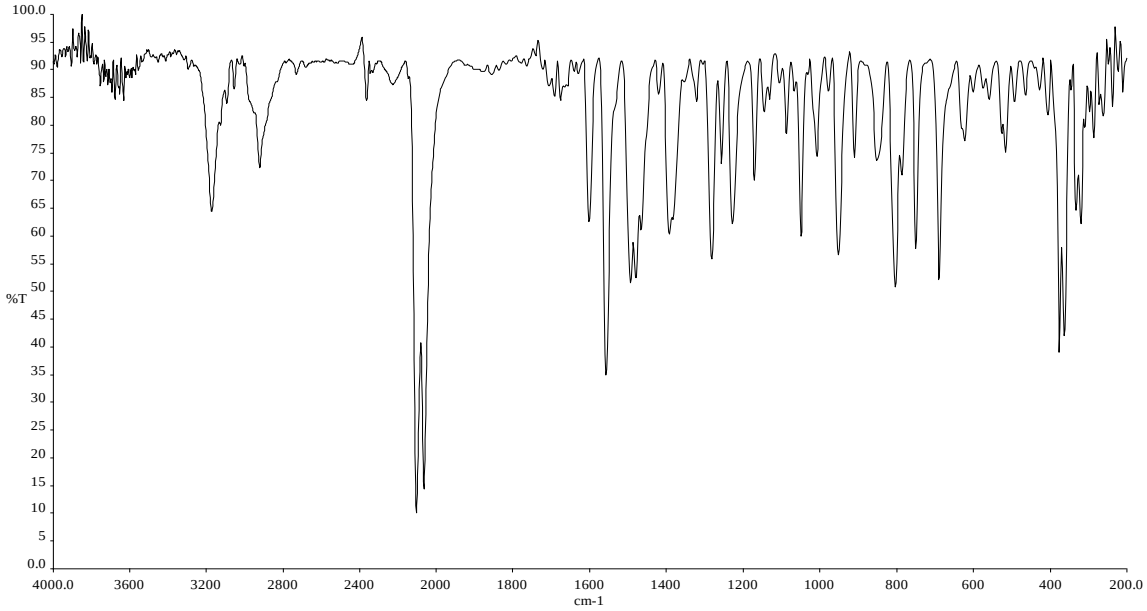

Fig.5(B).1 IR spectrum of $[Ni(bdpab)(NCSe)_2]$ (**1).**

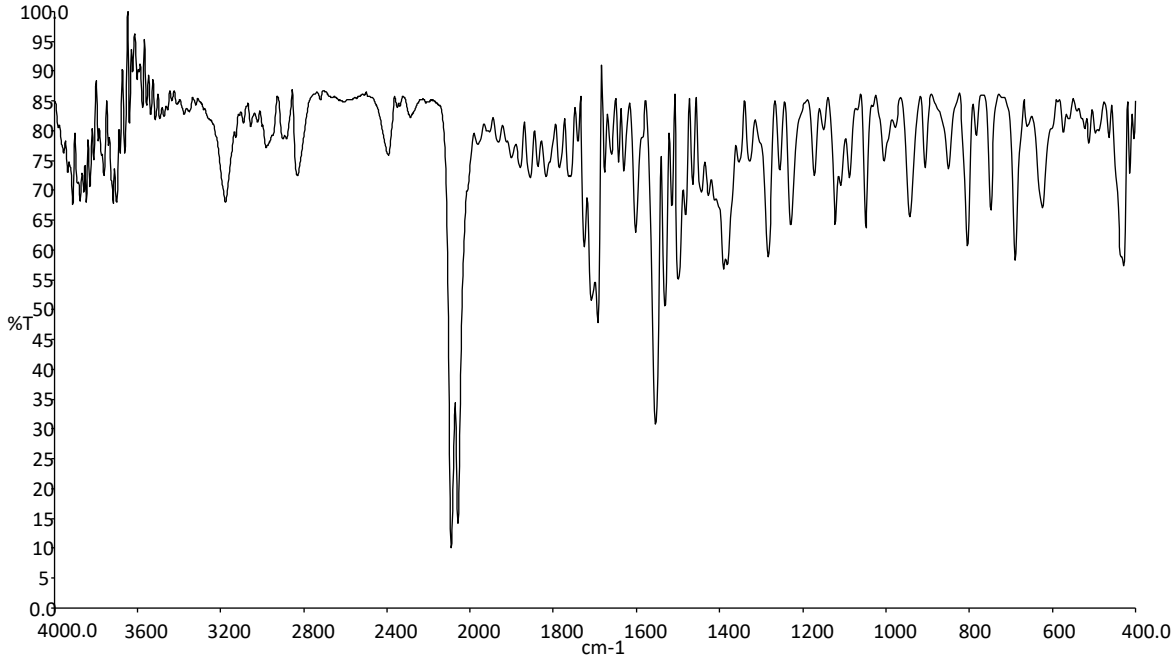

Fig.5(B).2. IR spectrum of $[Co(bdpab)(NCSe)_2]$ (**2**).

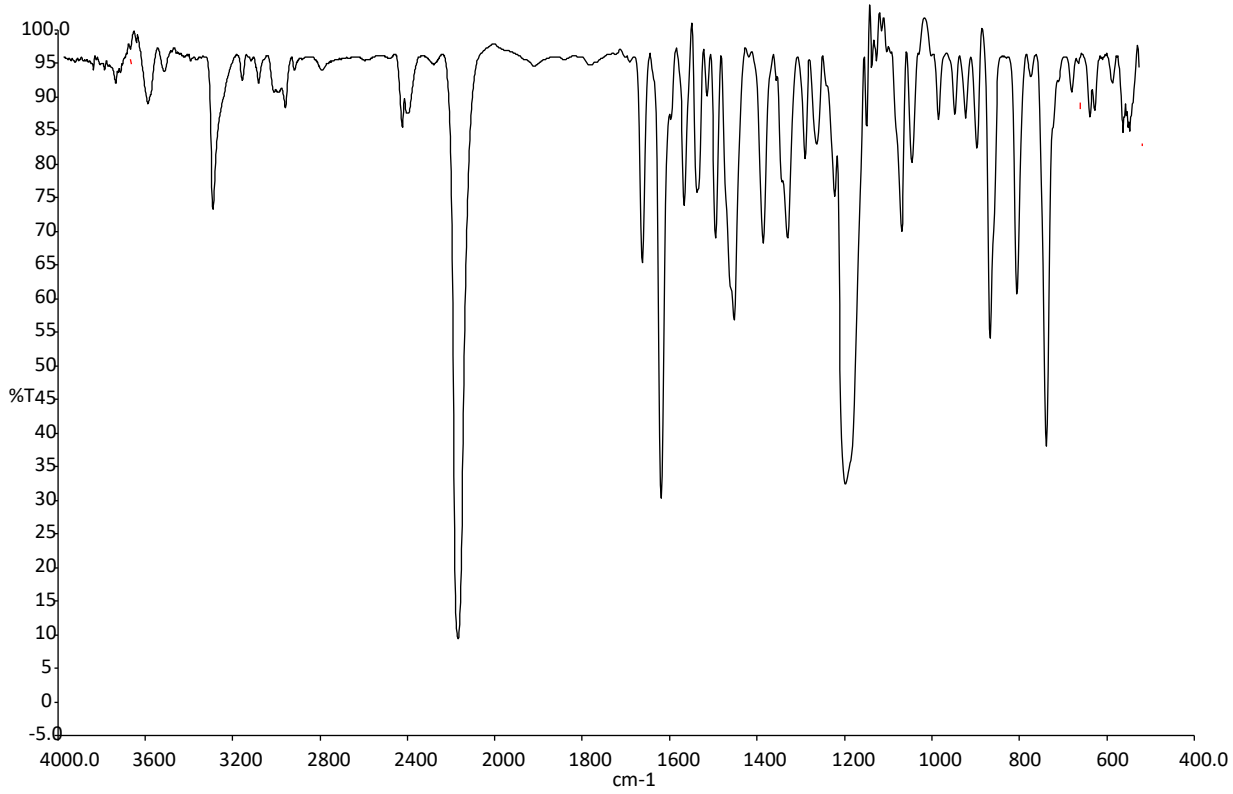

Fig.5(B).3. IR spectrum of [Zn(bdpab)(NCSe)]ClO_4 (**3**).

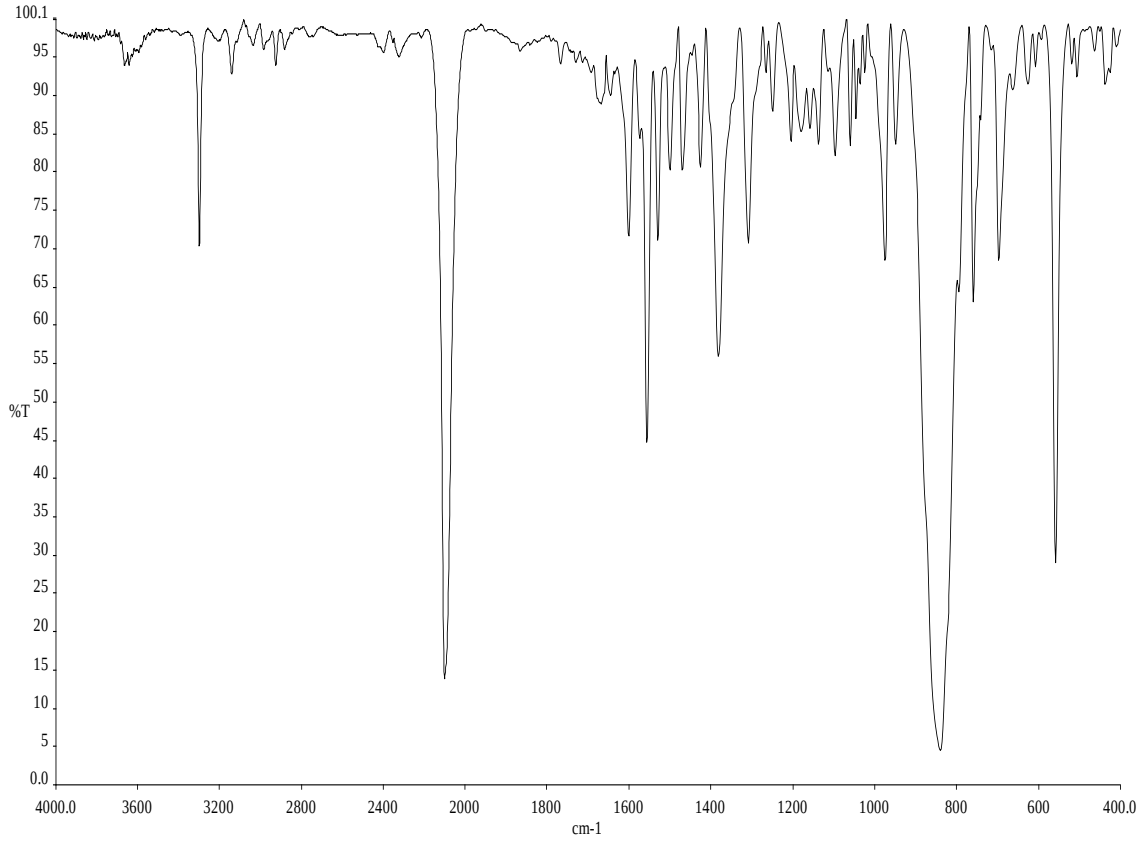

Fig.5(B).4. IR spectrum of [Zn(bdpab)(NCSe)]PF_6 (**4**).

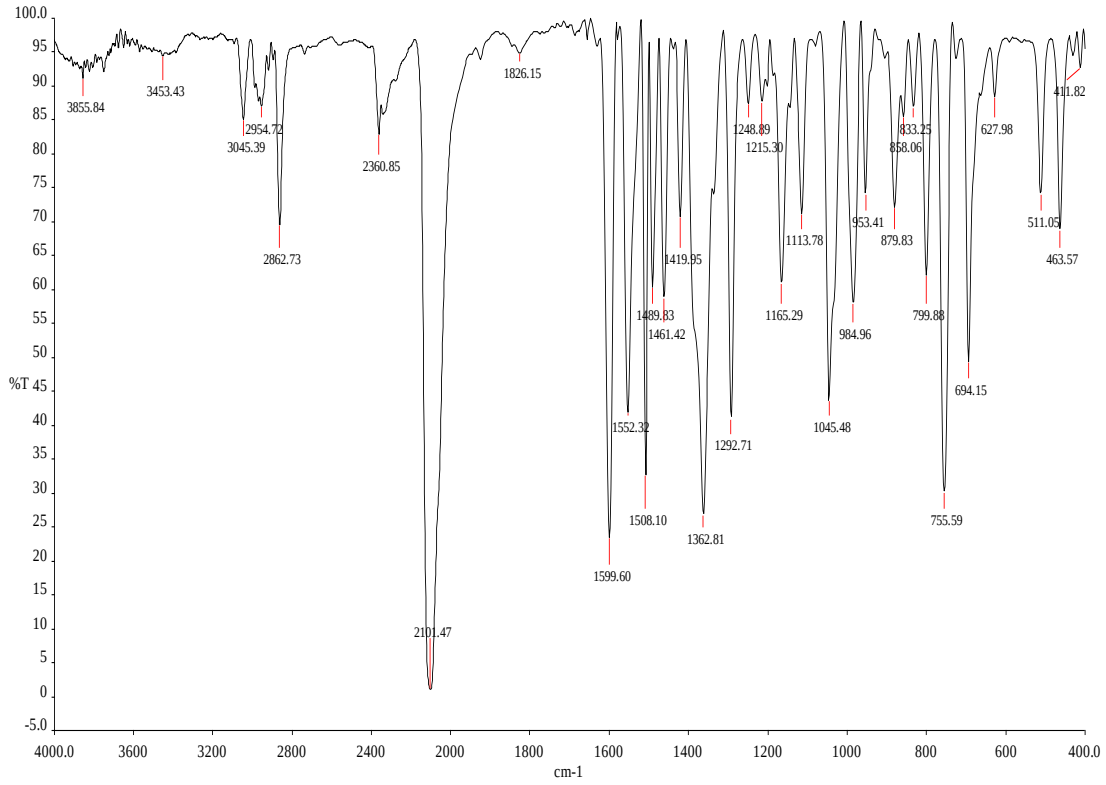

Fig.5(B).5. IR spectrum of $[Cd(dpip)(SCN)_2]_n$ (**5**).

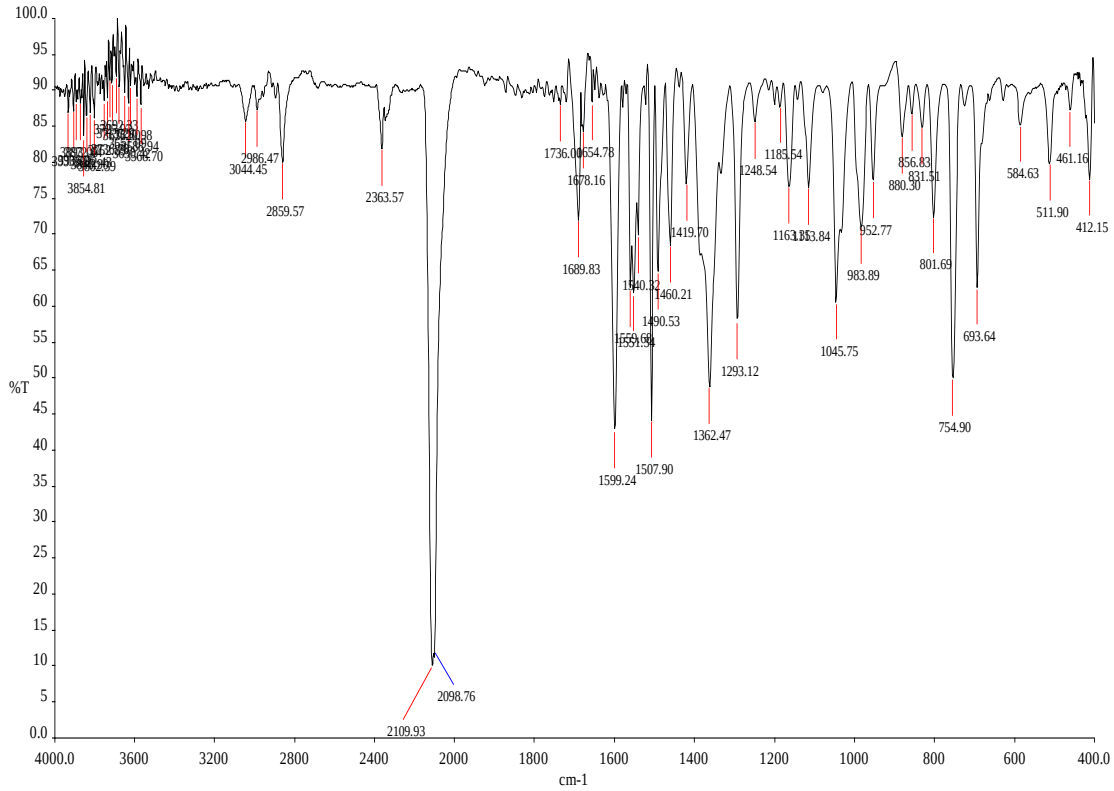

Fig.5(B).6. IR spectrum of $[Cd(dpip)(SeCN)_2]_n$ (**6**).

The ^{1}H NMR spectrum were recorded in DMSO-d_6 for complexes **5** and **6** and compared with the corresponding spectrum of free ligand bdpab, as described in the chapter **4**. Free ligand bdpab shows thirteen signals whereas the ^{1}H NMR spectrum of complexes **5** and **6** show ten signals for each symmetrically coordinated ligand dpip. Three signals at 2.32, 3.37 and 5.84 ppm of ligand bdpab are absent in both the complexes and these are due to loss of one pyrazolyl arm and one singlet of two protons attached to C-6 is shifted to up field position in both the complexes indicating the formation of new C-N bond. This also supports the formation of saturated imidazole ring during in situ complexation reaction.

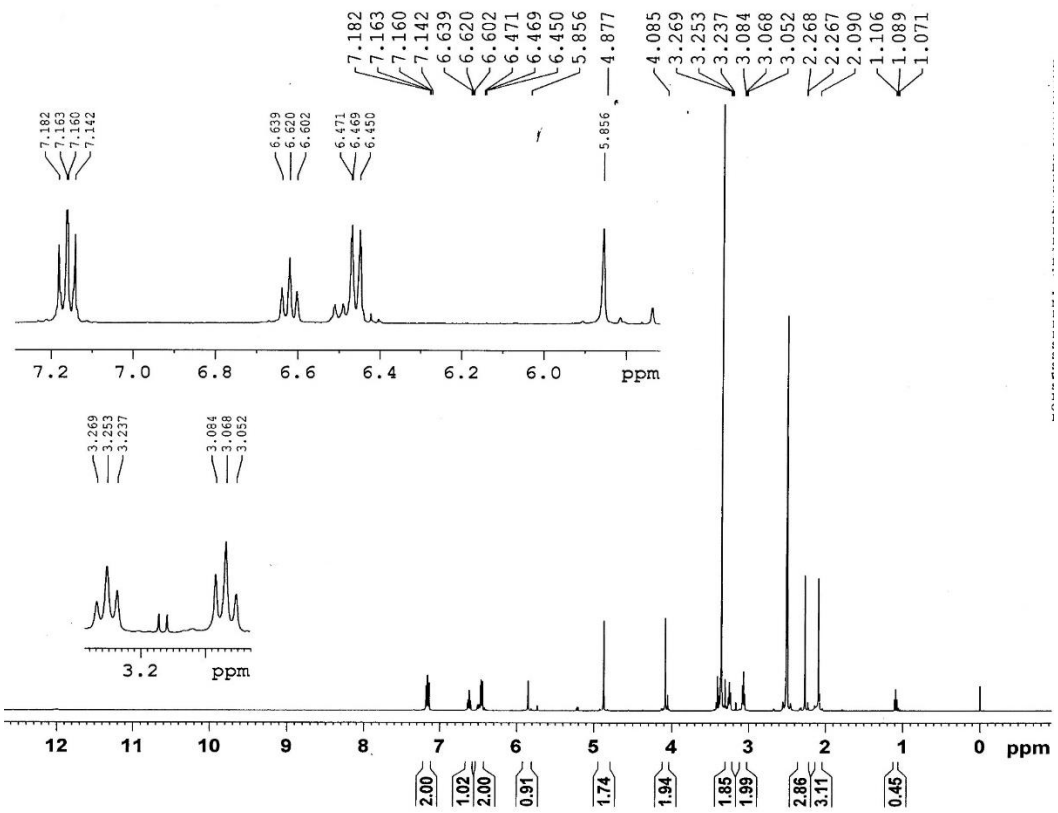

Fig.5(B).7. ^{1}H NMR spectrum of $[Cd(dpip)(SCN)_2]_n$ (**5**).

Complex **5** has two singlet at 2.09 and 2.27 ppm of six protons confirm the presence of two methyl group in pyrazole ring, one singlet of two protons appears at 4.09 due to -CH_2 group of C-5 attached to pyrazolyl ring and one singlet at 4.88 ppm due to two protons of C-6, which shifted to up field with respect to ligand bdpab due to formation of new saturated bond with N atom in the five membered ring. C-12

proton of pyrazole ring appeared as singlet at 5.86 ppm and the protons of phenyl ring appear at 6.45-7.18 ppm.

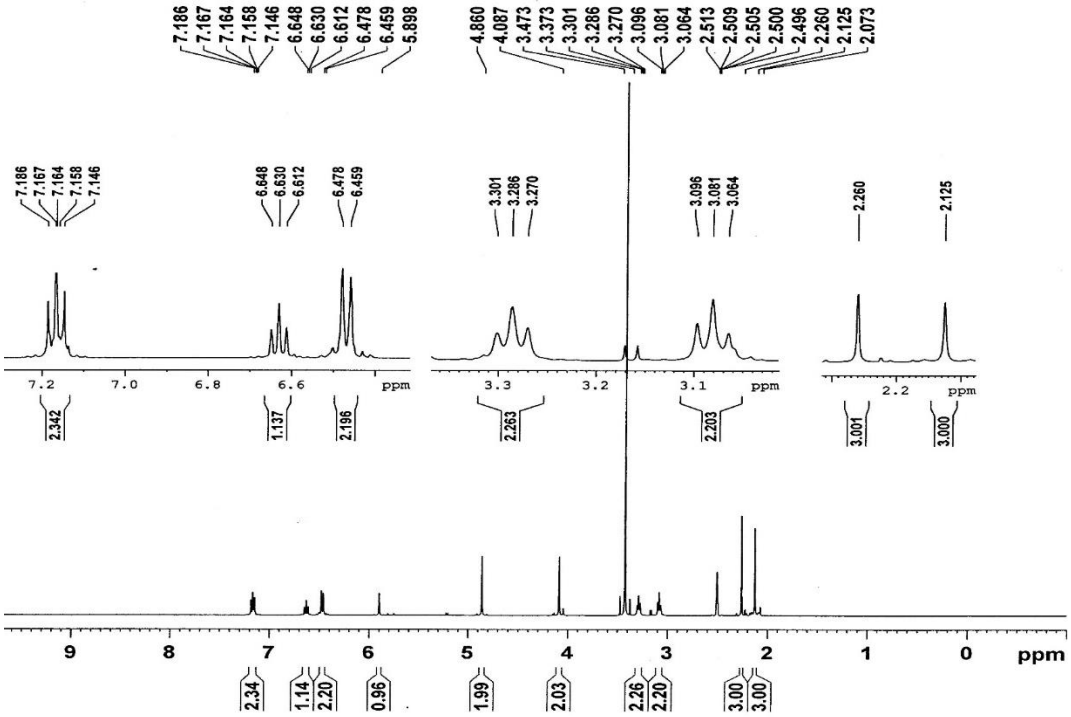

Fig.5(B).8. ^{1}H NMR spectrum of $[Cd(dpip)(SeCN)_2]_n$ (**6**).

Complex **6** has two singlet of six protons at 2.13 and 2.26 ppm which confirms the presence of two methyl group in the pyrazole ring, two singlet of two protons due to -CH_2 group of C-5 attached to pyrazolyl ring appears at 4.09 ppm. One singlet at 4.86 ppm due to two protons of C-6, which shifted to up field with respect to ligand bdpab due to formation of new saturated bond with N atom in the five membered ring. C-12 proton of pyrazole ring appeared as singlet at 5.89 ppm and the protons of phenyl ring appeared as multiplate at 6.46-7.60 ppm.

5(B).4.3. UV-Visible spectra and magnetic data

Electronic spectra were recorded of the complexes **1-4** in CH_3CN solution (~10^{-3} M). The Ni(II) complex shows two bands at 943 and 578 nm with very low molar extinction coefficients, arising from $^{3}A_{2g}(F) \rightarrow {}^{3}T_{2g}(F)$ and $^{3}A_{2g}(F) \rightarrow {}^{3}T_{1g}(F)$ transitions, respectively. The cobalt(II) complex shows two bands at 578 and 492 nm, assigned to $^{4}T_{1g}(F) \rightarrow {}^{4}A_{2g}(F)$ and $^{4}T_{1g}(F) \rightarrow {}^{4}T_{2g}(F)$ transitions, respectively. No bands were observed for the Zn(II) and Cd(II) complexes in the visible region. Bands

observed below 400 nm for all of these complexes are assigned charge transfer transitions.

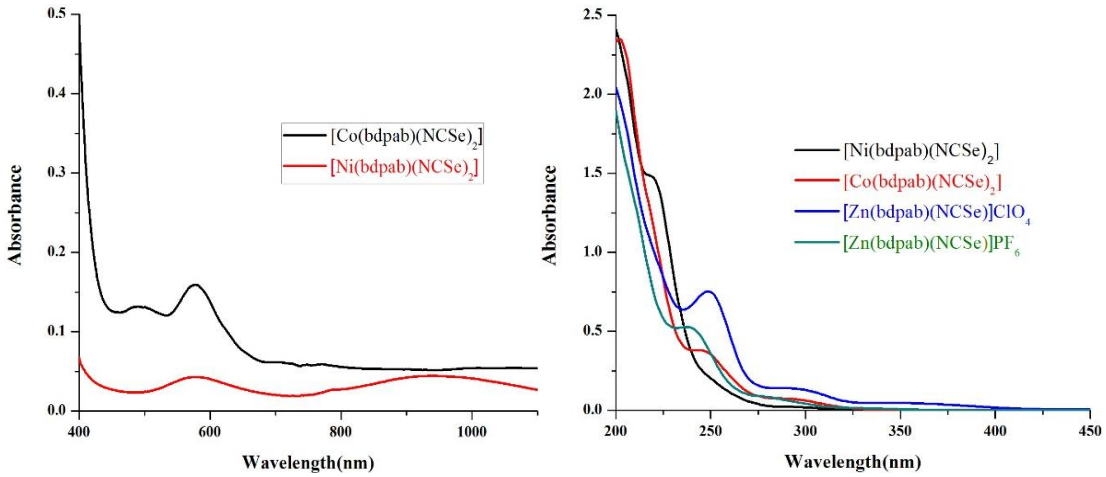

Fig.5(B).9. UV-Visible spectra of complexes **1-4** in CH_3CN (10^{-3} M).

Room temperature magnetic susceptibility measurements of the complexes show μ_{eff} ~ 2.75 BM for the nickel(II) complex, indicating two electron paramgnetism and μ_{eff} ~ 4.25 BM for the cobalt(II) complex, indicating three electron paramagnetism. The magnetic moments of others cobalt(II) complexes with tetradentate N_4-coordinate ligands also fall in this region [37].

5(B).4.4. Description of Crystal Structures

5(B).4.4.1. Crystal structures of [M(bdpab)(NCSe)2] [M= Ni(II) (1) and Co(II) (2)]

The molecular structures of complexes **1** and **2** with the atom-labeling schemes are shown in Figs.5(B).10(a) and 11(a), respectively. The ligand is tetradentate in both cases, utilizing its four nitrogen donor atoms N(1), N(2), N(4) and N(6) for coordination to the metal. In addition, the two selenocyanate ligands coordinate through their nitrogen atoms N(7) and N(8), giving a slightly distorted MN_6 coordination environment. Both compounds are iso-structural and crystallize in the monoclinic system with $P2_1/c$ space group.

In complex **1**, the geometry around nickel is distorted octahedral. The equatorial plane is occupied by three nitrogen atoms N(2), N(4) and N(6) from the bdpab ligand and one nitrogen atom N(8) of selenocyanate, and the axial plane is occupied by one nitrogen atom N(1) from the bdpab and N(7) from selenocyanate. The equatorial bond distances range from 2.018 (4) to 2.159 (3) Å and axial bond distances from 2.097(4) to 2.209(4) Å, with angles between 87.31 (12) and 179.88 (15)° (Table 5(B).2). The two NCSe ligands are nearly linear (~178°), but they are not linear with the nickel atom, as the bond angles are 147.67° for Ni-N(7)-C(21) and 169.70° for Ni-N(8)-C(22).

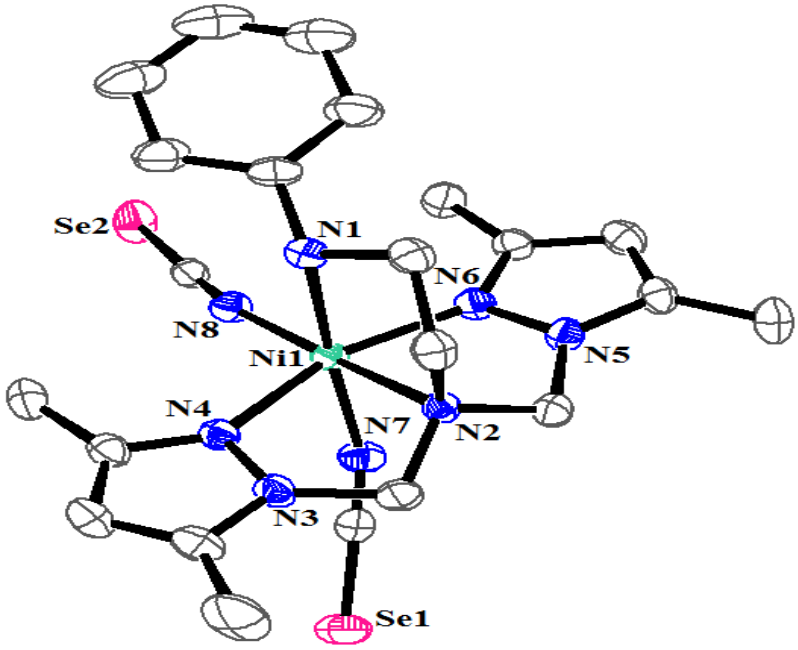

Fig.5(B).10(a). ORTEP diagram depicting the cationic part of the complex [Ni(bdpab)(NCSe)$_2$] (**1**) with atom numbering scheme (30% probability factor for the thermalellipsoids)

Table 5(B).2. Important bond lengths (Å) and bond angels (º) of complexes **1**, **2**, **3**, **5** and **6.**

Bond lengths (Å)									
[Ni(bdpab)(NCSe)$_2$] (1)		**[Co(bdpab)(NCSe)$_2$] (2)**		**[Zn(bdpab)(NCSe)]ClO$_4$ (3)**		**[Cd(dpip)(μ$_{1,3}$-SCN)$_2$]$_n$ (5)**		**[Cd(dpip)(μ$_{1,3}$-SeCN)$_2$]$_n$ (6)**	
Ni(1)-N(8)	2.018(4)	Co(1)-N(8)	2.032(6)	Zn(1)-N(2)	2.334(4)	Cd(1)-N(6)	2.316(7)	Cd(1)-N(4)	2.337(6)
Ni(1)-N(6)	2.068(4)	Co(1)-N(6)	2.097(6)	Zn(1)-N(1)	2.137(5)	Cd(1)-N(5)	2.324(7)	Cd(1)-N(5)	2.346(6)
Ni(1)-N(4)	2.089(3)	Co(1)-N(4)	2.118(6)	Zn(1)-N(6)	2.046(5)	Cd(1)-N(4)	2.345(6)	Cd(1)-N(6)	2.353(6)
Ni(1)-N(7)	2.098(4)	Co(1)-N(7)	2.133(6)	Zn(1)-N(3)	2.045(5)	Cd(1)-N(2)	2.489(5)	Cd(1)-N(2)	2.509(5)
Ni(1)-N(2)	2.158(3)	Co(1)-N(2)	2.233(5)	Zn(1)-N(7)	1.982(5)	Cd(1)-S(2)	2.6794(19)	Cd(1)-Se(1)	2.7474(8)
Ni(1)-N(1)	2.209(4)	Co(1)-N(1)	2.272(6)			C(7)-C(8)	1.533(13)	C(7)-C(8)	1.529(10)
						C(7)-N(1)	1.460(12)	C(7)-N(1)	1.460(10)
						Cd(1)-S(1)	2.650(2)	Cd(1)-Se(2)	2.7367(8)
						N(1)-C(17)	1.458(9)	N(1)-C(17)	1.463(8)
						N(2)-C(17)	1.483(9)	N(2)-C(17)	1.455(8)
						N(5)-C(15)	1.143(10)	N(5)-C(15)	1.136(10)
						N(6)-C(16)	1.143(11)	N(6)-C(16)	1.151(9)
						S(1)-C(15)	1.645(7)	Se(1)-C(15)	1.818(7)
						S(2)-C(16)	1.641(8)	Se(2)-C(16)	1.805(6)
						Cd(1)-Cd(1)i	5.724	Cd(1)-Cd(1)i	5.825

Bond angels (º) of complexes **1**, **2** and **3.**

Bond angles (º)					
[Ni(bdpab)(NCSe)$_2$] (1)		**[Co(bdpab)(NCSe)$_2$] (2)**		**[Zn(bdpab)(NCSe)]ClO$_4$ (3)**	
N(8)-Ni (1)-N(6)	99.89(15)	N(8)-Co(1)-N(6)	101.6(2)	N(1)-Zn(1)-N(2)	80.40(18)
N(8)-Ni(1)-N(4)	101.76 (15)	N(8)-Co(1)-N(4)	103.5(2)	N(6)-Zn(1)-N(2)	76.33(17)
N(6)-Ni(1)-N(4)	158.28 (15)	N(6)-Co(1)-N(4)	154.9(2)	N(6)-Zn(1)-N(1)	105.78(19)
N(8)-Ni(1)-N(7)	92.77 (16)	N(8)-Co(1)-N(7)	94.4(3)	N(3)-Zn(1)-N(2)	76.56(18)
N(6)-Ni(1)-N(7)	90.09 (16)	N(6)-Co(1)-N(7)	91.1(2)	N(3)-Zn(1)-N(1)	122.10(19)
N(4)-Ni(1)-N(7)	87.18 (15)	N(4)-Co(1)-N(7)	87.3(2)	N(3)-Zn(1)-N(6)	118.76(19)
N(8)-NI(1)-N(2)	176.88(15)	N(8)-Co(1)-N(2)	175.3(2)	N(7)-Zn(1)-N(2)	178.53(19)
N(6)-Ni(1)-N(2)	80.15(14)	N(6)-Co(1)-N(2)	78.6(2)	N(7)-Zn(1)-N(1)	101.1(2)
N(4)-Ni(1)-N(2)	78.33(13)	N(4)-Co(1)-N(2)	76.4(2)	N(7)-Zn(1)-N(6)	103.01(19)
N(7)-Ni(1)-N(2)	90.35(15)	N(7)-Co(1)-N(2)	90.3(2)	N(7)-Zn(1)-N(3)	102.7(2)
N(8)-Ni(1)-N(1)	95.00(15)	N(8)-Co(1)-N(1)	95.9(2)		
N(6)-NI(1)-N(1)	89.85(16)	N(6)-Co(1)-N(1)	88.3(2)		
N(4)-Ni(1)-N(1)	89.97(15)	N(4)-Co(1)-N(1)	88.8(2)		
N(7)-Ni(1)-N(1)	172.12(16)	N(7)-Co(1)-N(1)	169.6(3)		
N(2)-Ni(1)-N(1)	81.88(14)	N(2)-Co(1)-N(1)	79.4(2)		

Bond

Bond angels (º) of complexes **5** and **6.**

Bond angels (º)							
[Cd(dpip)($\mu_{1,3}$-SCN)$_2$]$_n$ (5)				**[Cd(dpip)($\mu_{1,3}$-SeCN)$_2$]$_n$ (6)**			
N(6)-Cd(1)-N(5)	172.8(3)	N(5)-Cd(1)-S(2)	94.02(18)	N(4)-Cd(1)-N(5)	87.4(2)	N(5)-Cd(1)-Se(1)	82.91(17)
N(6)-Cd(1)-N(4)	90.8(3)	N(4)-Cd(1)-S(2)	165.10(19)	N(4)-Cd(1)N(6)	91.3(2)	N(6)-Cd(1)-Se(1)	96.11(13)
N(5)-Cd(1)-N(4)	90.3(2)	N(2)-Cd(1)-S(2)	94.88(16)	N(5)-Cd(1)-N(6)	171.6(2)	N(2)-Cd(1)-Se(1)	93.92(13)
N(6)-Cd(1)-N(2)	89.7(2)	S(1)-Cd(1)-S(2)	93.60(8)	N(4)-Cd(1)-N(2)	71.29(18)	Se(2)-Cd(1)-Se(1)	95.25(3)
N(5)-Cd(1)-N(2)	84.0(2)	N(5)-C(15)-S(1)	178.4(7)	N(5)-Cd(1)-N(2)	89.1(2)	N(5)-C(15)-Se(1)	178.1(6)
N(4)-Cd(1)-N(2)	71.4(2)	N(6)-C(16)-S(2)	179.0(8)	N(6)-Cd(1)-N(2)	82.57(19)	N(6)-C(16)-Se(2)	178.4(6)
N(6)-Cd(1)-S(1)	98.0(2)	Cd(1)-S(1)-C(15)	94.81(2)	N(4)-Cd(1)-Se(2)	100.71(13)	Cd(1)-Se(1)-C(15)	96.87(18)
N(5)-Cd(1)-S(1)	88.7(2)	Cd(1)-S(2)-C(16)	100.37(3)	N(5)-Cd(1)-Se(2)	99.23(15)	Cd(1)-Se(2)-C(16)	91.81(18)
N(4)-Cd(1)-S(1)	100.7(2)	Cd(1)-N(5)-C(15)	152.02(6)	N(6)-Cd(1)-Se(2)	89.21(14)	Cd(1)-N(5)-C(15)	156.00(5)
N(2)-Cd(1)-S(1)	169.19(16)	Cd(1)-N(6)-C(16)	156.54(6)	N(2)-Cd(1)-Se(2)	168.29(13)	Cd(1)-N(6)-C(16)	149.89(5)
N(6)-Cd(1)-S(2)	83.1(2)	Cd(#)-Cd(1)-Cd(1i)	120.69	N(4)-Cd(1)-Se(1)	162.48(13)	Cd(#)-Cd(1)-Cd(1i)	121.64

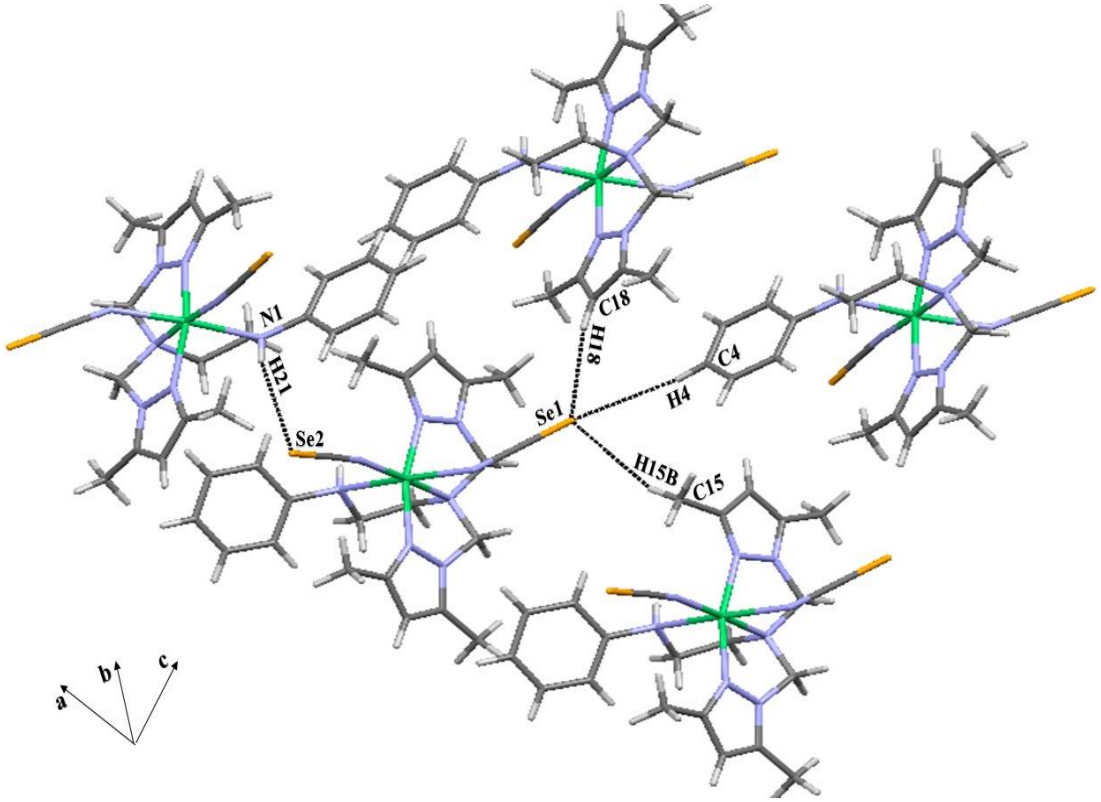

Fig.5(B).10(b). Intermolecular interactions of the complex **1.**

The selenium atoms of the two SeCN ligands show weak intermolecular interactions with the hydrogen atoms of neighboring molecules [Fig.5(B).10(b)]. Thus, Se(1) interacts with the three nearest molecules through H18 of H18C18 of the pyrazole molecule, H4 of H4C4 of the benzene ring, and H15B of H15BC15 of the methyl substituent on the pyrazole ring. Se(2) shows an intermolecular interaction with H21of H21N1 of the secondary amine attached to the benzene ring [Table 5(B).3.]. Hydrogen bonding with less electronegative selenium atom has been reported previously [38].

In complex **2**, the cobalt atom has a CoN_6 coordination environment with distorted octahedral geometry. Three nitrogen atoms N(1), N(4) and N(6) from the bdpab ligand and N(7) from one SeCN ligand occupy the equatorial positions, whilst the axial positions are occupied by N(2) of the bdpab ligand and N(8) of the second SeCN ligand. The lengths of the equatorial bonds Co-N(1), Co-N(4), Co-N(6) and Co-N(7) vary from 2.097(6) to 2.272(6) Å and the axial Co-N(8) [2.032(6) Å] bond is shorter than Co-N(2) [2.233(5) Å] [Table 5(B).2]. The two SeCN ligands are almost linear, with bond angles between Se(2)-N(8)-C(22) and Se(1)-N(7)-C(21) of 177.78

and 178.38° respectively, but the Co-N(8)-C(22) and Co-N(7)-C(21) bond angles are 162.47° and 146.90° respectively. The Co-N bond lengths involving both the pyrazole and SeCN ligands are comparable to those reported for other selenocyanate complexes [7]. In both complexes, the distance M-N(1) of the secondary amine is longer than other M-N bond distances (~2.209 Å).

Table 5(B).3. Intermolecular interaction of complexes **1**, **2** and **3**.

Compounds/ parameters	D-H(Å)	H---A(Å)	D----A(Å)	<(DHA)
[Ni(bdpab)(NCSe)$_2$] (1)				
N1-H21---Se2	0.702	2.965	3.667	154.79
C18-H18---Se1	0.929	3.066	3.995	142.82
C4-H4---Se1	0.930	3.051	3.981	162.02
C15-H15B---Se1	0.960	2.958	3.918	147.08
[Co(bdpab)(NCSe)$_2$] (2)				
N1-H21---Se2	0.679	2.956	3.635	160.45
C10-H10---Se1	0.930	3.056	3.986	142.35
C15-H15---Se1	0.930	3.048	3.978	159.47
C1-H1B---Se1	0.960	2.921	3.881	146.70
[Zn(bdpab)(NCSe)]ClO$_4$ (3)				
C6-H6----Se1	0.930	2.953	3.883	132.74
C18-H18---Se1	0.931	3.064	3.995	134.76

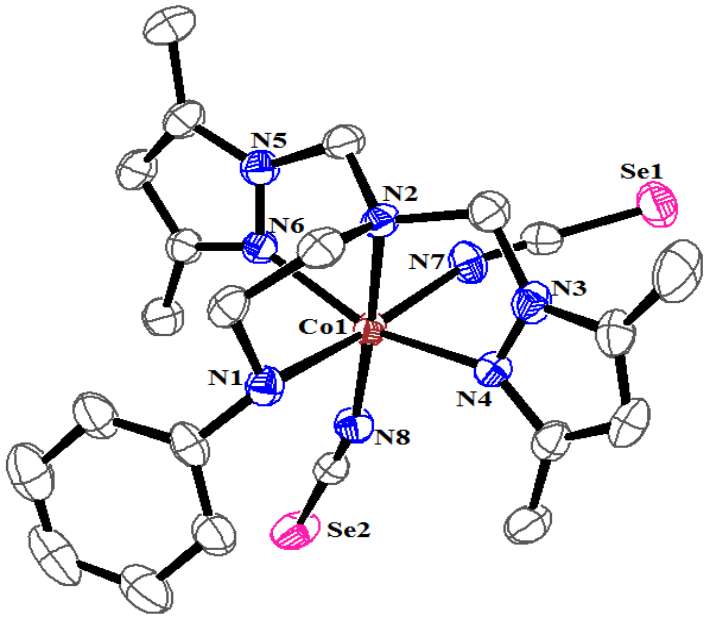

Fig.5(B).11(a). ORTEP diagram of the complex [Ni(bdpab)$(NCS)_2$] (**2**) with atom numbering scheme (30% probability factor for the thermal ellipsoids).

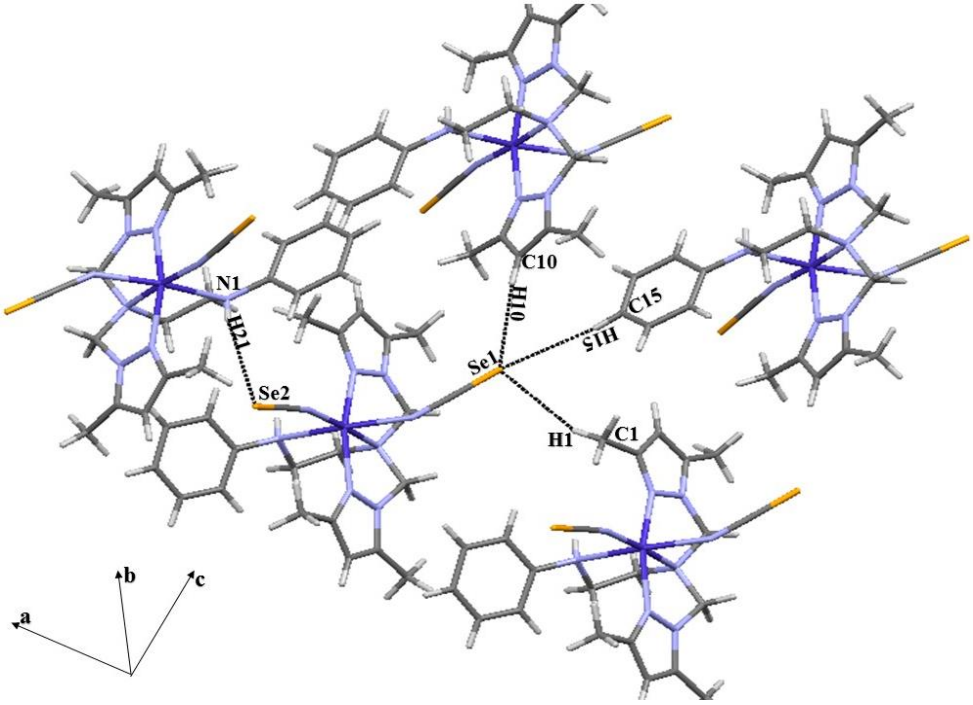

Fig.5(B).11(b). Intermolecular interactions of the complex **2.**

The selenium atoms of the two SeCN ligands show intermolecular interactions with hydrogen atoms of the nearest four molecules [Fig.5(B).11(b)]. Thus, Se(1) has weak intermolecular interactions with the three neighbouring molecules through H10 of H10C10 of the nearest pyrazole molecule, H15 of H15C15 of a benzene ring and

H1 of H1C1 of the methyl substituent on the pyrazole ring. Se(2) shows an intermolecular interaction with H21of H21N1 of the secondary amine attached to the benzene ring [Table 5(B).3].

5(B).4.4.2. Crystal Structure of [Zn(bdpab)(NCSe)]ClO_4 (3)

The molecular structure of the complex **3** is shown in Fig.5(B).12(a). The complex is crystallized in the triclinic system with *P-1* space group. The zinc atom is coordinated by four nitrogen atoms N(1), N(2), N(3) and N(6) of the bdpab ligand, plus one nitrogen atom N(7) of a selenocyanate ligand. Hence, the zinc atom has a ZnN_5 coordination environment with a trigonal bipyramidal geometry as revealed from the trigonality index ($\tau = 0.94$) [39]. The basal plane is occupied by N(1), N(3) and N(6) of the bdpab ligand and the axial positions are occupied by N(2) of bdpab and N(7) of the SeCN ligand. The bond lengths of the equatorial vary from 2.045(5) to 2.137(5) Å, whilst the axial bond length Zn-N(7) [1.982(5)Å] is shorter than Zn-N(2) [2.334(4) Å]. The axial bond angle N(2)-Zn-N(7) is linear [178.53(19)°] (Table 5(B).2). The Zn-N(2) (tertiary amine) [2.334(4) Å] bond is elongated in the complex. The SeCN ligand is linear, with bond angle N(7)-C(21)-Se(1) is 178.61°, whereas the Zn-N(7)-C(21) (164.37°) moiety is non-linear.

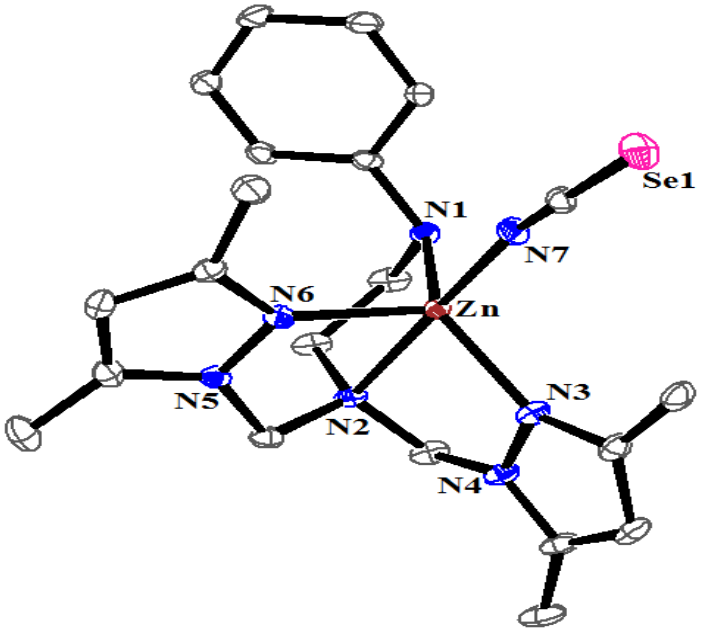

Fig.5(B).12(a). ORTEP diagram depicting the cationic part of the complex [Zn(bdpab)(NCSe)]ClO_4 (**3**) with atom numbering scheme (30% probability factor for the thermal ellipsoids).

The selenium atom of the SeCN ligand shows weak intermolecular interactions with hydrogen atoms of the two nearest neighbours [Fig.5(B).12(b)]. Thus, Se(1) shows weak intermolecular interactions with the two nearest molecules through H18 of H18C18 of the pyrazole moiety and H6 of H6C6 of the benzene ring [Table 5(B).3].

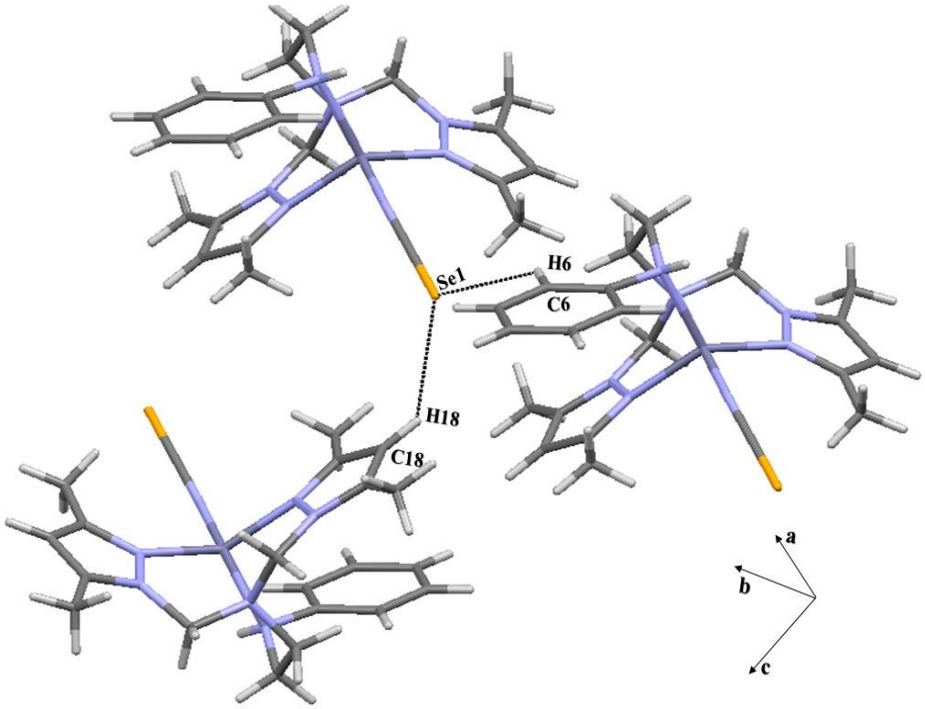

Fig.5(B).12(b). Intermolecular interactions of complex **3.**

5(B).4.4.3. Crystal Structures of $[Cd(dpip)(\mu_{1,3}\text{-}X)_2]_n$ [X = SCN (5) , SeCN (6)]

The asymmetric unit and polymeric unit of complexes **5** and **6** are shown in Figs.5(B). 13 (a and b) and 14 (a and b) and selected bond length and angles are given in Table 5(B).2. The structures of **5** and **6** consist of neutral chains of cadmium atoms bonded by four μ-1,3-(XCN) (X = S or Se) and two cadmium centres are bonded by two XCN ions in Cd-$(XCN)_2$-Cd chain. Thiocyanate is an ambidentate ligand and can bind cadmium(II) with both S and N coordination mode. Since selenocyanate ion is iso-electronic with thiocyanate ion, selenocyanate ion can also acts as bridging ligand and bridges the two cadmium centres like thiocyanate ion. Each cadmium atom has octahedral geometry with CdN_4S_2 and CdN_4Se_2 coordination environment, respectively and surrounded by a five member chelate ring and four μ-(XCN) bridges. The two nitrogen atoms N(5) and N(6) and one S2/Se2 from NCX and one nitrogen

N(4) of pyrazole ring defines the basal plane around cadmium **1** and the axial positions are occupied by another nitrogen atom N(2) from ligand dpip and S(4) /Se(4) of bridging SeCN ligand. The double μ-$(XCN)_2$ in Cd-$(XCN)_2$-Cd forms an eight membered ring and two sets of $\mu_{1,3}$-(XCN) bridges are not equivalent and giving alternating system produce zig-zag chain. Ligand dpip has formed a strain chelate ring around cadmium atom and the chelate ring strain may also be the reason for the in-equivalence of the two μ-$(XCN)_2$ around cadmium(II) and produce zig-zag chain. This type of eight membered ring and zig-zag μ-$(XCN)_2$ bridging compounds are reported in the literature [40-45] but number of compounds with SeCN are less reported in the literature [46]. The versatile bridging nature of μ-(SCN) as well as μ-(SeCN) ligands gives 1D polymeric chain along b-axis.

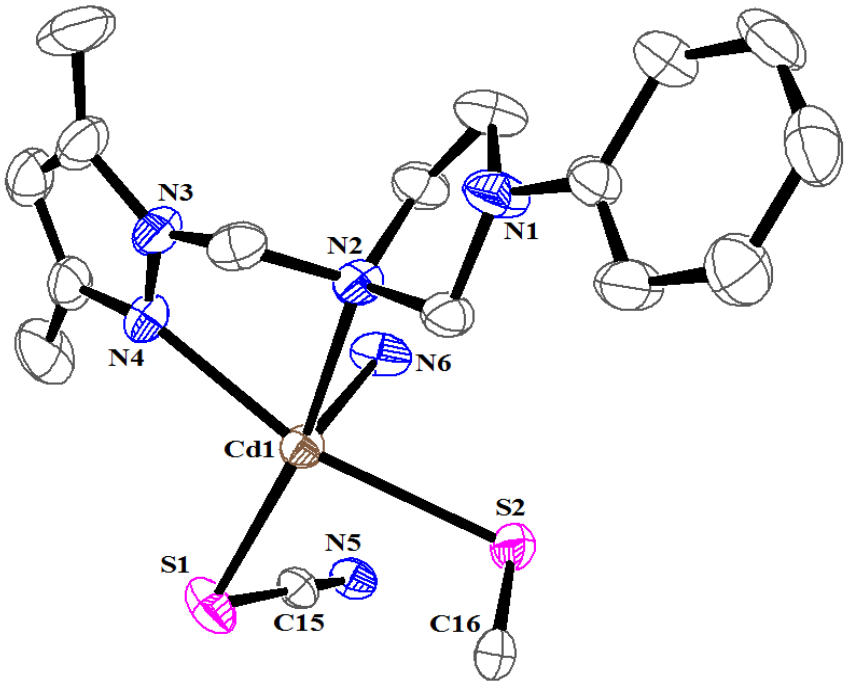

Fig.5(B).13(a). ORTEP diagram of aasymmetric unit of polymeric complex $[Cd(dpip)(\mu_{1,3}\text{-}SCN)_2]_n$ (**5**) with atom numbering scheme.

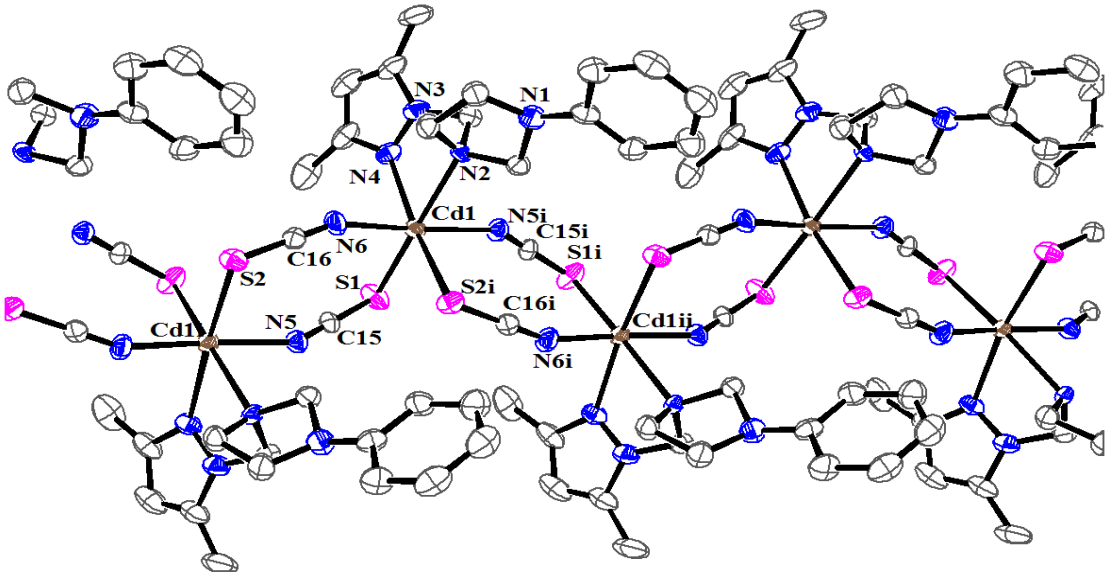

Fig.5(B).13(b). The 1D polymeric zig-zag chain of complex (**5**) along the b-axis, showing 8 membered rings (displacement ellipsoids are drawn at 30% probability level).

In $[Cd(dpip)(SCN)_2]_n$, the equatorial bond distances of Cd-N(5) [2.324(7) Å], Cd-N(6) [2.316(7) Å], Cd-N(4) [2.345(6) Å] and Cd-S(2) [2.6794(19) Å] are not equal and the cis-bond angels varies from 83.14(2)° to 172.8(3)°. The axial bond distances Cd-N(2) [2.489(5) Å] and Cd-S(1) [2.650(2) Å] are not equal and bond angle N(2)-Cd-S(1) is 169.19(16)°. Two Cd-N(organic ligand) bond distances are not equal and Cd-N(2) [2.489(5) Å] is longer than Cd-N(4) [2.345(6) Å] (Table 5(B).2). Two Cd-S bond lengths are nearly same but much longer than Cd-N (NCS or organic ligand) bond length, indicating two weak Cd-S bonds. The Cd-S bond lengths and angles with other atoms are comparable to thiocyanate bridged cadmium(II) complexes reported in the literature [47]. Two bridging bond angles Cd(1)-N(6)-C(16) [156.54(6)] and Cd(1)-S(1)-C(15) [94.81(2)] have wide differences but four bridging thiocyanate ions are nearly linear with bond angles ~ 178.45°. The distortion from ideal octahedral geometry in Fig.5(B).13 is due to unequal bond lengths [varies from 2.316(7) to 2.6794(19)Å] and bond angles [varies from 71.4(2) to 172.8(3)°]. The distance between two cadmium centers in Cd-$(NCS)_2$-Cd is 5.724 Å, comparable to other reported similar type cadmium compound [47-49].

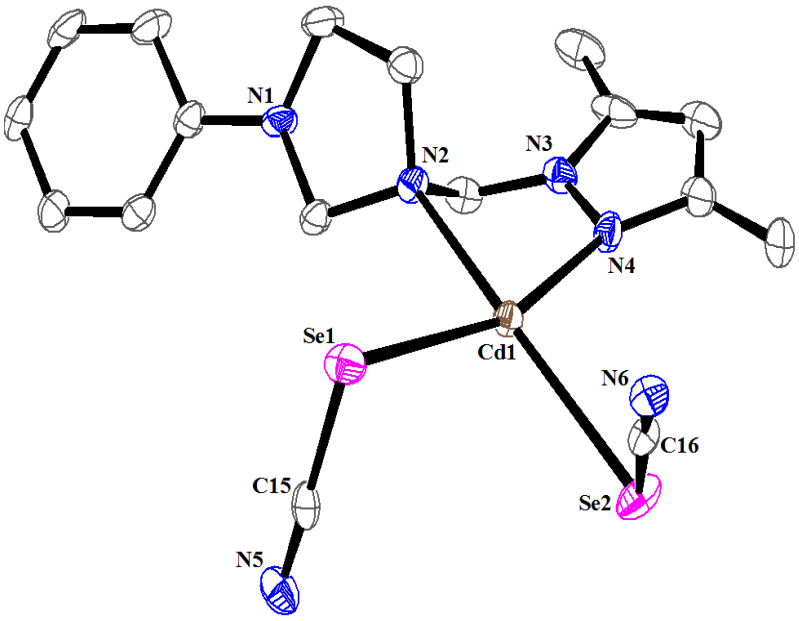

(a)

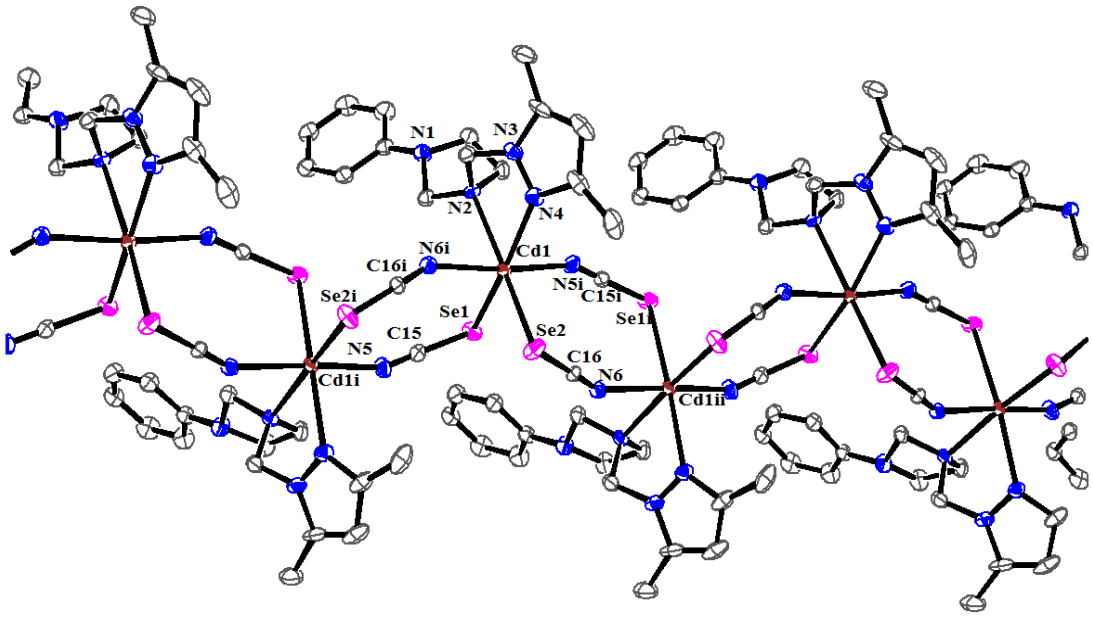

(b)

Fig.5(B).14(a). ORTEP diagram of asymmetric unit of polymeric complex $[Cd(dpip)(\mu_{1,3}\text{-}SeCN)_2]_n$ (**6**) with atom numbering scheme. **(b).** The 1D polymeric zig-zag chain of complex (**6**) along the b-axis, showing 8 membered rings (displacement ellipsoids are drawn at 30% probability level).

In $[Cd(dpip)(SeCN)_2]_n$, the equatorial bond distances of Cd-N(5) [2.346(6) Å], Cd-N(6) [2.353(6)Å], Cd-N(4) [2.337(6)Å] and Cd-Se(2) [2.7367(8)Å] are not equal and the cis-bond angels varies from 82.91(17)° to 96.11(13)°. The axial bond distances Cd-N(2) [2.509(5) Å] and Cd-Se(1) [2.7474(8)Å] are different and bond angle N(2)-Cd-Se(1) is 93.32(13)°. Two Cd-Se bond lengths are nearly same but much longer than Cd-N (both SeCN and dpip ligand), indicating much weaker bonding with selenium atoms. Two Cd-N bond distances of organic ligand are not equal and Cd-N(2)[2.509(5)Å] is much longer than Cd-N(4)[2.337(6)Å] (Table 5(B).2). The Cd-Se bond lengths and angles with other atoms are comparable to selenocyanate bridged cadmium(II) complexes reported in the literature. The distortion from ideal octahedral geometry in [Fig.5(B).14] is due unequal bond lengths [varies from 2.346(6) to 2.7474(8)º] and bond angles [varies from 82.57(19)° to 171.6(2)°]. Two bridging bond angles Cd(1)-N(5)-C(15)[156.00(5)°] and Cd(1)-Se(2)-C(16)[91.81(18)°] have wide differences but four bridging selenocyanates are nearly linear with bond angle 178.15°. The distance between two cadmium centers in Cd-$(NCSe)_2$-Cd is 5.825 Å and this is comparable to other reported similar type cadmium compounds [46, 50].

The C-N bond lengths varies from 1.459 – 1.485 Å and C-C bond length is ~1.534 Å in the new five membered saturated imidazole type ring formed during reaction and the data indicate they have single bond character.

5(B).4.5. Computational study

All calculations reported herein were carried out with Gaussian 09 program [51]. Molecular structures were visualized using the GaussView program [52]. The geometry were fully optimized using the B3LYP functional and 6-31+G* basis sets for H, N, O, C, Se, S and LANL2DZ basis set was employed for cadmium ion [53-55]. The solvent effect was included employing SCRF PCM solvent model in DMSO (ε = 46.82) [56]. The calculated structure of **5** and **6** using B3LYP/6-31+G* level of theory suggests that the geometrical parameters closely resembles to the crystal structures (Table 5(B).4). The Cd(II) complex with ligand dpip molecule and thiocyanate ligand is distorted octahedron (Fig.5(B).15).

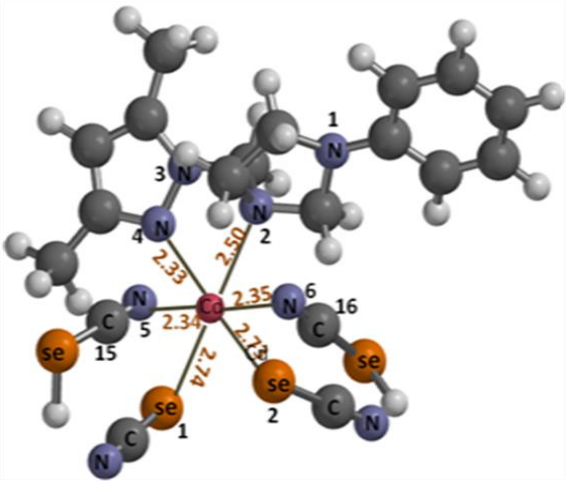

Fig.5(B).15(a). **Fig.5(B).15(b).**

Fig.5(B).15. B3LYP functional and 6-31+G* basis sets for H, N, O, C, Se, S and LANL2DZ basis set was employed for cadmium ion. Key: gray, C; blue, N; white, H; bright yellow S; Orange Se; and Red Cd:

The two nitrogen atoms N(2) and N(4) of the dpip [3,5-dimethyl-1-((3-phenylimidazolidin-1-yl)-methyl)-*1H*-pyrazole)] and sulfur atoms of thiocyanate groups occupy the equatorial positions and the nitrogens of thiocyanates occupies the apical positions. The complex **6** with selenocyanate ligand also exhibited similar structure and in good agreement with the crystal structure (Table 5(B).4). The Cd-S bond lengths are nearly equal but Cd-N bond distances are not equal in this distorted octahedral complexes, however, the Cd-S and Cd-Se bond lengths are nearly equal in each case (Fig.5(B).15). The distortions arises due to the difference in the bond angles Cd(1)-N(6)-C(16) [150.84)] and Cd(1)-S(1)-C(15)[95.74] [Table 5(B).4]. The thiocyanate groups are nearly linear with bond angles ~ 179.98°. The complex **6** with selenocyanate ligand also exhibited similar structure changes and in good agreement with the crystal structure (Table 5(B).4). For computational simplicity, only a small unit of the crystal structure was modeled in our DFT calculations.

Table 5(B).4. Important bond lengths (Å) and bond angels (º) of complexes **5** and **6.**

[Cd(dpip)(μ$_{1,3}$-SCN)$_2$]$_n$ (5)			**[Cd(dpip)(μ$_{1,3}$-SeCN)$_2$]$_n$ (6)**		
Crystallography data.		**DFT data.**	**Crystallography data.**		**DFT data.**
Cd(1)-N(6)	2.316(7)	2.258	Cd(1)-N(4)	2.337(6)	2.33
Cd(1)-N(5)	2.324(7)	2.296	Cd(1)-N(5)	2.346(6)	2.344
Cd(1)-N(4)	2.345(6)	2.294	Cd(1)-N(6)	2.353(6)	2.353
Cd(1)-N(2)	2.489(5)	2.507	Cd(1)-N(2)	2.509(5)	2.50
Cd(1)-S(1)	2.650(2)	2.645	Cd(1)-Se(2)	2.7367(8)	2.73
Cd(1)-S(2)	2.679(19)	2.678	Cd(1)-Se(1)	2.7474(8)	2.746
C(7)-C(8)	1.533(13)	1.54	C(7)-C(8)	1.529(10)	1.528
C(7)-N(1)	1.460(12)	1.46	C(7)-N(1)	1.460(10)	1.45
C(8)-N(2)	1.475(10)	1.47	C(8)-N(2)	1.478(8)	1.47
Bond angels (º)					
Crystallography data.		**DFT data.**	**Crystallography data.**		**DFT data.**
N(2)-Cd(1)-S(2)	94.88(16)	95.01	N(2)-Cd(1)-Se(1)	93.92(13)	93.927
N(5)-C(15)-S(1)	178.4(7)	179.98	N(5)-C(15)-Se(1)	178.1(6)	178.18
N(6)-C(16)-S(2)	179.0(8)	179.99	N(6)-C(16)-Se(2)	178.4(6)	178.39
Cd(1)-S(1)-C(15)	94.81(2)	95.74	Cd(1)-Se(1)-C(15)	96.87(18)	96.92
Cd(1)-S(2)-C(16)	100.37(3)	101.00	Cd(1)-Se(2)-C(16)	91.81(18)	96.92
Cd(1)-N(5)-C(15)	152.02(6)	146.33	Cd(1)-N(5)-C(15)	156.00(5)	155.99
Cd(1)-N(6)-C(16)	156.54(6)	150.84	Cd(1)-N(6)-C(16)	149.89(5)	149.91

5(B).5. Conclusion

Four mononuclear selenocyanate complexes [Ni(bdpab)$(NCSe)_2$], [Co(bdpab)$(NCSe)_2$] and [Zn(bdpab)(NCSe)]Y (Y = ClO_4^-, PF_6^-) and two new 1-D polymeric cadmium(II) complexes $[Cd(dpip)(\mu_{1,3}\text{-}SCN)_2]_n$ and $[Cd(dpip)(\mu_{1,3}\text{-}SeCN)_2]_n$ have been synthesized using tripodal ligand *N,N*-bis(3,5-dimethyl-*1H*-pyrazol-1-yl)methyl-N_2-phenylethane-1,2-diamine (bdpab) and thiocyanate or selenocyanate as co-ligands and characterized. Single crystal X-ray diffraction data shows that Co(II), Ni(II) and Zn(II) complexes are mononuclear with either octahedral or trigonal bipyramidal geometry whereas cadmium(II) complexes are distorted octahedral and form 1D zig-zag polymeric chain. Ligand 3,5-dimethyl-1-((3-phenylimidazolidin-1-yl)-methyl)-*1H*-pyrazole (dpip) is formed from tetradentate N_4-coordinate ligand *N,N*-bis(3,5-dimethyl-*1H*-pyrazol-1-yl)methyl-N_2-phenylethane-1,2-diamine (bdpab) during reaction. DFT calculations have been performed for the complexes $[Cd(dpip)(\mu_{1,3}\text{-}SCN)_2]_n$ and $[Cd(dpip)(\mu_{1,3}\text{-}SeCN)_2]_n$. and corroborated the experimental and theoretical data.

.

5(B).6. References:

[1] R. Kurtaran, H. Namli, C. Kazak, O. Turhan, O. Atakol, J. Coord. Chem. 60 (2007) 2133.

[2] Z.D. Georgousis, P.C. Christidis, D. Hadjipavlou-Litina, C.A. Bolos, J. Mol. Struct. 837 (2007) 30

[3] M.E. Farago, J.M. James, Inorg. Chem. 4 (12) (1965) 1706

[4] C. Pecile, G. Giacometi, A. Turco, Atti Accad. Lincei 28 (1960) 189.

[5] G. Marongiu, E.C. Lingafeller, P. Paoletti, Inorg. Chem. 8 (1969) 2763

[6] B.W. Brown, E.C. Lingafeller, Inorg. Chem. 17 (1964) 253.

[7] H. Takeda, K.Ohashi, A. Sekine, O. Ishitani, J. Am. Chem. Soc. 13 (2016) 4354.

[8] J. Palion-Gazda, B. Machura, F. Lloret, M. Julve, Cryst. Growth Des. 15 (2015) 2380.

[9] O.A. Babich, V.N. Kokozay, V.A. Pavlenko, Polyhedron 15 (1996) 2727.

[10] S. Roy, A. Bauza, A. Frontera, S. Chattopadhyay, Inorg. Chim. Acta 453 (2016) 51.

[11] A. Beheshti, W. Clegg, R. Hyvadi, H.F. Hekmat, Polyhedron 21 (2002) 1547.

[12] A.D. Jana, S.C. Manna, G.M. Rosair, M.G.B. Drew, G. Mostafa, N.R. Chaudhuri, Cryst. Growth Des.7 (2007) 1365.

[13] Y.-Q. Sun, D.-Z. Gao, W. Dong, D.-Z. Liao, C.-X. Zhang, Eur. J. Inorg. Chem. (2009) 2825.

[14] S. Wohlert, U. Ruschewitz, C. Nather, Cryst. Growth Des. 6 (2012) 2715.

[15] J. Palion-Gazda, B. Machura, F. Lloret, M. Julve, Cryst. Growth Des. 15 (2015) 2380.

[16] O.A. Babich, V.N. Kokozay, V.A. Pavlenko, Polyhedron 15 (1996) 2727.

[17] D. Bose, J. Banerjee, S.K.H. Rahaman, G. Mostafa, H.K. Fun, W.R.D. Bailey , M.J. Zaworotko, B.K. Ghosh, Polyhedron 23 (2004) 2045.

[18] S. Jana, S. Chattopadhyay, Polyhedron 81 (2014) 298.

[19] M.H. Sadhu, A. Solanki, S.B. Kumar, Polyhedron 100 (2015) 206.

[20] M.H. Sadhu, S.B. Kumar, Trans. Met. Chem. 40 (2015) 755.

[21] S. Bhattacharyya, T.J.R. Weakley, M. Chaudhury, Inorg. Chem. 38 (1999) 5453.

[22] M.R. Malachowski, A.S. Kasto, M.E. Adams, A.L. Rheingold, L.N.

Zakharov, L.D.Margerum, M. Greaney, Polyhedron 28 (2009) 393.

[23] S. Bhattacharyya, T.J.R. Weakley, M. Chaudhury, Inorg. Chem. 38 (1999) 633.

[24] H. Yang, Y. Tang, Polyhedron 28 (2009) 3491.

[25] A. Solanki, M. Monfort, S.B. Kumar, J. Mol. Struct. 1050 (2013) 197.

[26] Agilent, CrysAlis PRO. Agilent Technologies UK Ltd, Yarnton, England, (2011).

[27] G.M. Sheldrick, SAINT, 5.1 ed. Siemens Industrial Automation Inc., Madison, WI (1995).

[28] G.M. Sheldrick. SHELXL-97: Program for Crystal Structure Refinement, University of Gottingen, Gottingen (1997).

[29] L.J. Farrugia, J. Appl. Cryst. 32 (1999) 837.

[30] W.J. Geary, Coord. Chem. Rev.7 (1971) 81.

[31] T. Marino, N. Russo, M. Toscano, J. Am. Chem. Soc. 127 (2005) 4242.

[32] F.A. Cotton, D.M.L. Goodgame, M. Goodgame, T.E. Haas, Inorg. Chem. 1 (1962) 565.

[33] J.L. Burmeister, L. Williams, Inorg. Chem. 5 (1966) 1113.

[34] A. Turco, C. Pecile, Nature 191 (1961) 66.

[35] R.J.H. Clark, C.S. Williams, Spectrochim. Acta 22 (1966) 1081.

[36] K. Nakamoto, Infrared and Raman spectra of inorganic and coordination compounds, 3rd edn. Wiley, New York. (1978).

[37] F. Mani, G. Scapacci, Inorg. Chim. Acta 38 (1980) 151.

[38] M. Iwaoka, S. Tomoda, J. Am. Chem. Soc. 116 (1994) 4463.

[39] A.W. Addison, Y.N. Rao, J. Reedijk, J.V. Rijn,G.C. Verschoor, J. Chem. Soc. Dalton Trans. (1984)1349

[40] P.M. Secondo, J.M. Land, R.G. Baughman, H.L. Collier, Inorg. Chim. Acta 309 (2000) 13.

[41] S. Banerjee, B. Wu, P.-G. Lassahn, C. Janiak, A. Ghosh, Inorg. Chim. Acta 358 (2005) 535.

[42] T.K. Maji, I.R. Laskar, G. Mostafa, A.J. Welch, P.S. Mukherjee, N.R. Chaudhuri, Polyhedron 20 (2001) 651.

[43] M. Kobayashi, D. Savard, A.R. Geisheimer, K. Sakai, D.B. Leznoff, Inorg. Chem. 52 (2013) 4842.

[44] B. Zurowska, J. Mrozinski, M. Julve, F. Lloret, A. Maslejova, W. Sawka-Dobrowolska, Inorg. Chem. 41 (2002) 1771.

[45] Q. Jing, T. Yu-Zhang, T. Guo-Tao, W. Qing-Lun, L. Li-Cun, M. Yue, Y Guang-Ming, L. Dai-Zheng, Polyhedron 90 (2015) 123.

[46] C.R. Choudhury, S.K. Dey, N. Mondal, S. Mitra, V. Gramlich, Inorg. Chim. Acta 353 (2003) 217.

[47] B. Chand, U. Ray, G. Mostafa, L Tian-Huey, C. Sinha, Polyhedron 23 (2004) 1669.

[48] H. Chowdhury, R. Ghosh, S.K.H. Rahaman, B.K. Ghosh, Polyhedron 26 (2007) 5023.

[49] Y. Zhong-Lu, X. Han, Z. Guang-Ning, Z. Anorg. Allg. Chem. 634 (2008) 142.

[50] A.K. Ghosh, D. Ghoshal, M.G.B. Drew, G. Mostafa, N.R. Chaudhuri, Struct. Chem. 17 (2006) 85.

[51] M.J. Frisch et al., Gaussian 03, Revision C02 (Gaussian Inc., Pittsburgh PA, 2003).

[52] R. Dennington II, T. Keith, J. Millam, K. Eppinnett, W.L. Hovell, R. Gilliland, GaussView, Version 3.09 (Semichem, Inc., Shawnee Mission, KS, 2003).

[53] P.C. Hariharan, Pople, J. A. Mol. Phys. 27 (1974) 209.

[54] P.J. Hay, W. R. Wadt, J. Chem. Phys. 82 (1985) 270.

[55] P.J. Hay, W. R. Wadt, J. Chem. Phys. 82 (1985) 299.

[56] S. Miertus, E. Scrocco, J. Tomasi, Chem. Phys. 55 (1981) 117.